AD_____
(Leave blank)

Award Number: W81XWH-08-1-0660

TITLE: TPD52: A Novel Vaccine Target for Prostate Cancer

PRINCIPAL INVESTIGATOR: Robert K. Bright, Ph.D.

CONTRACTING ORGANIZATION: Texas Tech University Health Science Center
Lubbock, TX 79430-6591

REPORT DATE: September 2009

TYPE OF REPORT: Annual

PREPARED FOR: U.S. Army Medical Research and Materiel Command
Fort Detrick, Maryland 21702-5012

DISTRIBUTION STATEMENT: (Check one)

√ Approved for public release; distribution unlimited

□ Distribution limited to U.S. Government agencies only;
report contains proprietary information

REPORT DOCUMENTATION PAGE

Form Approved
OMB No. 0704-0188

1. REPORT DATE *(DD-MM-YYYY)*	2. REPORT TYPE	3. DATES COVERED *(From - To)*
01-09-2009	Annual	1 Sept 2008-31 Aug 2009

4. TITLE AND SUBTITLE

TPD52: A Novel Vaccine Target for Prostate Cancer

5a. CONTRACT NUMBER
W81XWH-08-1-0660

5b. GRANT NUMBER
PC073585

5c. PROGRAM ELEMENT NUMBER

6. AUTHOR(S)
Robert K. Bright, Ph.D.
Email: robert.bright@ttuhsc.edu

5d. PROJECT NUMBER

5e. TASK NUMBER

5f. WORK UNIT NUMBER

7. PERFORMING ORGANIZATION NAME(S) AND ADDRESS(ES)
Texas Tech University Health Sciences Center, Lubbock, Texas, 79430-6591

8. PERFORMING ORGANIZATION REPORT NUMBER

9. SPONSORING / MONITORING AGENCY NAME(S) AND ADDRESS(ES)
U.S. Army Medical Research and Materiel Command Fort Detrick, Maryland 21702-5012

10. SPONSOR/MONITOR'S ACRONYM(S)

11. SPONSOR/MONITOR'S REPORT NUMBER(S)

12. DISTRIBUTION / AVAILABILITY STATEMENT
Approved for public release; distribution unlimited

13. SUPPLEMENTARY NOTES

14. ABSTRACT
As outlined in our approved statement of work, the goals of this Award are to test the efficacy of TPD52-based vaccines in the TRAMP murine model of prostate cancer, and to characterize vaccine induced mechanisms of tumor immunity. Specifically, we have begun to evaluate the ability of TPD52-DNA-based vaccines given intramuscularly to induce immune responses capable of rejecting the formation of subcutaneous tumors following challenge with TRAMP-C1 or TRAMP-C2 tumor cells. Over the past 12-18 months we have made the following significant findings or accomplishments; First, DNA vaccines encoding the human orthologue of TPD25 (hD52) induced increased protection from tumor challenge compared to murine TPD52 (mD52) DNA vaccines suggesting the xenogeneic antigen may be more immuno-potent. Second, TPD52-DNA vaccines administered intramuscularly appear to be less effective than TPD52-DNA vaccines admixed with soluble GMSCF protein administered subcutaneously. Our recent work in other murine tumor models suggests that protein-based TPD52 vaccines may be more effective than DNA-based TPD52 vaccines. To prepare to address this in the TRAMP prostate tumor model we established efficient, reliable methods for generating and purifying both murine and human TPD52 recombinant protein for future xenogeneic, prime-boost vaccine studies.

15. SUBJECT TERMS
Human tumor protein D52 (hD52); murine tumor protein D52 (mD52); transgenic adenocarcinoma mouse prostate (TRAMP); xenogeneic antigen

16. SECURITY CLASSIFICATION OF:			17. LIMITATION OF ABSTRACT	18. NUMBER OF PAGES	19a. NAME OF RESPONSIBLE PERSON
a. REPORT	b. ABSTRACT	c. THIS PAGE			USAMRMC
U	U	U	UU	58	19b. TELEPHONE NUMBER *(include area code)*

Table of Contents

Introduction

Anti-cancer vaccines targeting self-proteins or auto-antigens have been applied to treat or prevent multiple cancers in preclinical studies and clinical trials [1, 2]. Tumor protein D52 (TPD52) is a novel and potentially important tumor associated auto-antigen (TAA) due to its' over expression in a number of fatal and common cancers to include prostate [3, 4, 5], breast [6, 7, 8, 9] and ovarian [10] carcinomas. Recent studies have identified TPD52 as one of 12 important markers, along with MUC-1 and PSA, that can be used as a molecular fingerprint of human prostate cancer enabling more accurate and sensitive diagnosis and prognosis of aggressive disease [11]. Our laboratory independently identified and cloned TPD52 from human prostate cancer cells, isolated from patients undergoing radical prostatectomy, using differential gene expression analysis of our novel paired cancer and normal human prostate epithelial cell cultures. The human orthologue of TPD52 has been identified as a candidate breast cancer TAA by using sera from breast cancer patients to screen a library of expressed genes from breast cancers, demonstrating that TPD52 is capable of inducing IgG antibodies which would have required induction of T cell help [12]. This report suggests that TPD52 may be immunogenic in humans and also capable of inducing a cellular immune response, thus warranting study of TPD52 as an anti-cancer vaccine to induce cellular immunity. The murine orthologue of *TPD52* (m*D52*) naturally mirrors h*D52* with respect to known function and over-expression in tumor cells, and shares 86% protein identity with the human orthologue [13]. Recently we demonstrated that transfection and stable expression of *mD52* cDNA in mouse 3T3 fibroblasts (3T3.mD52) induced increased proliferation, anchorage independent cell growth, and the ability to form subcutaneous tumors and spontaneous lethal lung metastases *in vivo* when 3T3.mD52 cells were inoculated subcutaneously into naïve, syngeneic, immuno-competent mice [14]. Together, these data strongly suggest that *TPD52* expression may be important for initiating and perhaps maintaining a tumorigenic and metastatic phenotype and thus may be important for tumor cell survival. Moreover, we recently demonstrated, for the first time, that mD52 is immunogenic when administered as recombinant protein-based vaccine admixed with CpG/ODN in mice. The immune response generated was capable of rejecting tumor cells that naturally over-express mD52 protein without inducing harmful autoimmunity [15]. These data suggest that hD52 protein may also be a potent vaccine antigen that could be administered to patients to treat or prevent cancers that over express *hD52*.

Reported herein we describe our initial efforts to evaluate DNA based, intramuscular vaccination targeting TPD52 in a murine model of prostate cancer. Briefly, we compared immunization with mD52-DNA to immunization with hD52-DNA as a xeno-antigen and assessed induction of anti-tumor immunity *in vivo*. In addition, we evaluated the efficacy of xenogeneic prime-boost vaccine strategies involving immunizing first with mD52-DNA followed by hD52-DNA or the reverse and assessed the induction of anti-tumor immunity *in vivo*. The present study was undertaken to further investigate the potential of targeting TPD52 in tumors through active vaccination.

BODY

The following research efforts reflect the ten month period from November 1, 2008 through August 30, 2009. Funding was not made available to our laboratory to begin ordering animals and supplies until October 13, 2008. In an effort to quickly begin addressing the goals of the proposal, in light of the loss of nearly two months time, we chose to use the pcDNA3.1 plasmid DNA constructs encoding the full length human or mouse orthologue cDNAs of TPD52 that were in hand, previous confirmed and immediately ready for vaccine studies. Our efforts to use the vaccine approved plasmid DNA vector, pVax, as stated in the original statement of work, will be described following our discussion of our initial DNA vaccine experimental efforts. It should be noted, however, that pVax was derived from pcDNA3.1, and is essentially the exact same vector excluding the G418 selection marker present in pcDNA3.1.

Research Accomplishments

Our initial experiments to address intramuscular administration of TPD52-DNA as a vaccine to induce immunity against TRAMP tumor cells that naturally over-express TPD52 protein, we immunized groups of male C57BL/6 mice with plasmid DNA encoding either murine TPD52 (mD52) or human TPD52 (hD52) as a xenogenic tumor associated antigen. Our hypothesis was that the ~15% difference in amino acid content between hD52 and mD52 may impart greater immunogenicity to hD52 in mice yet afford the possibility that intramolecular epitope spreading [16] would result in immunity to the native murine form of TPD52 expressed by murine tumor cells. Our rationale was that if our hypothesis were true perhaps the reverse would be true for vaccination of humans with TPD52-DNA. Seventy percent of mice (7/10) immunized with hD52-DNA were capable of long term rejection of TRAMP-C1 tumor cells challenge (Fig.1B and Fig. 2A) whereas only 50% of mice (5/10) immunized with mD52-DNA were protected from TRAMP-C1 tumor cell challenge (Fig.1A and Fig. 2A). Interestingly, mice immunized with mD52-DNA and challenged with TRAMP-C2 tumors were only 40% protected (Fig.1C and Fig. 2B). Both TRAMP-C1 and TRAMP-C2 tumor cells were derived from spontaneous tumors that arose in male TRAMP mice and were found to be tumorigenic *in vivo* when inoculated into naïve, male C57BL/6

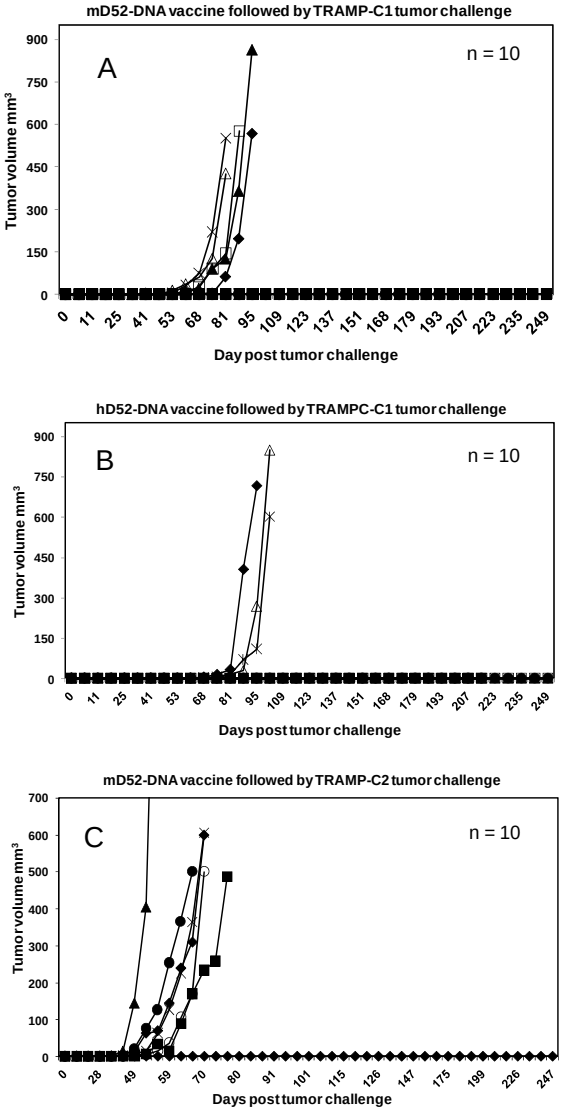

Figure 1. Immunization with TPD52 DNA induces protection against tumor challenge. Groups of male C57BL/6 mice were immunized with 50 micrograms of TPD52-DNA administered i.m. in saline every 10 days for a total of 4 injections. Two weeks after the 4th injection the mice were challenged s.c. with TRAMP-C1 or TRAMP-C2 tumor cells. **A)** Mice were immunized with murine TPD52 (mD52)-DNA and challenged with 5 x 10^6 autochthonous TRAMP-C1 tumor cells (right flank). **B)** Mice were immunized with human TPD52 (hD52)-DNA then challenged with 5 x 10^6 autochthonous TRAMP-C1 tumor cells (right flank). **C)** Mice were immunized with murine TPD52 (mD52)-DNA then challenged with 2 x 10^6 autochthonous TRAMP-C2 tumor cells (right flank). Tumor size was determined by taking perpendicular measurements with calipers every 2 to 3 days and tumor volume (mm^3) was calculated using the following formula: (a x b^2) / 2, where b is the smaller of the two measurements. n = 10 for each group.

immuno-competent mice ($5x10^6$ and $2x10^6$ cells, respectively) [17]. The majority of mice immunized with empty vector plasmid or saline alone developed tumors (Fig. 2). Though we hoped for complete protection from tumor challenge, and feel that mD52-DNA immunization yields results that were more negative than positive, we were encouraged by the results with hD52-DNA as a xenogenic antigen. There are two possibilities contributing to the lack of complete protection that we can address. First, TPD52 is a non-mutated, tumor associated antigen that is expressed by several normal tissues at levels less than observed for malignant cells [14, 15]. Making it by definition a tumor associated auto-antigen and subject to peripheral mechanisms of immune suppression, namely the action of CD25+, Foxp3+ regulatory T cells (Tregs). To address this possibility in future experiments we will *in vivo* deplete CD25+ cells along with TPD52 vaccination by administration of PC61 monoclonal Ab shown to target and deplete CD25+ Tregs in mice. We have recently demonstrated the efficacy of this approach in other murine tumor models (unpublished observation). Second, it is possible that the published tumorigenic doses for TRAMP-C1 and TRAMP-C2 do not represent the minimal tumorigenic dose, making the therapeutic window of efficacy too small to observe positive effects from vaccination. We have begun *in vivo* tumor titration studies to determine the minimal tumorigenic dose, described below.

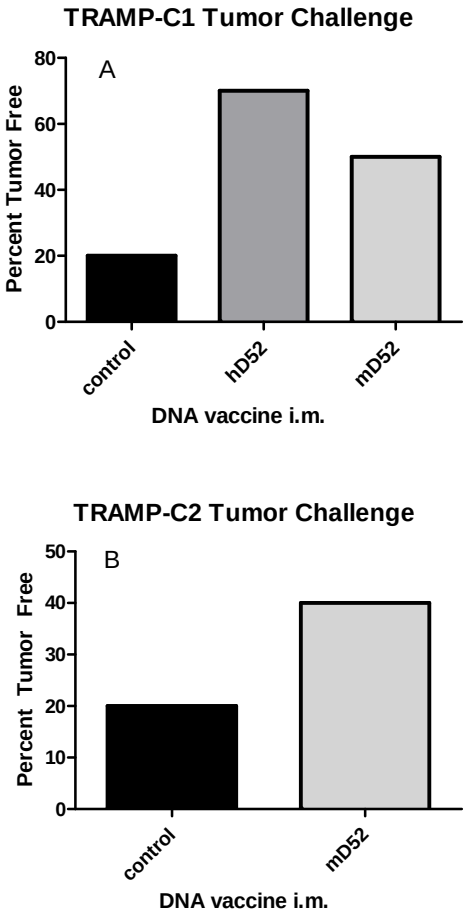

Figure 2. Protection from TRAMP tumor cell challenge following TPD52 immunization. Groups of male C57BL/6 mice were immunized with 50 micrograms of TPD52-DNA administered i.m. in saline every 10 days for a total of 4 injections. Two weeks after the 4th injection the mice were challenged s.c. with TRAMP-C1 or TRAMP-C2 tumor cells. Subcutaneous tumor growth was measured over time and compared for each immunization group as % tumor free mice on day 250 post tumor challenge. **A)** Represents mice challenged with TRAMP-C1 tumor cells. **B)** Represents mice challenged with TRAMP-C2 tumor cells. All control immunizations are shown as a single representative bar graph (control) and include saline alone and empty vector DNA in saline alone.

To further assess the immunopotency of hD52 as a xenogeneic antigen we conducted a prime-boost vaccine study. Mice were primed with either mD52- or hD52-DNA and boosted with the opposite orthologue of TPD52 as a DNA vaccine and challenged with TRAMP-C1 tumor cells. For mice that developed tumors in each group, the time to onset was similar. Interestingly, 7/10 of mice in the group that received hD52-DNA as a boost were protected from tumor challenge (Fig. 3B) compared to 6/10 that were primed with hD52 and boosted with mD52-DNA (Fig. 3A). These data were closer to what we observed for mice immunized with hD52-DNA alone suggesting that a xenogeneic prime-boost approach may be sufficiently immunopotent. For future experiments we will include *in vivo* depletion of CD25+ Tregs along with xenogeneic prime-boost vaccination in an attempt to increase the number of mice protected from tumor challenge.

To address whether long term immunologic memory was developed in mice that were immunized and protected from TRAMP-C1 tumor challenge, we inoculated the survivors with TRAMP-C2 tumor cells in the opposite flank approximately five months (~138 days) after TRAMP-C1 tumor inoculation (not shown). This secondary challenge experiment is ongoing. We anticipate terminating the experiment and evaluating T cell function and specificity in surviving mice by early November 2009. However, a large number of the mice that were immunized with either hD52-DNA alone or boosted with hD52-DNA after being primed with mD52-DNA remain tumor free to date. These data suggest that hD52-DNA immunization may lead to superior long term immunity capable of rejecting mD52 expressing tumors.

Overall our initial efforts to induce tumor immunity following intramuscular TPD52-DNA immunization have been promising. It appears that hD52 may be a more immuno-potent antigen in mice resulting in superior tumor immunity. We predicted this to be so given the success of others involving the application of murine or rodent tumor associated antigens in human clinical trials.

To expand our DNA vaccine efforts to include the clinically approved plasmid vector pVax we subcloned the full length cDNAs for both mD52 and hD52 from the pcDNA3.1 plasmids used for our initial DNA vaccine studies into pVax plasmids. Restriction digestion confirmed the full length cDNAs for mD52 and hD52 were successfully subcloned into pVax (Fig. 4 and Fig. 5, respectively). To further confirm the subclones, PCR with specific primers was performed. PCR amplification of the correct size bands indicated the presence of the corresponding cDNA clone for either mD52 or hD52 (Fig. 6). Finally, the pVax clones were sequenced and the results confirmed the correct orientation and presence of full length cDNAs for each mD52 and hD52 in the pVax vectors (not shown).

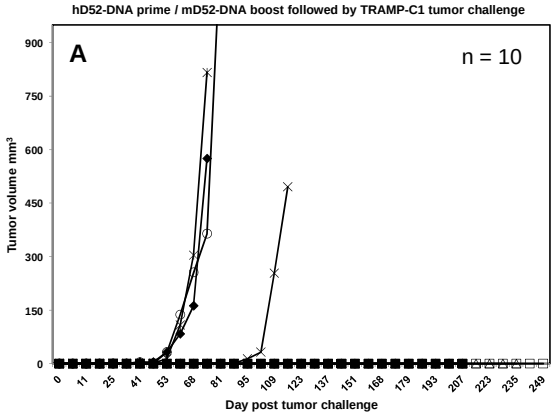

Figure 3. Xenogenic prime-boost Immunization with TPD52 DNA induces protection against tumor challenge. Groups of male C57BL/6 mice were immunized with 50 micrograms of TPD52-DNA administered i.m. in saline every 10 days for a total of 4 injections. Two weeks after the 4th injection the mice were challenged s.c. with TRAMP-C1 tumor cells. **A)** Mice were immunized with human TPD52 (hD52)-DNA twice at 10 day intervals followed by immunization with murine TPD52 (mD52)-DNA twice at 10 day intervals then challenged with 5 x 10^6 autochthonous TRAMP-C1 tumor cells (right flank). **B)** Mice were immunized with murine TPD52 (mD52)-DNA twice and 10 day intervals followed by immunization with human TPD52 (hD52)-DNA twice at 10 day intervals then challenged with 5 x 10^6 autochthonous TRAMP-C1 tumor cells (right flank). Tumor size was determined by taking perpendicular measurements with calipers every 2 to 3 days and tumor volume (mm^3) was calculated using the following formula: (a x b^2) / 2, where b is the smaller of the two measurements. n = 10 for each group.

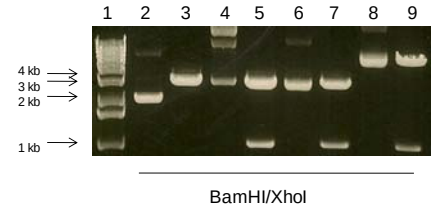

Figure 4. Restriction enzyme digestion of mD52-pVax: Lane1,1kb ladder; lane 2, pVax vector uncut (3kb); lane 3, pVax vector cut BamHI/XhoI (3kb); *lane 4, mD52-pVax1 uncut (4.4kb); lane 5 mD52-pVax1 cut BamHI/XhoI (1.4kb full length mD52 cDNA and 3kb pVax vector); *lane 6, mD52-pVax uncut (4.4kb); lane 7, mD52-pVax cut BamHI/XhoI (1.4kb full length mD52 cDNA and 3kb pVax vector); lane 8, mD52-pcDNA uncut (6.8kb); lane 9, mD52-pcDNA cut BamHI/XhoI (1.4kb full length mD52 cDNA and 5.4kb pcDNA vector). * Two different mini-preps of mD52-pVax plasmid DNA.

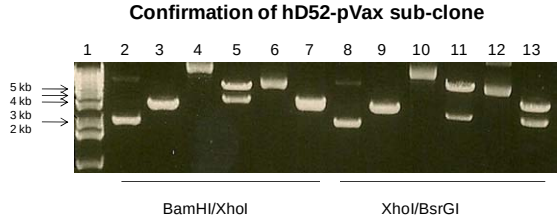

Figure 5. Restriction enzyme digestion of hD52-pVax: Lane 1, 1Kb ladder; lane 2, pVax vector uncut (3kb); lane 3, pVax vector cut BamHI/XhoI (3kb); lane 4, hD52-pcDNA uncut (8.7kb); lane 5, hD52-pcDNA cut BamHI/XhoI (3.3kb full length hD52 cDNA and 5.4kb pcDNA vector); lane 6, hD52-pVax uncut (6.6kb); lane 7, hD52-pVax cut BamHI/XhoI (3.3kb full length hD52 cDNA and 3.0 kb pVax, slight doublet); lane 8, pVax vector uncut (3kb); lane 9, pVax vector cut XhoI/BsrGI (3kb with shift); lane 10, hD52-pcDNA uncut (6.6kb); lane 11, hD52-pcDNA cut XhoI/BsrGI (2.4kB partial hD52, 6.3 (0.9+5.4kb) rest of hD52 with pcDNA vector); lane 12, hD52-pVax uncut (6.6kb); lane 13, hD52-pVax cut XhoI/BsrGI (2.4kB partial hD52, 3.9kb(0.9+3) with pVax vector).

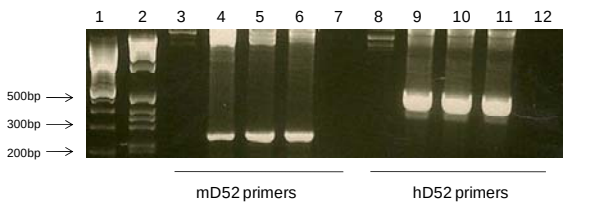

Figure 6. PCR conditions using mD52 primers: 62ºC (annealing temperature), 30 cycles, expected mD52 band= 250bp. Lane 1, 100bp ladder; lane 2, 1kB ladder; lane 3, pVax vector with mD52 primers; *lane 4, mD52-pVax1 with mD52primers; *lane 5, mD52-pVax with mD52 primers; lane 6, mD52-pcDNA with mD52 primers; lane 7, no template (water) with mD52 primers. ***PCR conditions using hD52 primers***: 60ºC (annealing temperature), 30 cycles, expected hD52 band ~500bp. Lane 8, pVax vector with hD52 primers; lane 9, hD52-pVax with hD52 primers; *lane 10, hD52-pcDNA 1 with hD52 primers; *lane 11, hD52-pcDNA with hD52 primers; lane 12, no template (water) with hD52 primers. *Different mini-preps of respective sub-clones.

Western analysis for TPD52 expression from pVAX plasmid constructs

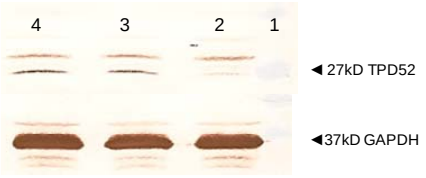

Figure 7. Western blot showing expression of hD52 (lane 4) and mD52 (lane 3) in 3T3 murine fibroblasts following transient transfection (72hrs) with pVAX plasmid encoding full length mD52 or hD52 cDNA: Lane1 is a molecular weight ladder, lane 2 is 3T3 lysate (representative mock transfection), lane 3 is 3T3.pVaxmD52 lysate, lane 4 is 3T3pVaxhD52 lysate. To detect TPD52 protein expression 1ug of TPD52 antibody was added. For GAPDH detection a 1:1000 dilution of antibody was used to probe. For Western analysis method details see appendix reprints.

The mD52 and hD52 pVax clones were tested for the ability to express the respective proteins when transfected into 3T3 fibroblast cells using our previously published methods [14]. Since the pVax vector does not contain a eukaryotic selection marker the transfection experiments were done transiently, with 72 hours determined to be sufficient for optimum protein expression. We previously demonstrated by real-time RT-PCR that 3T3 fibroblasts express detectable amounts of mD52, albeit less than what was detected for tumor cells [14, 15]. Western analysis demonstrated that both pVax.mD52 and pVax.hD52 constructs produced much more protein when transfected transiently into 3T3 fibroblasts than what was detected in mock or non-transfected 3T3 fibroblasts using a rabbit polyclonal IgG antibody specific for TPD52 that cross-reacts with both mD52 and hD52 (Fig. 7). See reference 15 for details on Western analysis using this antibody. Together these data demonstrate that we now have in hand the pVax-DNA constructs coding either mD52 or hD52 making it possible for us to repeat our DNA vaccine studies with the clinically approved DNA vector.

Western analysis of recombinant mD52 protein purification

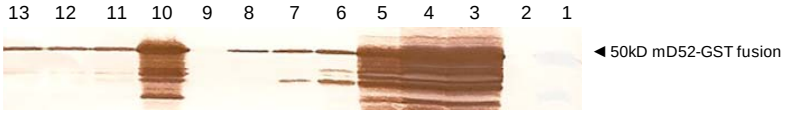

Figure 8. Western blot showing purification of mD52 protein: Lane 1 is a molecular weight ladder, lane 2 is skipped, lane 3 is a sample post lysis of *E. coli* cells expressing mD52 protein, lane 4 is flow through, lane 5 is wash 1, lane 6 is wash 2, lane 7 is wash 3, lane 8 is wash 4, lane 9 is wash 5, lane10 is eluate 1, lane 11 is eluate 2, lane12 is eluate 3, lane 13 is eluate 4. lanes 11-13 represent purified mD52-GST fusion protein. To detect TPD52 protein expression 1ug of TPD52 antibody was added. For Western analysis method details see appendix reprints.

38 Days post tumor inoculation

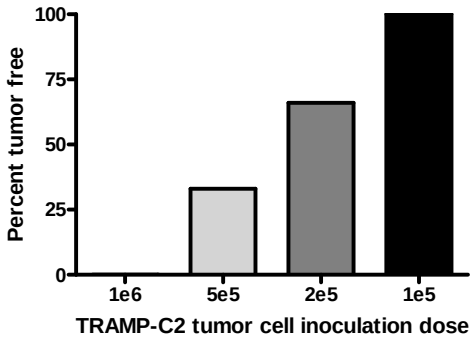

***Figure 9. In vivo titration of TRAMP-C2 tumor cells*.** Groups of male C57BL/6 mice were injected s.c. with varying doses of TRAMP-C1 tumor cells in saline. Tumor cells doses were; $1x10^6$ (1e6), $5x10^5$ (5e5), $2x10^5$ (2e5) and $1x10^5$ (1e5). Tumor size was determined by taking perpendicular measurements with calipers every 2 to 3 days and was calculated using the following formula: $(a \times b^2) / 2$, where b is the smaller of the two measurements. Results are shown as percentage of mice with a tumor on day 38 post tumor inoculation. n = 3 for each group.

In addition to studying the efficacy of DNA-based vaccines coding TPD52 we proposed to study TPD52 protein-based vaccines in the TRAMP model of prostate cancer. The full length cDNAs for mD52 and hD52 were sub-cloned separately into the pGEX-3X bacterial expression vector containing glutathione S-transferase (GST) as a purification tag. Both mD52- and hD52-GST fusion proteins have a molecular weight of approximately twice that of each protein alone (~50kD). We are able to easily generate 5-10 mg of highly purified fusion protein for our vaccines studies as depicted for mD52-GST protein in figure 8. As this report was being finalized we confirmed similar quantities and level of purification for hD52-GST protein as well (not shown). We and others have demonstrated the efficacy of using GST as a carrier to increase the immunogenicity of self or auto-antigens when administered as vaccines in murine tumor models [15, 18]. Together these results suggest we will have similar success in the coming months using protein to induce anti-TPD52 immune responses capable of protecting mice from TRAMP tumor cell challenge.

Finally, in order to ensure a more linear window of vaccine efficacy for tumor rejection we titrated TRAMP-C2 tumor cells in vivo in order to determine the minimal tumorigenic dose. We focused initially on TRAMP-C2 cells since it reportedly take 2.5 times as many TRAMP-C1 cells to form tumors when inoculated *in vivo*. The reported tumorigenic dose for TRAMP-C2 cells is $2x10^6$ cells injected

subcutaneously [17]. We started the titration with $1x10^6$ cells as depicted in figure 9. Thirty eight days following inoculation of tumor cells 100% of mice that were inoculated with $1x10^6$ cells had tumors. In our experience with this tumor model 6-7 weeks is necessary to determine tumor growth *in vivo*. We anticipate that the minimum tumorigenic dose (100% tumor take) for TRAMP-C2 cells will be between $5x10^5$ and $1x10^6$ cells, a dose that is 2-4 times less than what we previously used. These data support our hypothesis that $2x10^6$ tumor cells is too great a tumor burden to see optimal vaccine effects, and suggests that a more empirically determined dose will provide opportunities for testing our vaccine in a treatment scenario as well.

Future Work

In the next few weeks we will perform T cell function assays on survivors from the experiments described in figures 1-3. EliSpot assays for IFN-gamma production will be performed. ELISA based cytokine capture assays for the production of IL-4, IL-10, IL-17 and IFN-gamma will also be performed to assess the role of various T Helper cell subsets, and CTL-mediated killing assays will be performed to demonstrate T cell effector function against tumor cell targets. Details on the specific T cell assay methods can be found in appendix items 2 and 3.

For the upcoming year, we anticipate evaluating protein-based vaccine strategies as well as the pVax-DNA constructs for the ability to induce protective tumor immunity. In addition, we will assess the role of T cell subsets *in vivo* during TPD52 vaccination by administering antibodies to deplete CD4+ or CD8+ T cells (see appendix item 4 for detailed methods). Since TPD52 is an intracellular protein and does not contain membrane anchor motifs, we don't anticipate that specific antibodies will play a role in tumor rejection following TPD52 vaccination. Our previous work with TPD52 vaccines indicates that CD8+ cytotoxic T cells (CTLs) are the main mediators of tumor killing following TPD52 vaccination (appendix items 2 and 3), and will be the focus of our upcoming immune mechanism studies.

KEY RESEARCH ACCOMPLISHMENTS

(the research accomplishments outlined below were completed by a 50% FTE associate, a graduate student and myself at 30% effort)

- We demonstrated that TPD52-DNA vaccines delivered intramuscularly in saline are effective at inducing anti-tumor immunity in the TRAMP model of prostate cancer.
- We demonstrated that the human orthologue of TPD52 (hD52) delivered as a DNA-based vaccine is more effective at inducing protective tumor immunity than murine TPD52 (mD52) in the TRAMP model of prostate cancer.
- Concurrent, related studies, but not supported by this award mechanism, demonstrated that *in vivo* antibody-mediated depletion of CD25+ Treg cells resulted in significant increase in the number of tumor free mice following TPD52 vaccination in a Balb/c, kidney sarcoma model (not shown or discussed in the body). Since this study was undertaken before September 1, 2008 and was supported by institutional funds it was not included in this progress report. However, the findings are novel, significant and support our hypothesis of why our initial DNA-based vaccine studies were less than 100% effective in the TRAMP model. These results will play a critical role in guiding our efforts during year 2 of funding.
- We also demonstrated that TPD52, DNA-based vaccines delivered subcutaneously with soluble GM-CSF as an adjuvant were effective in protecting mice from challenge with TRAMP-C1 tumor cells. This was the first demonstration in the TRAMP model of DNA-based vaccine mediated tumor immunity. This study represents an extension of our original statement of work and was undertaken prior to the award of W81XWH-08-1-0660 in an effort to generate additional proof for future funding. Since this study was undertaken before September 1, 2008 and was supported by institutional funds it was not included in this progress report. These results will play a critical role in guiding our efforts during year 2 of funding. These results can be viewed in appendix item 3.

- In addition to generating data that are critical for our future TPD52-vaccine study design and success, we spent a significant amount of time generating and validating critical vaccine components to include hD52.pVax DNA, mD52.pVax DNA, highly purified recombinant mD52 protein and recombinant hD52 protein. The pVax vectors are FDA approved for trial in humans and along with the recombinant proteins are critical for addressing the majority of our tasks outlined in the original statement of work. Details on these efforts are provided in the body of this report (see figures 4-8).
- Finally, in order to optimize our therapeutic window following vaccine studies and tumor challenge *in vivo*, we performed tumor cell titrations in naïve mice to determine a minimal tumorigenic dose for TRAMP tumor cells. This has not been previously reported. Early indications from our data suggest that the "common" dose used by others and reported in the literature [see reference 17] is 2-4 times greater than what is necessary to obtain 100% tumor take in unprotected mice. This information will be important for our ongoing vaccine studies and useful to others working with the TRAMP model of prostate cancer.

REPORTABLE OUTCOMES

We anticipated that our reportable outcomes for year one of funding will be less than subsequent years and beyond the termination of funds in year three. This is due to the time it takes for TRAMP tumor cells to grow *in vivo* and the amount of time it takes to publish peer reviewed data. However, we have published novel findings supported by other funds that are critical for the future progress and success of our project supported by award W81XWH-08-1-0660.

Manuscripts: (see appendix)

Presentations:

(Data presented was generated with institutional funds prior to award of W81XWH-08-1-0660, but is critical to and in support of the work proposed in award W81XWH-08-1-0660. Presenter is in bold)

- Lewis JD, Payton LA, De Riese W, Byrne JA and **Bright RK**. Memory and Cellular Immunity Induced by a DNA Vaccine Encoding Self Antigen TPD52 Administered with Soluble GM-CSF. Cancer Immunology and Immunotherapy: realizing the promise. NIH/NCI, Bethesda, MD 2008
- Department of Urology, TTUHSC, Grand Rounds. **Bright RK.** "TPD52: a novel vaccine target for prostate cancer." February 15, 2008
- Hollings Cancer Center, Medical University of South Carolina. **Bright RK.** "Mining Immunogens in Tumors: targeting self to kill cancer?" June 10, 2008
- Pfizer Cancer Vaccine Center, LaJolla, CA. **Bright RK.** "Mining Immunogens in Tumors: targeting self to kill cancer" January 15, 2009

Degrees:

- Heather Schultz with defend her master thesis entitled: "Vaccination against the Self-Tumor Associated Antigen Tumor Protein D52 (TPD52)", October 2009. I served as Mrs. Schultz's mentor for her research. Though she was supported by institutional funds her thesis work was directly related to our proposed studies in the TRAMP model and will be included in future progress reports.

Funding applied for in year 2:

(No funding was applied for in year 1. The following are proposal to be submitted during year 2 of funding that are supported by findings from year 1 research accomplishments. The following are "either or" submissions but do not overlap in any way with our current funding, specifically award W81XWH-08-1-0660)

- Cancer Prevention Research Institute of Texas (CPRIT); to be submitted 10/08/09; Robert Bright (PI); "Induction of Immunity to Tumor Associated Auto-Antigens"; total direct costs: $450,000

- National Cancer Institute; NIH 1 RO1; to be submitted 02/05/10; Robert Bright (PI); "Induction of Immunity to Tumor Associated Auto-Antigens"; 30% effort; total direct costs: $1,250,000

CONCLUSIONS

Overall our initial efforts to induce tumor immunity following intramuscular TPD52-DNA immunization have been promising. It appears that hD52 may be a more immuno-potent antigen in mice resulting in superior tumor immunity. We predicted this to be so given the success of others involving the application of murine or rodent tumor associated antigens as xenogeneic vaccines in human clinical trials. We will explore this further in year 2, along with immune mechanism studies outlined as task 2 in our original statement of work. In TPD52 immunize mice that were protected from tumor challenge we saw no evidence for the development of auto-immuity, this supports our previously published findings (see appendix item 2).

In concurrent, independently supported studies we determined that CD25+ Treg cells do play a role in inhibiting TPD52-based immunity following vaccination, this was expected given that TPD52 is a novel, classic, tumor associated-auto-antigen. These data are critical for guiding and driving our efforts in year 2. In addition, we demonstrated for the first time that TPD52-DNA delivered subcutaneously with GM-CSF as an adjuvant induced anti-tumor immunity in the TRAMP model (see appendix item 3). Although these studies were undertaken prior to our receiving funding under award W81XWH-08-1-0660, the findings are important and will be critical for guiding and driving our efforts in year 2 as well.

Relevance "So What":

TPD52 is involved in the induction of transformation and metastasis and has been shown by us and other investigators to be over expressed in human prostate, breast, lung, ovarian and colon cancers. Recent studies have identified TPD52 as one of twelve important protein markers, along with MUC-1 and PSA, that can be used as a molecular fingerprint of human prostate cancer enabling more accurate and sensitive diagnosis and prognosis of aggressive disease. Our preliminary data suggest that TPD52 vaccination induces immunity capable of rejecting tumors in vivo without evidence of the induction of autoimmunity or other harmful side effects. We believe the results generated by our research will demonstrate that TPD52 is capable of inducing tumor immunity when administered as a vaccine, and that this immunity will specifically destroy prostate tumor cells.

TPD52-based vaccines defined and characterized by this study could be clinically developed to treat advanced cancer or for preventing progression and metastasis. Recombinant TPD52 protein and/ or synthetic peptide(s) could be used to stimulate and expand T cells from patients ex vivo for therapeutic transfer back to the patient as adoptive cell therapies (ACT). All these vaccine approaches are relatively easy to generate making the cost much less than other immunotherapy approaches such as dendritic cell (DC)-based vaccines. DNA, protein and peptide vaccines have already proven to have little to no toxicity in patients when studied in clinical trials, making these approaches very safe.

References

1. Gilboa E. (2004) The promise of cancer vaccines. Nat Rev Cancer 4:401-411.
2. Lewis JD, Reilly BD and Bright RK. (2003) Tumor associated antigens: from discovery to immunity. Int Rev Immunol 22:81-112.
3. Wang R, Xu J, Saramaki O, Visakorpi T, Sutherland WM, Zhou J, Sen B, Lim SD, Mabjeesh N, Amin M, Dong JT, Petros JA, Nelson PS, Marshall FF, Zhau He and Chung LW. (2004). *PrLZ*, a novel prostate-specific and androgen-responsive gene of the TPD52 family, amplified in chromosome 8q21.1 and overexpressed in human prostate cancer. Cancer Res. 64, 1589–1594.
4. Wang R, Xu J, Mabjeesh N, Zhu G, Zhou J, Amin N, He D, Marshall FF, Zhau He and Chung LW. (2007). PrLZ is expressed in normal prostate development and in human prostate cancer progression. Clin. Cancer Res. 13: 6040-6048.
5. Rubin MA, Varambally S, Beroukhim R, Tomlins SA, Rhodes DR, Paris PL, Hofer MD, Storz-Schweizer M, Kuefer R, Fletcher JA, Hsi BL, Byrne JA, Pienta KJ, Collins C, Sellers WR, and Chinnaiyan AM (2004). Overexpression, Amplification and Androgen-regulation of TPD52 in Prostate Cancer. Cancer Res. 64: 3814-3822.
6. Balleine RL, Fejzo MS, Sathasivam P, Basset P, Clarke CL and Byrne JA. (2000). The hD52 (TPD52) gene is a candidate target gene for events resulting in increased 8q21 copy number in human breast carcinoma. Genes Chromosom Cancer 29: 48-57.
7. Byrne JA, Tomasetto C, Granier JM, Rouyer N, Mattei MG, Bellocq JP, Rio MC and Basset P. (1995). A screening method to identify genes commonly overexpressed in carcinomas and the identification of a novel complementary DNA sequence. Cancer Res. 55: 2896-2903.
8. Pollack JR, Sorlie T, Perou CM, Rees CA, Jeffrey SS, Lonning PE, Tibshirani R, Botstein D, Borresen-Dale AL and Brown PO. (2002). Microarray analysis reveals a major direct role of DNA copy number alteration in the transcriptional program of human breast tumors. Proc. Natl. Acad. Sci. USA. 99: 12963-12968.
9. Shehata M, Bieche I, Boutros R, Weidenhofer J, Fanayan S, Spalding L, Zeps N, Byth K, Bright RK, Lidereau R and Byrne JA. (2008). Nonredundant functions for tumor protein D52-like proteins supports specific targeting of TPD52. Clin Cancer Res. 14: 5050-5060.
10. Byrne JA, Balleine RL, Schoenberg Fejzo M, Mercieca J, Chiew Y-E, Livnat Y, St. Heaps L, Peters G, Byth K, Karlan BY, Slamon DJ, Harnett P, and deFazio A (2005). Tumor Protein D52 (TPD52) is overexpressed and a gene amplification target in ovarian cancer. Int. J. Cancer 117: 1049-1054.
11. Bismar TA, Demichelis F, Riva A, Kim R, Varambally S, He L, Kutok J, Aster JC, Tang J, Kuefer R, Hofer MD, Febbo PG, Chinnaiyan AM and Rubin MA. (2006). Defining aggressive prostate cancer using a 12-gene model. Neoplasia 8: 59-68.
12. Scanlan MJ, Gout I, Gordon CM, Williamson B, Stockert E, Gure AO, Jager D, Chen YT, Mackay A, O'Hare MJ, Old LJ. (2001) Humoral immunity to human breast cancer: antigen definition and quantitative analysis of mRNA expression. Cancer Immunity 1:4-20.
13. Byrne JA, Mattei MG and Basset P. (1996) Definition of the tumor protein D52 (TPD52) gene family through cloning of D52 homologues in human (hD53) and mouse (mD52). Genomics 35:523-532.
14. Lewis JD, Payton LA, Whitford JG, Byrne JA, Smith DI, Yang L and Bright RK. (2007) Induction of tumorigenesis and metastasis by the murine orthologue of tumor protein D52. Mol Cancer Res 5:133-144.
15. Payton LA, Lewis JD, Byrne JA and Bright RK. (2008) Vaccination with metastasis-related tumor associated antigen TPD52 and CpG/ODN induces protective tumor immunity. Cancer Immunol Immunother 57:799-811.
16. Lewis JD, Shearer MH, Kennedy RC and Bright RK. (2005) Surrogate tumor antigen vaccination induces tumor-specific immunity and the rejection of spontaneous metastases. Cancer Res 65:2938-2946.

17. Foster BA, Gingrich JR, Kwon ED, Madias C and Greenberg NM. (1997) Characterization of prostatic epithelial cell lines derived from transgenic adenocarcinoma of the mouse prostate (TRAMP) model. Cancer Res 57:3325-3330.
18. Acres B, Apostolopoulos V, Balloul J-M, Wreshner D, Xing P-X, Ali-Hadji D, Bizouarne N, Kieny MP and McKenzie IFC. (2000) MUC1-specific immune responses in human MUC1 transgenic mice immunized with various human MUC1 vaccines. Cancer Immunol Immunother 48:588-594.

Appendices

1) Lewis et al. Molecular Cancer Research, 2007
2) Payton et al. Cancer Immunology and Immunotherapy, 2008
3) Lewis et al. Cancer Immunology and Immunotherapy, 2009
4) Kennedy et al. Cancer Research, 2003

Induction of Tumorigenesis and Metastasis by the Murine Orthologue of Tumor Protein D52

Jennifer D. Lewis,[1] Laura A. Payton,[1] Jill G. Whitford,[2] Jennifer A. Byrne,[3] David I. Smith,[4] LiBang Yang,[5] and Robert K. Bright[1]

[1]Department of Microbiology and Immunology and the Southwest Cancer Treatment and Research Center, Texas Tech University Health Sciences Center, Lubbock, Texas; [2]Vaccine and Gene Therapy Institute, Oregon Health Sciences University, Portland, Oregon; [3]The University of Sydney Discipline of Paediatrics and Child Health, Childrens Hospital at Westmead, NSW, Australia; [4]Department of Laboratory Medicine and Pathology, Mayo Foundation and Clinic, Rochester, Minnesota; and [5]Division of Gastroenterology, Hepatology, and Nutrition, Department of Pediatrics, University of Minnesota, Minneapolis-St. Paul, Minnesota

Abstract

Expression studies have consistently identified tumor protein D52 (TPD52) overexpression in tumor cells. Murine TPD52 (mD52) shares 86% identity with the human orthologue. To study a possible role for *TPD52* in transformation, 3T3 fibroblasts were transfected with the full-length cDNA for *mD52*. Expression of mD52 was confirmed by reverse transcription-PCR (RT-PCR), real-time PCR, and Western blot analysis compared with 3T3 and vector-transfected 3T3 (3T3.V), and the resultant cell line was designated 3T3.mD52. At 4 weeks, 3T3.mD52 gained a 2-fold increase in growth rate, lost contact inhibition, and exhibited a marked phenotype change. Further characterization revealed an acquired ability for anchorage-independent cell growth. To determine whether 3T3.mD52 had become tumorigenic, naïve, healthy, immunocompetent syngeneic mice were inoculated subcutaneously with varying cell doses. Tumors measuring >1 cm^2 were detected 60 days postinoculation with 3T3.mD52, and a 50% subcutaneous tumor incidence was obtained with as few as 5×10^5 3T3.mD52 cells. Remarkably, when lungs from 3T3.mD52 tumor-bearing mice were analyzed, numerous tumor nodules were observed, ranging from nodules less than 10 to nodules too numerous to count (inoculation with 1×10^5 and 5×10^6 cells, respectively). Further support for the metastatic capacity of 3T3.mD52 was the demonstration that transforming growth factor (TGF)-βR1 (receptor) expression decreased and TGF-β1 secretion increased in 3T3.mD52 compared with 3T3 controls. cDNA microarray analysis showed a gene expression pattern that further supported *mD52*-induced transformation and metastasis. Together, these data suggest that mD52 expression in 3T3 cells initiated cellular transformation, tumorigenesis, and progression to metastasis.

(Mol Cancer Res 2007;5(2):133–44)

Introduction

The human *TPD52* gene family (1) is comprised of four genes, *hD52* or *PrLZ* (2, 3), *hD53* (1, 4), *hD54* (5, 6), *hD55* (7). The first *D52*-like gene to be identified, human *TPD52*(*hD52*), was found to be overexpressed in ~40% of breast carcinomas (2). Subsequent reports have shown that *hD52* is overexpressed in cancers of the lung (8, 9), prostate (3, 10, 11), colon (12), and ovary (13), as well as in B cell malignancies (14). The *hD52* gene has been localized to human chromosome 8q21 (2), a region frequently gained in breast and prostate carcinomas (15-18). It has been reported that *hD52* represents a target for gene amplification in human breast cancer (19), where *hD52* was the first chromosome 8q21 target gene proposed in any cancer type. Additional studies suggest that *hD52* and *hD53* genes encode markers or regulators of cancer cell proliferation (1), suggesting that tumor protein D52 (TPD52) may be important for initiating and perhaps maintaining a tumorigenic and metastatic phenotype. Interestingly, Scanlan et al. (20) identified *hD52* as a breast cancer antigen by screening a library of expressed genes from breast cancers with sera from breast cancer patients, demonstrating that hD52 is capable of inducing immunoglobulin G (IgG) antibodies. This suggests a lack of normal immunologic tolerance to hD52, and that hD52 may be sufficiently immunogenic to be explored as an anticancer vaccine.

The *D52*-like family members encode hydrophilic polypeptides containing between 180 and 200 amino acid residues that include a coiled-coil motif (1, 6). The coiled-coil motif is required for multimer formation and heterologous interaction with other proteins (5, 21-23). A murine orthologue of *TPD52* (*mD52*) has been cloned and, based on the sequence information, is predicted to be 86% identical to TPD52 (1).

Received 8/7/06; revised 12/13/06; accepted 1/2/07.
Grant support: NIH grant CA 77351, grant RPG-00-207-01 from the American Cancer Society, funds from the Southwest Cancer Treatment and Research Center and by a Howard Hughes Medical Institute grant through the Undergraduate Biological Sciences Education Program to Texas Tech University.
The costs of publication of this article were defrayed in part by the payment of page charges. This article must therefore be hereby marked *advertisement* in accordance with 18 U.S.C. Section 1734 solely to indicate this fact.
Note: Supplementary data for this article are available at Molecular Cancer Research Online (http://mcr.aacrjournals.org/).
J.D. Lewis and L.A. Payton contributed equally to this study.
Requests for reprints: Robert K. Bright, Department of Microbiology and Immunology, Texas Tech University Health Sciences Center, 3601 4th Street, MS 6591, Lubbock, TX 79430. Phone: 806-743-4592; Fax: 806-743-2334; E-mail: robert.bright@ttuhsc.edu

doi:10.1158/1541-7786.MCR-06-0245

In the present study, we sought to further explore the role of murine *TPD52* (*mD52*) in cell proliferation, and whether *mD52* may be involved in the transformation of nonmalignant cells. To this end, we stably expressed the full-length complementary DNA (cDNA) of *mD52* in an early version of nontransformed, contact-inhibited 3T3 fibroblasts (24). Transfection of 3T3 cells with *mD52* resulted in increased proliferation, anchorage-independent cell growth, and the ability to form subcutaneous tumors and spontaneous lethal lung metastases *in vivo* when inoculated into naïve, syngeneic, immunocompetent mice.

Results

Expression of mD52 in Transfected 3T3 Cells

To generate a cell line with elevated expression of mD52 protein, Swiss albino 3T3 cells were transfected with pcDNA.*mD52* plasmid containing the full-length cDNA for *mD52*. The resultant cell line was designated 3T3.mD52. Parental 3T3 cells (24) were simultaneously transfected with pcDNA3.1 plasmid to serve as an empty vector control and designated 3T3.V. Forty-eight hours after transfection, 3T3.V and 3T3.mD52 were selected with G418 at increasing concentrations over time until reaching a concentration of 1 mg/mL. Expression of *mD52* mRNA was confirmed by reverse transcription-PCR (RT-PCR) using methods our laboratory previously published (25, 26). Expression of *mD52* was not detected in either the untransfected parental 3T3 cell line or the empty vector control, 3T3.V (Fig. 1A). However, 3T3.mD52 cells expressed *mD52* message detectable by RT-PCR (Fig. 1A). Protein expression of mD52 was confirmed by Western blot analysis using an anti-mD52 antibody. A band of ~27 kDa was observed for the 3T3.mD52 cell line (Fig. 1B). Examination of the 3T3.V empty vector control cell line revealed no detectable levels of mD52 protein expression by Western blot analysis (Fig. 1B).

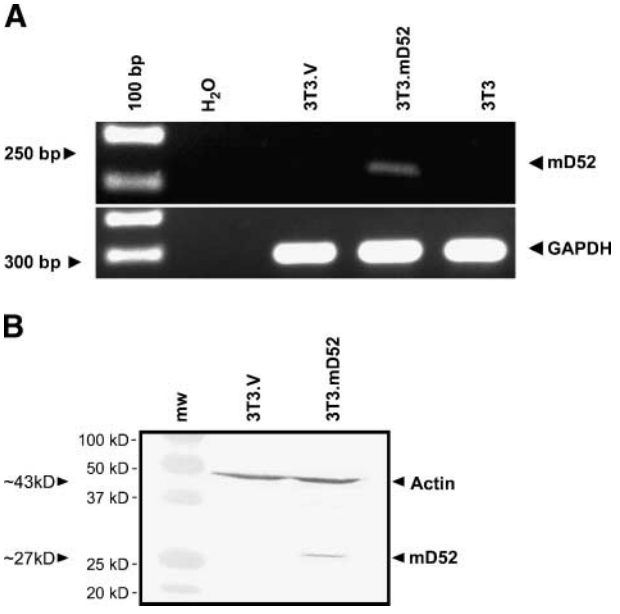

FIGURE 1. Murine TPD52 (mD52) expression in transfected 3T3 cells. **A.** RT-PCR demonstrating *mD52* expression in 3T3 murine fibroblasts following transfection with a plasmid encoding the full-length cDNA for *mD52*. 3T3 and 3T3.V (transfected with empty vector) served as negative controls. *GAPDH* expression served as an internal reference control. **B.** Western blot analysis of murine tumor cell lysates generated from 1×10^8 cell equivalents demonstrating mD52 protein expression using a rabbit polyclonal antibody with specificity for mD52 (~27 kDa). 3T3.V served as a negative control. Actin (~43 kDa) served as a control for protein loading.

To further evaluate the expression of *mD52* by 3T3.mD52 cells, real-time RT-PCR was done Fig. 2A. Consistent with end-point RT-PCR results, only 3T3.mD52 expressed *mD52* at detectable levels at 30 cycles of amplification. The ΔRn for *mD52* expression in 3T3.mD52 at 30 cycles of amplification was >3, compared with nearly 0 for both 3T3 and 3T3.V (Fig. 2A). Similarly, the ΔRn for *mD52* expression in 3T3.mD52 was ~5 by 33 cycles, whereas the ΔRn for *mD52* expression in both 3T3 and 3T3.V was <1 (Fig. 2A). Of note is the observation that the *mD52* cDNA amplification curves for 3T3 and 3T3.V were not significantly different, and that the ΔRn for *mD52* expression in 3T3.mD52 at 31 cycles of amplification (see Fig. 2A, arrow) was 7-fold higher than either 3T3 or 3T3.V at the same time point relative to the respective ΔRn for *GAPDH* expression for the respective cell line at 31 cycles (Fig. 2A, inset). The difference in the amplification curves for real-time RT-PCR and the lack of detection of mD52 protein in 3T3 and 3T3.V show a significant increase in mD52 expression in 3T3.mD52 compared with 3T3 and 3T3.V cells.

mD52 Expression–Induced Transformation of 3T3 Cells

Next, we evaluated whether expression of mD52 protein affected the growth kinetics and morphology of 3T3 cells *in vitro*. 3T3.mD52 grown in complete medium was compared with 3T3 and 3T3.V by plating 5×10^5 cells in 2 mL of complete medium in duplicate wells of a six-well plate, followed by incubation at 37°C for 48 h. Figure 3A represents standard phase contrast micrographs of each cell line. Both 3T3 and 3T3.V exhibited the characteristic broad, flat fibroblast appearance of 3T3 cells, whereas 3T3.mD52 cells exhibited a smaller, rounded morphology typical of rapidly dividing cells (Fig. 3A). Growth kinetics over time was evaluated using a standard, commercially available 3-(4,5-dimethylthiazol-2-yl)-2,5-diphenyltetrazolium bromide (MTT) assay (Fig. 3B). By 48 h, 3T3.mD52 showed increased cell proliferation. The growth rate for 3T3.mD52 after 48 and 72 h was significantly greater ($P < 0.001$) than the growth rates for either 3T3 or 3T3.V (Fig. 3B).

To further assess whether mD52 expression resulted in the transformation of 3T3 cells, we tested the ability of the three cell lines to form foci in soft agar, demonstrating the capacity for anchorage-independent growth and indication of transformation. As expected from the morphology and proliferation data and previously published information (24), neither 3T3 nor 3T3.V were capable of forming colonies in soft agar (Fig. 4A). Strikingly, 3T3.mD52 consistently formed large foci in soft agar visible after 7 to 10 days of culture. 3T3.mD52 had formed >150 (mean of three determinations) large colony foci in 10 microscopic fields compared with less than 10 (mean of three determinations) small clusters of cells for 3T3 and 3T3.V (Fig. 4B). When cultured beyond 10 days, there was no change in 3T3 and 3T3.V, whereas 3T3.mD52 colonies became easily visible to the naked eye. These data indicate that mD52 expression in 3T3 cells confers the ability to grow in an anchorage-independent fashion in soft agar.

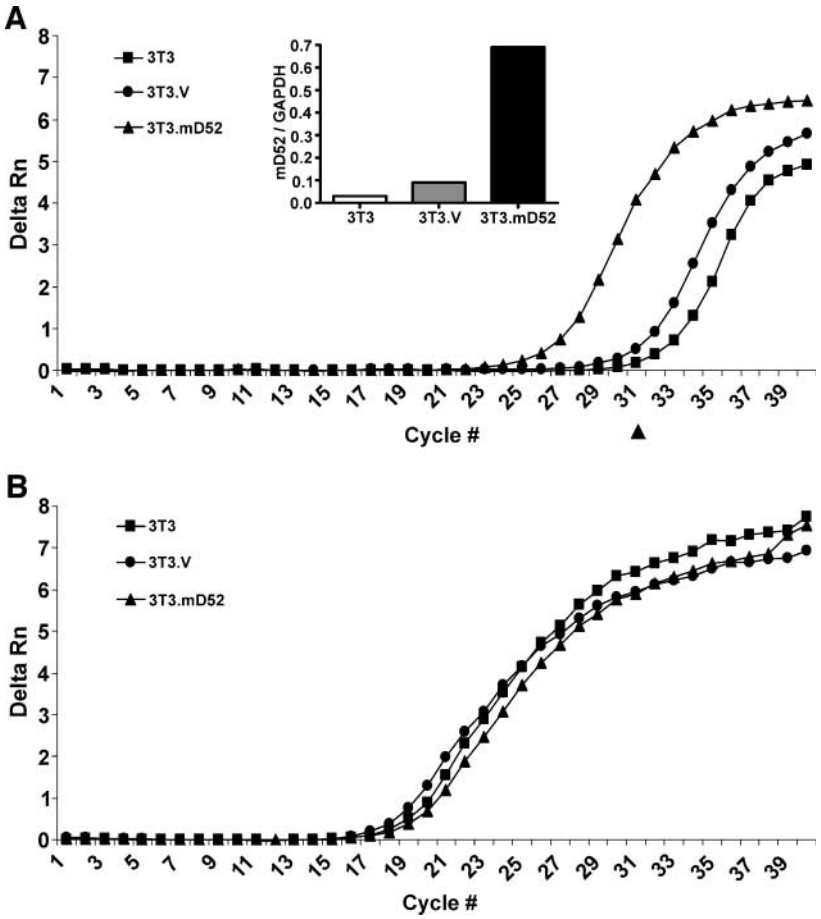

FIGURE 2. **A.** Real-time RT-PCR showing comparative *mD52* expression in 3T3, 3T3.V, and 3T3.mD52 cell lines. Inset, relative expression of mD52 corrected for *GAPDH* levels for a given cell line as determined by real-time RT-PCR for 31 cycles. **B.** Real-time RT-PCR showing comparative *GAPDH* expression as an internal reference control. Representative of three separate experiments.

To determine whether anchorage-independent growth observed for bulk cultures of 3T3.mD52 represented a stable phenotype, individual single cell clones of both 3T3.mD52 and 3T3.V were tested for the ability to form foci in soft agar. Consistent with the results for the bulk parental cell lines, no single cell clones of 3T3.V were capable of anchorage-independent growth, whereas individual single cell clones of 3T3.mD52 formed foci that ranged from 130 to 190 large colony foci in 10 microscopic fields (mean of three determinations; Fig. 4C). When cultured beyond 10 days, there was no change in any 3T3.V clone observed. Similar to what was observed for bulk cultures of 3T3.mD52, colonies of 3T3.mD52 clones became easily visible to the naked eye (data not shown). These data suggest that the transformed phenotype for 3T3.mD52, as assessed by growth in soft agar, is stable.

In vivo *Growth and Spontaneous Metastasis of 3T3.mD52 Cells*

To determine whether 3T3.mD52 cells were capable of *in vivo* growth indicative of tumorigenesis, we inoculated syngeneic, naïve, immunocompetent mice subcutaneously, with 5×10^6 viable 3T3.mD52 cells. Within 37 days of inoculation with 3T3.mD52 cells, 100% of mice ($n = 5$) had a palpable subcutaneous tumor, and by day 60, all tumors had grown near or beyond 1000 mm^3 (Fig. 5A). In repeat experiments, a total of 20 mice were inoculated subcutaneously with 5×10^6 viable 3T3.mD52 cells, and tumors grew with similar kinetics in all 20 animals. Surprisingly, 3T3.mD52 tumor-bearing mice also had lung metastases (Fig. 5B). Figure 5B (a and b) shows representative lungs taken from two individual immunocompetent, syngeneic mice that were bearing tumors 60 days following subcutaneous inoculation with 5×10^6 3T3.mD52 cells. These lungs bore visible lung tumor metastases unlike lungs from uninoculated control animals [Fig. 5B (c)].

In light of these results, we were interested in determining a minimal tumorigenic inoculum for 3T3.mD52 cells in syngeneic, immunocompetent mice. Groups of mice were injected subcutaneously with varying numbers of viable 3T3.mD52 cells, ranging from 1×10^6 to 1×10^5 cells (Fig. 5C). Measurable subcutaneous tumors grew in mice from all the dose groups. Figure 5A (inset) represents a day 39 curve of tumor growth for an inoculum of 5×10^6 3T3.mD52 cells, with the *X*- and *Y*-axes adjusted for direct comparison to tumor growth curves in Fig. 5C. Strikingly, even the lowest subcutaneous inoculation dose (1×10^5 cells) resulted in the generation of spontaneous lung metastases in 25% of animals ($n = 4$) bearing subcutaneous tumors (Fig. 5D). These data suggest that the 50% tumorigenic dose is between 5×10^5 and 1×10^6 3T3.mD52 cells, and a minimal 100% tumorigenic dose is $\sim 1 \times 10^6$ 3T3.mD52 cells. Moreover, these data show that even relatively low-dose subcutaneous inoculation with 3T3.mD52 cells results in spontaneous lung metastases in tumor-bearing animals.

To determine whether the *in vivo* growth ability observed for bulk cultures of 3T3.mD52 represented a stable phenotype, we inoculated syngeneic, naïve, immunocompetent mice subcutaneously with 5×10^6 viable independent single cell clones of 3T3.mD52 cells. Inoculation of mice with 5×10^6 viable independent single cell clones of 3T3.V served as controls. As expected, none of the single cell clones of 3T3.V were capable of subcutaneous growth (Fig. 6D). Interestingly, subcutaneous inoculation of mice with clones of 3T3.mD52 resulted in variable growth patterns that could be divided into three groups: 3T3.mD52 clones that formed progressively growing subcutaneous tumors similar to the bulk 3T3.mD52 cell line (Fig. 6A); 3T3.mD52 clones that formed palpable subcutaneous tumors early that spontaneously regressed over time (Fig. 6B); and 3T3.mD52 clones that failed to form detectable subcutaneous tumors (Fig. 6C). Of note, all 3T3.mD52 clones capable of forming progressively growing subcutaneous tumors also formed spontaneous lung metastases (data not shown) similar to what was observed for the bulk 3T3.mD52 cell line (Fig. 5B). These data suggest that the bulk 3T3.mD52 cell line comprised clones that are aggressively tumorigenic, less tumorigenic, and nontumorigenic.

Induction of TGF-β1 Expression and Secretion in 3T3.mD52 Cells

It is widely accepted that the family of transforming growth factors (TGF), particularly TGF-β1, plays a role in tumorigenesis, metastasis, and immune suppression (27). Immune suppression enables the nascent tumor to escape immune surveillance and subsequent destruction. TGF-β1 is also involved in antiproliferative mechanisms within normal cells where TGF-β1 secreted by a cell binds to its own TGF-β1 receptor and inhibits cell growth in an autocrine manner (28). Expression of both TGF-β1 and TGF-βR1/ALK-5 by 3T3, 3T3.V, and 3T3.mD52 cells was determined by RT-PCR using commercially available primer sets and PCR conditions. Following 35 cycles of RT-PCR amplification, only cDNA from 3T3.mD52 cells produced a detectable TGF-β1 product. TGF-β1 transcripts were not detected in either 3T3 or 3T3.V cells using these PCR conditions and reagents (Fig. 7A, top). Conversely, TGF-βR1/ALK-5 transcript levels were reduced in 3T3.mD52 cells compared with both 3T3 and 3T3.V, which showed similar TGF-βR1 levels (Fig. 7A, middle). Flow cytometry analysis of surface expression of TGF-βR1/ALK-5 protein supported these RT-PCR data (data not shown). To analyze TGF-β1 protein expression and secretion by 3T3.mD52 cells, we did a standard antigen capture ELISA with supernatants from cultured 3T3, 3T3.V, and 3T3.mD52 cells. The amount of secreted TGF-β1 produced by 3T3.mD52 was significantly greater ($P < 0.001$) than either 3T3 or 3T3.V cells at multiple supernatant dilutions (Fig. 7B). This equated to 3T3.mD52 secreting TGF-β1 concentrations of 1,300 pg/mL/24 h and 600 pg/mL/24 h for 1:2 and 1:4 dilutions of the

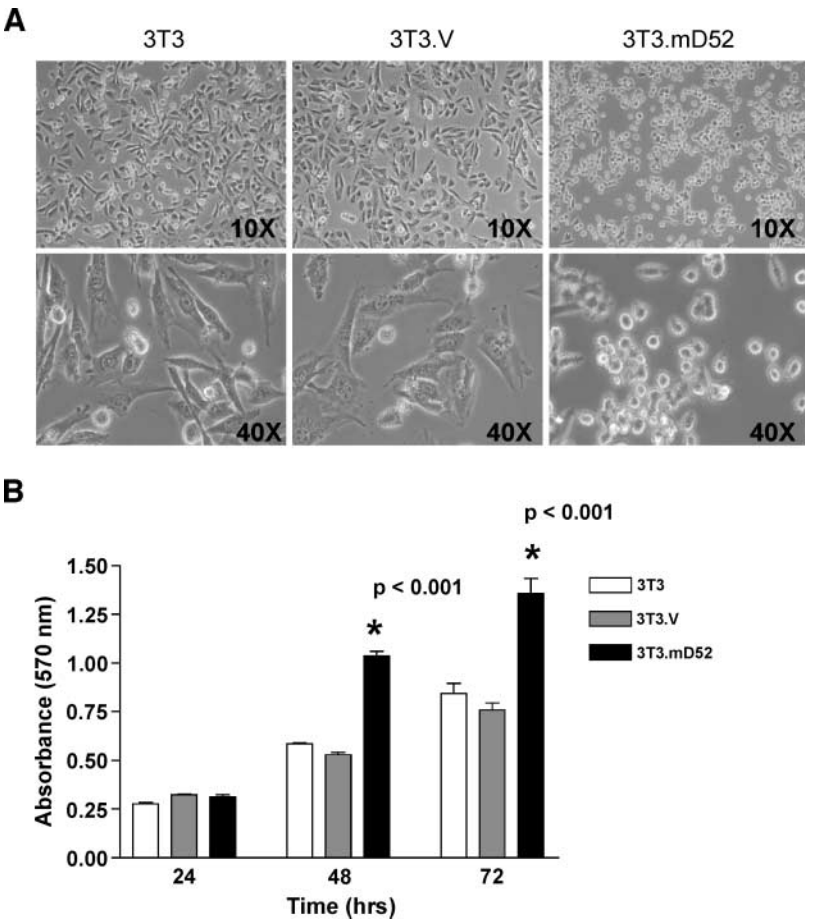

FIGURE 3. Increased *in vitro* proliferation by 3T3.mD52 cells. **A.** Representative phase-contrast photomicrographs at 10× and 40× magnification depicting *in vitro* morphology of 3T3, 3T3.V, and 3T3.mD52. **B.** Cell proliferation was measured at 24-, 48-, and 72-h intervals using a nonradioactive cell proliferation assay (Promega). Statistical analysis at 48 and 72 h showed a significant difference in proliferation rate between 3T3.mD52 and either 3T3 or 3T3.V. *, $P < 0.001$. Columns, mean of triplicate determinations at three time points; bars, SE.

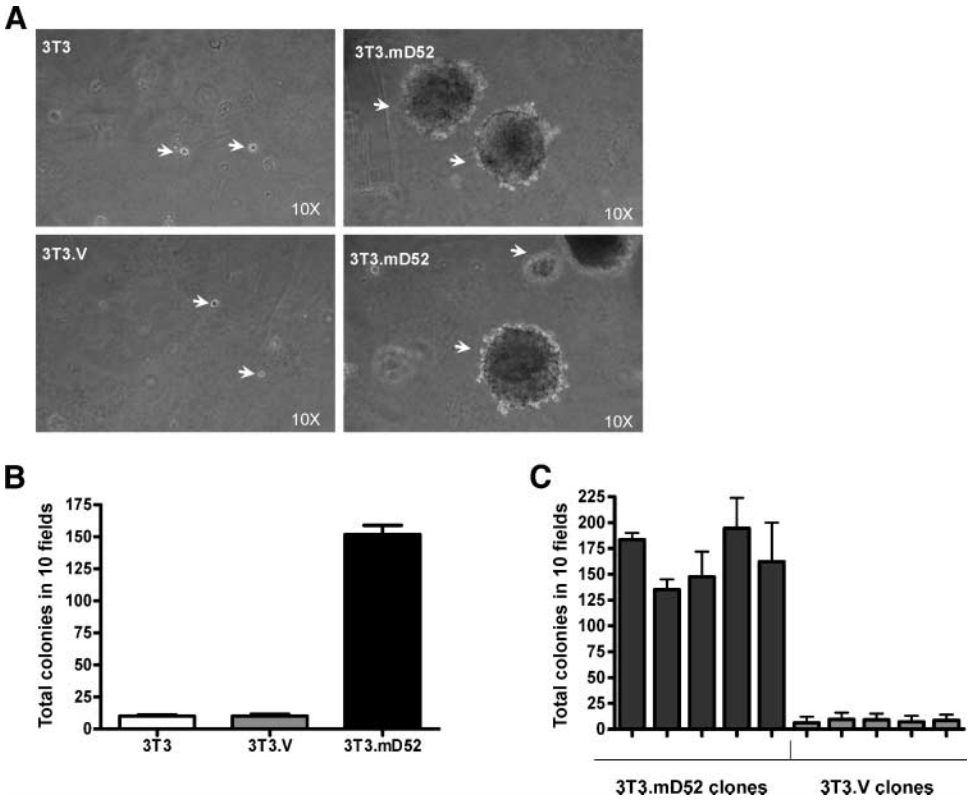

FIGURE 4. mD52 expression in 3T3 cells confers anchorage-independent growth capacity. **A.** Representative phase-contrast photomicrographs (10× magnification) depicting colony formation in soft agar for 3T3, 3T3.V, and 3T3.mD52. Arrows, individual cells for 3T3 and 3T3.V, compared with large colonies for 3T3.mD52. **B.** Total soft agar colony counts for bulk 3T3, 3T3.V, and 3T3.mD52 cell lines were done by three independent investigators microscopically visualizing individual colonies (clusters of 15 or more cells) in 10 random microscopic fields. **C.** Total soft agar colony counts for independent single cell clones of 3T3.mD52 and 3T3.V were done by three independent investigators microscopically visualizing individual colonies (clusters of 15 or more cells) in 10 random microscopic fields. Columns, mean number of colonies in 10 fields as determined by three independent investigators; bars, SE. Representative of three separate experiments.

supernatant, respectively (Fig. 7C). The concentration of TGF-β1 secreted by 3T3 cells was similar to that of 3T3.V cells, and both secreted significantly lower ($P < 0.001$) TGF-β1 concentrations than 3T3.mD52 (Fig. 7C). These data show that expression of mD52 in 3T3 cells produced increased TGF-β1 expression and secretion and reduced TGF-β1 receptor expression.

Analysis of Differential Gene Expression in 3T3.mD52 versus 3T3 Cells

It is unlikely that TGF-β1 alone produced the malignant phenotype and gain of metastatic ability observed in 3T3.mD52 cells. To determine other gene expression changes in 3T3.mD52 cells, we did cDNA microarray analysis. Differential gene expression was assessed by comparing gene expression in 3T3 and 3T3.mD52 cells using the Affymetrix (Santa Clara, CA) GeneChip Mouse Genome 430 2.0 Array, containing over 39,000 transcripts. In addition to a 24-fold increase in *mD52* expression, several genes involved in cancer progression and metastasis showed increased expression in 3T3.mD52 cells (Table 1). Up-regulated genes include the oncogenes *Vav3* (29), *Myc*, and homologue U of *Ras*, as well as adhesion molecules integrin-α3, integrin-α6 (30-32), and lamanin-α5 (*Lama5*; ref. 33). 3T3.mD52 cells also showed 16- and 12-fold increased expression of *cathepsin H* and *cathepsin C*, respectively (Table 1). In addition, the expression of several putative tumor suppressor genes was significantly down-regulated. For example, the expression of *cadherin 2, cadherin 11*, and *protocadherins 7* and *18* showed 155-, 122-, 124- and 8-fold decreases in expression, respectively (Table 1). A 10-fold decrease in expression of *caveolin* was also observed in 3T3.mD52 cells. Decreased expression of *caveolin* has been reported as correlating with cancer progression (34). Tumor-induced generation of new blood vessels or angiogenesis is a critical step in tumor progression and metastasis. *Thrombospondin-2*, implicated in preventing angiogenesis (35), showed a 39-fold decrease in expression in 3T3.mD52 cells compared with 3T3 cells (Table 1). Numerous other genes also showed significant changes in expression in 3T3.mD52 cells (Supplementary Data).

Discussion

To study the effect of *mD52* expression on nontransformed cells, contact inhibited murine 3T3 fibroblasts were transfected with the full-length cDNA for *mD52*. Expression of mD52 was confirmed by RT-PCR and Western blot analysis (Fig. 1), and the resultant cell line was designated 3T3.mD52. At 4 weeks of culture, 3T3.mD52 cells gained a 2-fold increase in growth rate, lost contact inhibition, and exhibited a marked morphologic change (Fig. 3). Further characterization revealed an acquired ability for anchorage-independent cell growth for the bulk 3T3.mD52 cell line and independent single cell clones of 3T3.mD52 (Fig. 4). To determine whether 3T3.mD52 cells were also tumorigenic, naïve, immunocompetent syngeneic mice were inoculated subcutaneously with different doses of 3T3.mD52 cells. Tumors measuring >1 cm^2 were detected 60 days postinoculation with 5×10^6 3T3.mD52, and a 50% subcutaneous tumor incidence could be obtained with as few as

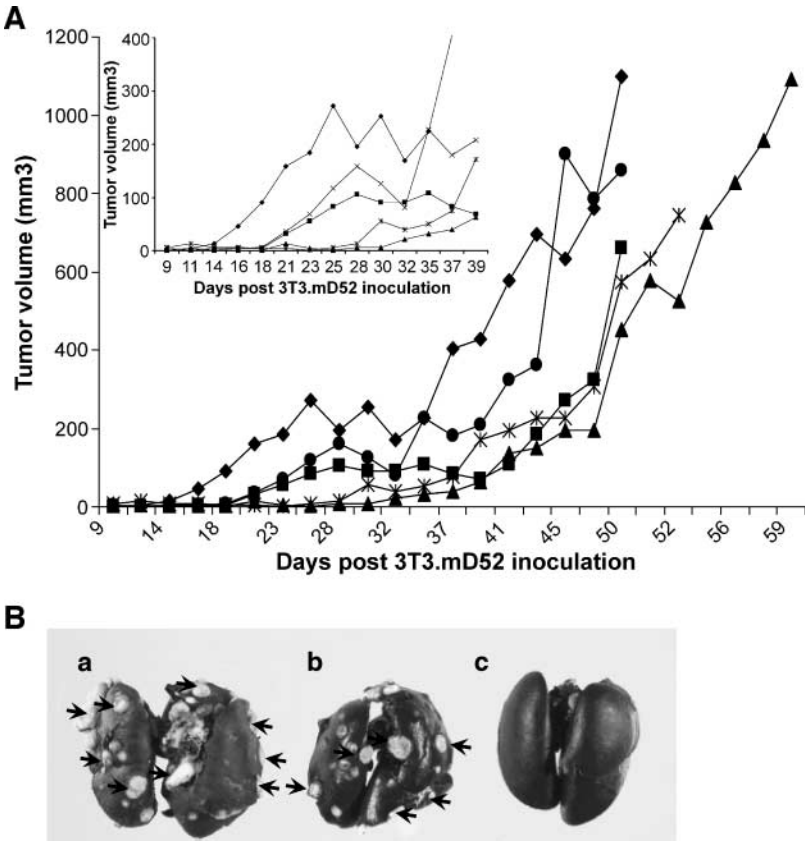

FIGURE 5. *In vivo* growth and spontaneous metastasis of 3T3.mD52 cells. **A.** Naïve, syngeneic, immunocompetent mice were inoculated subcutaneously with 5×10^6 viable 3T3.mD52 cells, and tumor growth was assessed by taking perpendicular measurements. Curves, representative of three independent experiments consisting of five mice for each. Inset, 3T3.mD52 tumor growth curve from Fig. 5A adjusted on the *Y*-axis to a maximum of 400 and the *X*-axis to an end point of 39 d for direct comparison to similar growth curves in Fig. 5C. **B.** Spontaneous 3T3.mD52 lung metastases. Individual mice were sacrificed on day 60 postinoculation with 5×10^6 3T3.mD52 cells, the lungs removed, and injected with India ink to visualize individual tumor nodules; **a** and **b,** arrows, tumor nodules in the lungs from two representative mice; **c,** lungs from a representative control naïve mouse depicting the absence of tumor nodules.

5×10^5 3T3.mD52 cells. Remarkably, when lungs from 3T3.mD52 tumor-bearing mice were analyzed, numerous tumor nodules were observed, with nodules ranging from less than 10 to nodules too numerous to count (inoculation with 1×10^5 and 5×10^6 cells, respectively; Fig. 5D). Interestingly, independent single cell clones of the bulk 3T3.mD52 cell line showed subcutaneous tumor growth patterns that could be divided into three groups: those that formed progressively growing tumor, those that spontaneously regressed over time, and those that failed to grow (Fig. 6A-C, respectively). These data suggest that the bulk 3T3.mD52 cell line comprised clones that are aggressively tumorigenic, less tumorigenic, and nontumorigenic. This differed somewhat from what was expected given that all single cell clones of 3T3.mD52 were capable of anchorage-independent growth (Fig. 4C). In addition, single cell clones of 3T3.mD52 capable of forming progressively growing subcutaneous tumors (Fig. 6A) also formed spontaneous lung metastases (data not shown). Taken together, the data on single cell clones show that the transformed and tumorigenic phenotype was not likely due to a spontaneous event because none of the single cell clones of the vector-transfected cell line 3T3.V were capable of anchorage-independent growth (Fig. 4C) or subcutaneous growth *in vivo* (Fig. 6D). Further support for the metastatic capacity of 3T3.mD52 cells was the demonstration that TGF-β1 secretion increased in 3T3.mD52 cells compared with 3T3 controls (Fig. 7). Finally, cDNA microarray analysis showed a gene expression pattern that further supported *mD52*-induced transformation and metastasis (Table 1; Supplementary Data). Of note, what seemed to be metastases were also observed, by gross visual examination, in the spleens and livers of 3T3.mD52 tumor-bearing mice (data not shown).

Recently, Wang et al. (3) reported the discovery of a novel, prostate-specific, and androgen-responsive *TPD52* isoform *PrLZ*, which was shown to be amplified on chromosome 8q21.1 in human prostate cancer. *PrLZ* was overexpressed in prostate cancer cell lines regardless of androgen receptor status. Similar to *TPD52* and 8q amplification in breast cancer (19), *PrLZ* is the first and possibly only prostate-specific gene associated with 8q amplification in prostate cancer identified to date and may play a role in malignant transformation of normal prostate epithelial cells. A fourth *TPD52*-like gene (*TPD52L3, hD55*) was recently identified in human testis using cDNA microarray (7). *hD55* contains a coiled-coil motif and was shown to interact with *hD52, hD53, hD54*, and itself (*hD55*) in pull-down assays and was determined to be expressed 5.6-fold higher in adult testis compared with fetal testis, suggesting a role for *hD55* in testis development and spermatogenesis. Previously, expression of *hD52* (termed PC-1) in murine NIH3T3 cells [American Type Culture Collection (ATCC; Manassas, VA) CRL-1658] produced increased growth rate, the ability to grow in soft agar, and the ability to form subcutaneous tumors in immune-deficient nude mice (36). In the present study, our data showed the formation of subcutaneous tumors in immunocompetent mice and the gain of metastatic ability in the independent 3T3 cell line (ATCC CCL 92) following the expression of *mD52,* the murine orthologue of *hD52*.

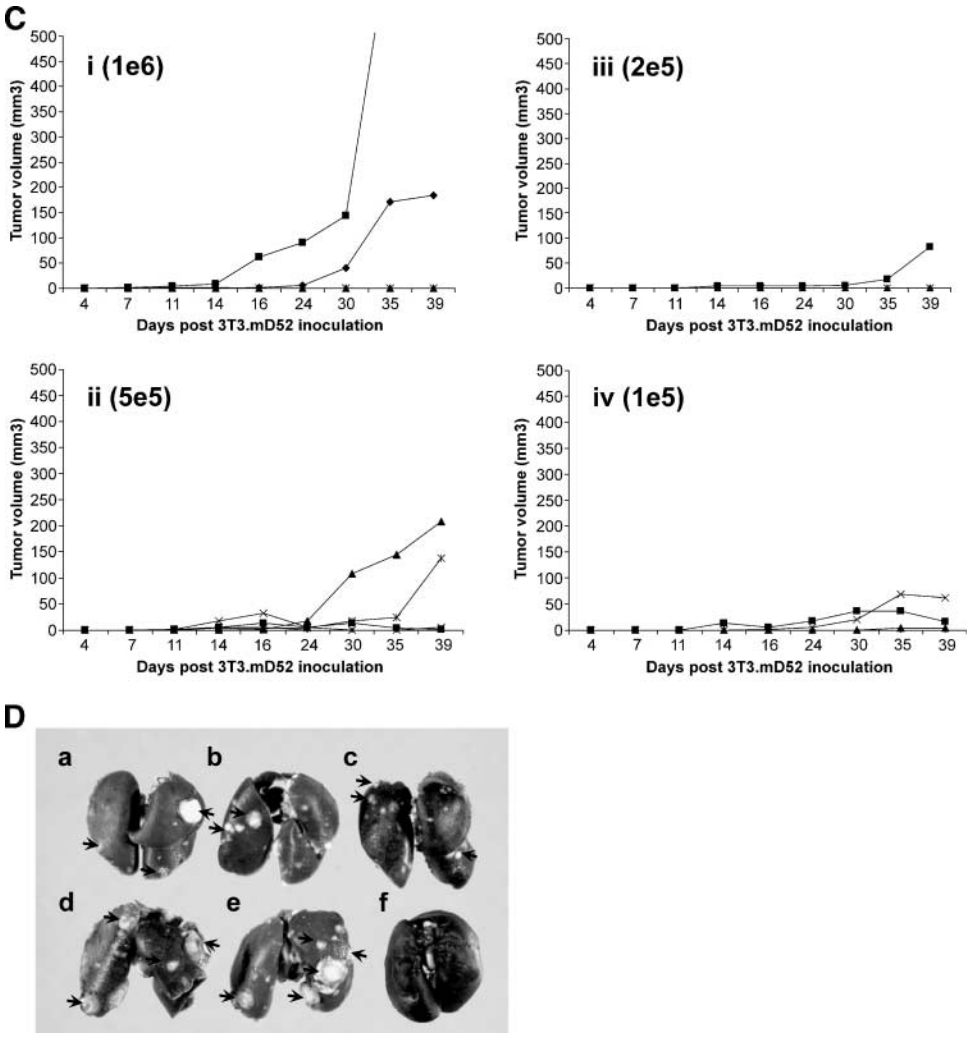

FIGURE 5 *Continued.* **C.** Subcutaneous dose titration of 3T3.mD52 cells and corresponding lung metastases. Naïve, syngeneic, immunocompetent mice were inoculated subcutaneously with varying numbers of viable 3T3.mD52 cells (i, 1×10^6; ii, 5×10^5; iii, 2×10^5; iv, 1×10^5, respectively, as compared with 5×10^6 3T3.mD52 cells, *inset*), and tumor volume was calculated by taking perpendicular measurements. Curves, representative of three independent experiments consisting of four mice for each. **D. a-e,** spontaneous lung metastases corresponding to inoculum doses of 5×10^6, 1×10^6, 5×10^5, 2×10^5, 1×10^5 3T3.mD52 cells, respectively. Arrows, tumor nodules. **f,** representative control naïve mouse lungs with an absence of tumor nodules.

It has been proposed that cancer is the result of a succession of genetic changes that lead to the transformation of normal cells into malignant cells, and that this progression to malignancy involves six essential alterations: self-sufficiency in growth signals, insensitivity to growth-inhibitory signals, evasion of apoptosis, limitless replicative potential, angiogenesis, and tissue invasion and metastasis (37). Others have suggested that the steps in progression to metastasis include additional gained functions of the malignant cell to include embolization, survival in the circulation, arrest, extravasation, evasion of host defenses, and progressive growth at distant sites in the host (37). Regardless of the initiating events and the amount of time needed to progress to metastasis, it is becoming clear that there are genes in which expression seems critical for the generation of a metastatic cell, and that these genes fit into the previously proposed essential alterations and steps toward metastasis (37, 38). Among these genes are those that are up-regulated in 3T3.mD52 cells, including *Vav3* (29), the antiapoptosis gene *CARD10* (39), and *integrin-α3* and *integrin-α6,* two members of the *integrin* family involved in the inhibition of apoptosis, growth stimulation, adhesion, and metastasis (30-32). Several genes that may be important in preventing tumor formation and metastasis were down-regulated in 3T3.mD52 cells, including *caveolin* (34), four members of the *cadherin* gene family (40), specifically *cadherins 11* and *2* and *protocadherins 7* and *18*, as well as the antiangiogenesis gene *thrombospondin 2* (35). The candidate tumor suppressor *Plagl1* (41, 42) was also down-regulated in 3T3.mD52 cells.

In addition to these and other genes (Supplementary Data) that were differentially expressed in 3T3.mD52 cells, we measured an increase in TGF-β1 expression and secretion and a decrease in expression of its receptor (TGF-βR1/ALK-5). Malignant cells often secrete elevated amounts of TGF-β1, which aid in increased invasion and metastasis. It is clear that TGF-β1 can act as both a transformation inhibitor for benign cells and as a progressive factor for malignant transformation, invasion, and metastasis (43-45). In addition, TGF-β1 has shown roles in each of the aforementioned six essential alterations that make up the hallmarks of cancer (37): self-sufficiency in growth signals, insensitivity to growth-inhibitory signals, evasion of apoptosis, limitless replicative potential, angiogenesis, and tissue invasion and metastasis (reviewed in ref. 46). Increased secretion of TGF-β1 in the tumor

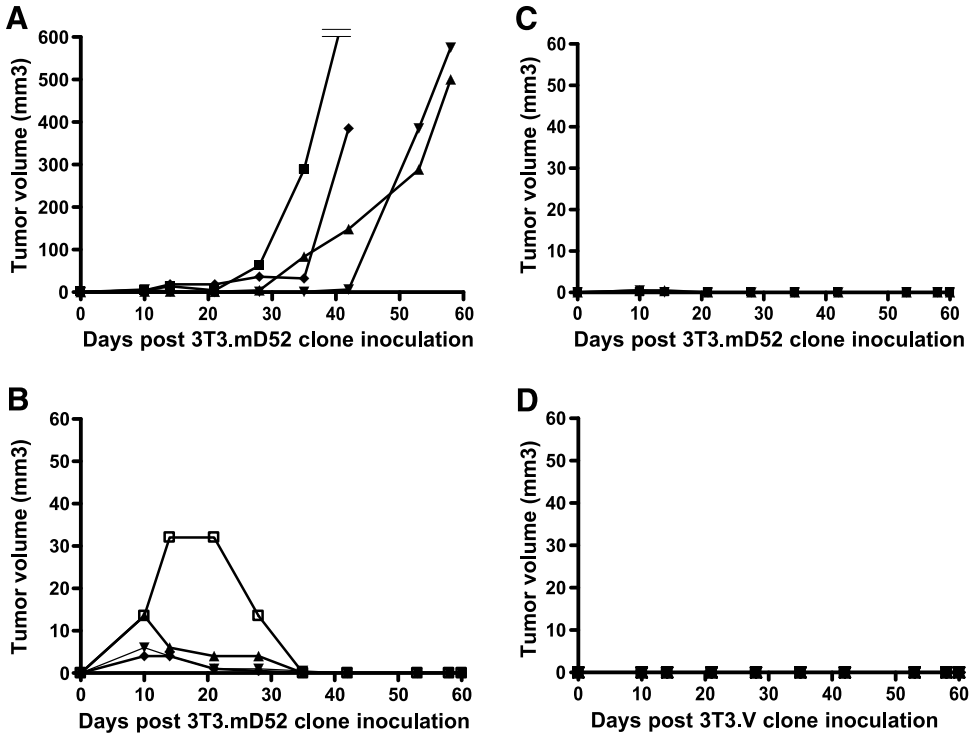

FIGURE 6. Naïve, syngeneic, immunocompetent mice (n = 5) were inoculated subcutaneously with either 5×10^6 viable single cell clones of 3T3.mD52 cells or viable single cell clones 3T3.V cells, and tumor growth was assessed by taking perpendicular measurements. **A.** Representative of four independent 3T3.mD52 single cell clones that formed progressive subcutaneous tumors. **B.** Representative of four independent 3T3.mD52 single cell clones that formed palpable subcutaneous tumors and spontaneously regressed over time. **C.** Representative of four independent 3T3.mD52 single cell clones that failed to form subcutaneously tumors. **D.** Representative of five independent 3T3.V single cell clones that failed to form subcutaneous tumors. Curves, tumor growth curves for individual mice from repeat experiments.

microenvironment has been shown to activate proteases that enable the degradation of the extracellular matrix, enabling invasion and subsequent metastasis (reviewed in refs. 27, 28). Concomitant with increased secretion of TGF-β1 by cancer cells is an observed decrease in expression of receptors for TGF-β1 such as TGF-βR1, which has been shown to lead to increased cancer risk, tumorigenicity, and metastasis in several human cancers to include cancers of the kidney and bladder (47), colon (48), pancreas (49) and prostate (50). The decrease or loss of expression of a TGF-βR is often through mutations that alter its signaling functions (43).

The present study suggests that *mD52* is capable of initiating cellular transformation, tumorigenesis, and progression to metastasis, and that 3T3.mD52 cells may represent a model to study *TPD52* involvement in tumorigenesis and metastasis. Furthermore, the ability of a single gene to produce changes in cell function and behavior supports the importance of *TPD52* and its role in cancer.

Materials and Methods

Subcloning of mD52 *cDNA for Eukaryotic Expression*

Previously, the full-length cDNA encoding *mD52* (1) was cloned into the pTL1 vector and termed pTL1mD52. For eukaryotic expression studies, *mD52* cDNA was first subcloned from pTL1mD52 into pMT/V5-His (Invitrogen Corp., Carlsbad, CA). Next, pMT/V5-His was digested, and the *mD52* cDNA fragment was ligated into the *Eco*RV and *Xho*I site of pcDNA3.1(+) (Invitrogen). The pcDNA.*mD52* clone was confirmed by digesting minipreps with *Bam*HI and *Xho*I (Promega Corp., Madison, WI) and by DNA sequencing (Texas Tech University Molecular Biology core).

Mice and Cell Lines

Female, 6- to 8-week-old BALB/c mice were purchased from the NIH (Frederick, MD). All animals were cared for and treated according to institutional guidelines. Cells were cultured in RPMI 1640 (Fisher Scientific, Pittsburgh, PA) supplemented with 10% heat-inactivated fetal bovine serum, 2 mmol/L L-glutamine, 250 ng/mL Fungizone, 50 IU/mL penicillin, 50 μg/mL streptomycin, 50 μg/mL gentamicin sulfate, and 10 mmol/L HEPES. The 3T3.mD52 and 3T3.V (vector control) cell lines were generated by transfecting parent 3T3 fibroblasts (Swiss albino 3T3 cells that were not immortalized or virally transduced and known to be contact inhibited ATCC CCL 92; ref. 51) with pCDNA3.1 containing the full-length cDNA for *mD52* (pcDNA.*mD52*) or empty pCDNA3.1(+), respectively, using LipofectAMINE Plus reagent (Invitrogen) and methods previously described (25). Forty-eight hours following transfection, 3T3.V and 3T3.mD52 were selected and subsequently maintained in 1 mg/mL G418.

RNA Isolation and RT-PCR Analysis

Total RNA was isolated from 3T3 (negative control), 3T3.V (vector alone), and 3T3.mD52 (*mD52* cDNA transfected) cell lines using the TRIzol reagent (Bio Whittaker, Walkersville, MD), and 1 μg was reverse transcribed to obtain cDNA. *mD52* amplification reactions were carried out using the following primers: *mD52* forward: 5′-TGCTGAAGACAGAGCCGG-3′; and *mD52* reverse: 5′-ACGTCTTGCCACCCTTTG-3′; and previously described PCR conditions for 30 cycles and an annealing temperature of 62°C (26). RT-PCR for the detection of *TGF-β1* and *TGF-βR1/ALK-5* (receptor) was carried out using cDNA generated as described above with commercially

available primers and the manufacturer's recommended annealing temperature (55°C) and cycle number (ref. 36; R&D Systems, Inc., Minneapolis, MN). All PCR reactions were carried out in 50 μL, and the results were visualized on 2% agarose gels containing ethidium bromide. Amplification of glyceraldehyde-3-phosphate dehydrogenase (*GAPDH*) using an annealing temperature of 60°C and 25 cycles served as an internal reference control.

Real-time RT-PCR Analysis

Real-time PCR was done using cDNA samples generated as described above and the ABI Prism 7000 Sequence Detection System and ABI SYBR green PCR core reagents kit according to the manufacturer's instructions (Applied Biosystems, Foster City, CA). PCR conditions for 40 cycles were 50°C for 2 min, 95°C for 10 min, 95°C for 15 s, and an annealing temperature of 62°C for 1 min for *mD52* primers (60°C annealing temperature was used for *GAPDH* control reactions). Additional controls were no template and no enzyme and were included in all real-time PCR reactions.

Western Blot Analysis

The cell lines 3T3.V, 3T3.mD52 were grown to confluency in RPMI supplemented as described above. Cells were harvested and counted, and whole cell protein lysates were prepared at a concentration of 1×10^8 cell equivalents/mL using methods previously described (25). Briefly, 10 μL of lysate were loaded onto a standard SDS-PAGE (4% stacking, 12% resolving) and run at 200 V for 15 min and 150 V for 40 min, followed by electrolytic transfer onto nitrocellulose. The nitrocellulose membrane was blocked for 1 to 2 h at room temperature in 0.0067 mol/L phosphate-buffered NaCl solution/0.02% Tween containing 1% normal goat serum and 1% evaporated milk. To visualize the expression of mD52 protein, the membrane was probed overnight at 4°C with 25 μg/mL of anti-TPD52 polyclonal antibody [generated by immunizing rabbits with NH_2-terminal, carrier-conjugated peptide **GC***AYKKTSETLSQAGQKAS* (italics represents a region of the TPD52 protein that is conserved between human and mouse; Bio Synthesis, Inc., Lewisville, TX). The membrane was simultaneously probed with a 1:500 dilution of polyclonal goat anti-actin antibody (clone I-19, Santa Cruz Biotechnology, Inc., Santa Cruz, CA) to serve as a control reference for protein loading. Following three washes with 0.0067 mol/L phosphate-buffered NaCl solution/0.02% Tween, goat anti-rabbit IgG and rabbit anti-goat IgG horseradish peroxidase–conjugated secondary antibodies were added at 1:1,000 dilutions for 2 h at room temperature. Finally, the membrane was washed and developed with 3,3′-diaminobenzidine reagent as a substrate (Sigma, St. Louis, MO).

Cell Proliferation Assay

Confluent cultures of 3T3, 3T3.V, and 3T3.mD52 cells were harvested and plated in 96-well flat-bottomed plates, in

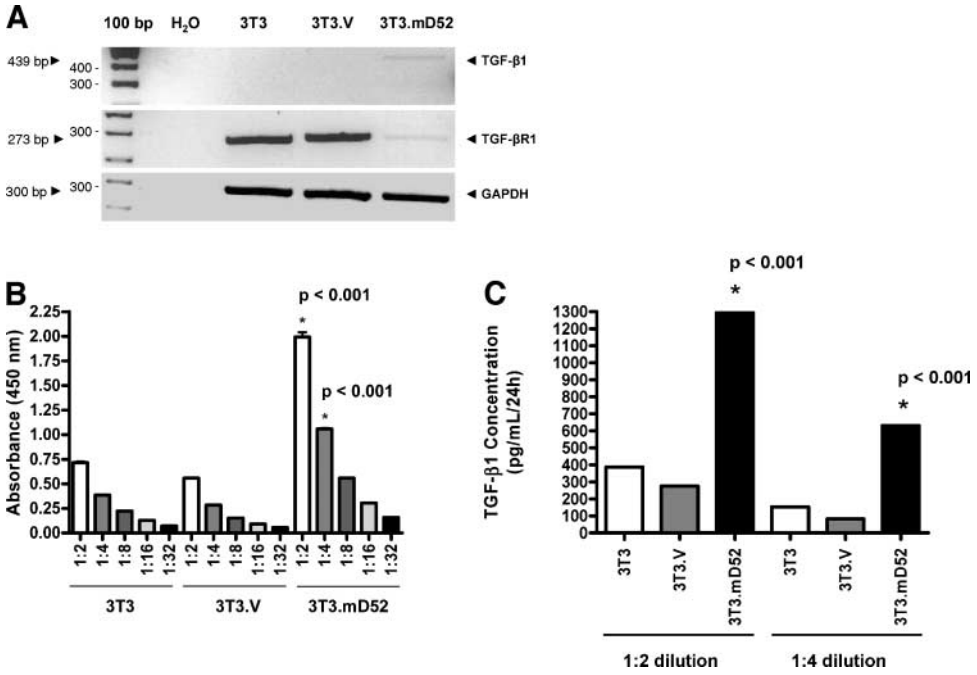

FIGURE 7. TGF-β1 and TGF-βR1 expression in control and transfected 3T3 cells. **A.** Top, RT-PCR demonstrating *TGF-β1* expression in 3T3.mD52 cells. *TGF-β1*–specific primers amplify a 439-bp product from cell line cDNA (R&D Systems). Middle, RT-PCR demonstrating decreased expression of *TGF-βR1* in 3T3.mD52 versus to 3T3 and 3T3.V cells using specific primers (273 bp; R&D Systems). Bottom, *GAPDH* amplification (300 bp) served as an internal reference control. **B.** Quantitative analysis of TGF-β1 secretion by 3T3, 3T3.V, and 3T3.mD52 cells. Cell supernatants were collected and serially diluted for analysis of TGF-β1 by antigen capture ELISA. TGF-β1 was measured and quantified using a Quantikine Mouse/Rat/Porcine TGF-β1 Immunoassay kit (R&D Systems). Statistical analysis showed a significant increase in TGF-β1 secretion by 3T3.mD52 cells compared with 3T3 and 3T3.V cells. *, $P < 0.001$. Columns, mean of duplicate determinations for supernatants from individual cell lines at varying dilutions; bars, SE. **C.** Concentration of TGF-β1 (pg/mL/24 h) secreted by 3T3, 3T3.V, and 3T3.mD52 cells. Statistical analysis showed a significant increase in the concentration of TGF-β1 secreted by 3T3.mD52 compared with 3T3 and 3T3.V cells. *, $P < 0.001$. Representative of three separate experiments.

TABLE 1. Differential Gene Expression by 3T3.mD52 Cells

Gene	Fold Change (Up)	Gene	Fold Change (Down)
mD52	24	*Cadherin 2*	155
Vav3 oncogene	22	*Protocadherin 7*	124
Myc oncogene	20	*Cadherin 11*	122
Cathepsin H	16	*CXCL12*	99
STEAP	15	*Serpinf1*	63
Cathepsin C	12	*Smoc2*	54
CD38	9	*Daf 2*	50
Estrogen R-α	8	*Thrombospondin 2*	39
MAP3K1	7	*Daf 1*	22
Ras homolog U	7	*Gas 6*	18
Rb l1 (p107)	7	*Caveolin*	10
Ephrin B2	6	*Protocadherin 18*	8
Ifld2	14	*Gas2*	11
Card10	8	*Plagl1*	22
Itga3	8	*Ripk3*	9
Itga6	13		
Lama5	6		

NOTE: Partial list of differentially expressed genes in 3T3.mD52 as determined by Affymetrix. GeneChip Mouse Genome 430 2.0 Array containing over 39,000 transcripts. Shown is the fold change up (increased expression) or down (decreased expression) of genes in 3T3.mD52 cells that are reported to be important in tumorigenesis and/or metastasis. For a complete list of differentially expressed genes in 3T3.mD52, see Supplementary Data.

triplicate at 5×10^3 cells per well. Cell proliferation was measured at 24-, 48-, and 72-h intervals using Cell Titer 96 Non-Radioactive Cell Proliferation Assay (MTT based; Promega) according to the manufacturer's instructions. Briefly, cells were incubated at 37°C and 5% CO_2, then 15 μL of the dye solution was added to each well at the above time intervals. Next, 100 μL of stop solution was added to each well, and the plates were incubated at room temperature for 1 h. Finally, absorbance at 570 nm was measured on a Victor3 automated plate reader (Wallac, Perkin-Elmer, Boston, MA).

Single Cell Cloning of Transfected 3T3 Cell Lines

Clonal populations of 3T3 cells transfected with either pCDNA3.1 empty vector (3T3.V) or pCDNA3.1.mD52 (3T3.mD52) were generated to assess transformation *in vitro* and tumorigenicity *in vivo* compared with the bulk parental cell lines using previously published methods (51). Briefly, confluent cultures of the parental 3T3.V and 3T3.mD52 were harvested with trypsin, washed, and counted. Cells were serially diluted to a concentration of 4 to 5 cells/mL in medium and dispensed into five individual 96-well flat-bottomed microculture plates at 200 μL/well. Confluent wells originating from dilutions of <1 cell per well were expanded to 24-well plates and then to T25 tissue culture flasks to ensure enough cells for *in vitro* experiments, *in vivo* inoculation, and cryopreservation.

Assay for Anchorage-Independent Cell Growth

Anchorage-independent growth was determined using a modification of previously described methods (52). Briefly, a base layer of 0.6% agar in complete medium was plated in six-well plates and allowed to solidify (1 mg/mL G418 was added to wells containing 3T3.V, 3T3.mD52 or single cell clones from both 3T3.V and 3T3.mD52). Next, duplicate wells were overlaid with 5×10^4 cells per well in a 0.3% agar. A growth control well was included with 5×10^4 cells in medium alone (no agar) for each cell line. The plates were incubated at 37°C, 5% CO_2 for 10 to 15 days and checked every 2 to 3 days for colony formation. At day 15, individual colonies (defined as clusters of 15 or more cells) were counted in 10 random fields.

In vivo *Tumor Growth*

Naïve female BALB/c mice were inoculated subcutaneously in the right flank with different numbers of viable 3T3.mD52 cells (5×10^6, 1×10^6, 5×10^5, 2×10^5, 1×10^5), and tumor growth was monitored every 2 to 3 days using calipers to measure perpendicular angles. For single cell clones of 3T3.mD52 and 3T3.V, naïve female BALB/c mice were inoculated subcutaneously in the right flank with 5×10^6 viable cells. Tumor volume (mm^3) was calculated using the following formula: $(a \times b^2)/2$, where b is the smaller of the two measurements (25).

Evaluation of Spontaneous Lung Metastases

To analyze tumor metastasis to the lungs, mice were sacrificed, and their lungs removed and injected with India ink to visualize individual tumor nodules as described previously (25). Briefly, an India ink solution was injected through the trachea and allowed to fill the lungs. The lungs were removed and placed in Fekete's solution (70% ethanol, 10% formaldehyde, 5% acetic acid) for destaining. Tumor nodules do not absorb India ink, which results in the normal lung tissue staining black and the tumor nodules remaining white.

ELISA for TGF-β1 Production

To analyze the comparative secretion of TGF-β1, 3T3, 3T3.V, and 3T3.mD52 cell lines were plated in duplicate in 12-well plates at 5×10^5 cells per well. Cells were grown to confluency (~72 h) in complete medium, then washed and incubated for 24 h in medium without serum. After the final incubation, cell supernatants were collected, and like wells were pooled for analysis of TGF-β1 protein secretion by antigen capture ELISA. TGF-β1 was measured and quantified for duplicate determinations using a Quantikine Mouse/Rat/Porcine TGF-β1 Immunoassay kit (R&D Systems), and absorbance at 450 nm was measured on a Victor3 automated plate reader (Wallac, Perkin-Elmer).

Microarray Analysis of Differential Gene Expression in 3T3.mD52 Cells

Quality RNA samples obtained from 3T3 and 3T3.mD52 cells were analyzed using GeneChip Mouse Genome 430 2.0 arrays containing over 39,000 transcripts (Affymetrix). Double-stranded cDNA and biotinylated complementary RNA (cRNA) were synthesized from total RNA and hybridized onto microarrays. The array hybridization, washing, and staining procedures were done according to the manufacturer's protocols. All data used were derived from Affymetrix 5.0 software. GeneChip output files were given as a signal that represents the difference between the intensities of the sequence-specific perfect match probe set and the mismatch probe set or as detection of present, marginal, or absent signals as determined by the program's algorithm. Gene arrays were scaled to an

average signal of 1,500 and then analyzed independently. After raw image DAT data files were initially processed to create CEL files, DNA-Chip analyzer (dCHIP; Version 1.3)[6] was used for data quality checking and high-level analysis. A fold-change analysis was done in which the ratio of the geometric means of the expression intensities of the relevant gene fragments was computed. This ratio was reported as the fold change (up or down). Only genes with differences between 3T3.mD52 and 3T3 control greater than 2.0-fold (90% lower bound) were considered to be differentially expressed in 3T3.mD52 cells.

Statistical Analysis

For microarray analyses, confidence intervals and P values on the fold change were calculated with the use of a two-sided, Welch-modified two-sample t test. P values of 0.01 or less were considered significant. For proliferation and TGF-β1 secretion, one-way ANOVA and Tukey-Kramer multiple comparison tests were done. For ANOVA, P values <0.05 were considered significant. For Tukey-Kramer, if $q > 5.910$, then $P < 0.05$ and is considered significant (GraphPad InStat).

Acknowledgments

We thank Dr. Curt M. Pfarr and Steven C. Platten for imaging assistance.

[6] http://www.dchip.org/

References

1. Byrne JA, Mattei MG, Basset P. Definition of the D52 gene/protein family through cloning of *D52* homologues in human (*hD53*) and mouse (*mD52*). Genomics 1996;35:523–32.

2. Byrne JA, Tomasetto C, Garnier JM, et al. A screening method to identify genes commonly overexpressed in carcinomas and the identification of a novel complementary DNA sequence. Cancer Res 1995;55:2896–903.

3. Wang R, Xu J, Saramaki O, et al. PrLZ a novel prostate-specific and androgen-responsive gene of the TPD52 family, amplified in chromosome 8q21.1 and overexpressed in human prostate cancer. Cancer Res 2004;64:1589–94.

4. Byrne JA, Mattei MG, Basset P, Gunning P. Identification and *in situ* hybridization mapping of a mouse *Tpd52l1* (*D53*) orthologue to chromosome 10A4–2. Cytogenet Cell Genet 1998;81:199–201.

5. Byrne JA, Nourse CR, Basset P, Gunning P. Identification of homo- and heteromeric interactions between members of the breast carcinoma-associated D52 protein family using the yeast two-hybrid system. Oncogene 1998;16:873–82.

6. Nourse CR, Mattei MG, Gunning P, Byrne JA. Cloning of a third member of the D52 gene family indicates alternative coding sequence usage in D52-like transcripts. Biochim Biophys Acta 1998;1443:155–68.

7. Cao Q, Chen J, Zhu L, et al. A testis-specific and testis developmentally regulated tumor protein D52 (TPD52)-like protein TPD52L3/hD55 interacts with TPD52 family proteins. Biochem Biophys Res Commun 2006;344:798–806.

8. Chen S-L, Maroulakou IG, Green JE, et al. Isolation and characterization of a novel gene expressed in multiple cancers. Oncogene 1996;12:741–51.

9. Zhu H, Lam DC, Han KC, et al. High resolution analysis of genomic aberrations by metaphase and array comparative genomic hybridization identifies candidate tumour genes in lung cancer cell lines. Cancer Lett 2006. Epub ahead of print.

10. Dhanasekaran SM, Barrette TR, Ghosh D, et al. Delineation of prognostic biomarkers in prostate cancer. Nature 2001;412:822–6.

11. Rubin MA, Varambally S, Beroukhim R, et al. Overexpression, amplification, and androgen regulation of TPD52 in prostate cancer. Cancer Res 2004;64:3814–22.

12. Malek RL, Irby RB, Guo QM, et al. Identification of Src transformation fingerprint in human colon cancer. Oncogene 2002;21:7256–65.

13. Byrne JA, Balleine RL, Fejzo MS, et al. Tumor protein D52 (TPD52) is overexpressed and a gene amplification target in ovarian cancer. Int J Cancer 2005;117:1049–54.

14. Tiacci E, Orvietani PL, Bigerna B. Tumor protein D52 (TPD52): a novel B-cell/plasma-cell molecule with unique expression pattern and Ca^{2+}-dependent association with annexin VI. Blood 2005;105:2812–20.

15. Kallioniemi A, Kallioniemi OP, Piper J, et al. Detection and mapping of amplified DNA sequences in breast cancer by comparative gemonic hybridization. Proc Natl Acad Sci U S A 1994;91:2156–60.

16. Forozan F, Karhu R, Kononen J, Kallioniemi A, Kallioniemi OP. Genome screening by comparative genomic hybridization. Trends Genet 1997;13:405–9.

17. Cher ML, Bova GS, Moore DH, et al. Genetic alterations in untreated metastases and androgen-independent prostate cancer detected by comparative genomic hybridization and allelotyping. Cancer Res 1996;56:3091–102.

18. Virgin JB, Hurley PM, Cher MP, et al. Isochromosome 8q is associated with 8p loss of heterozygosity in a prostate cancer cell line. Prostate 1999;41:49–57.

19. Balleine RL, Schoenberg Fejzo M, Sathasivam P, Basset P, Clarke CL, Byrne JA. The *D52* (*TPD52*) gene is a candidate target gene for events resulting in increased 8q21 copy number in human breast carcinoma. Genes Chromosomes Cancer 2000;29:48–57.

20. Scanlan MJ, Gout I, Gordon CM, et al. Humoral immunity to human breast cancer: antigen definition and quantitative analysis of mRNA expression. Cancer Immun 2001;1:4–20.

21. Proux V, Provot S, Felder-Schmittbuhl MP, Laugier D, Calothy G, Marx M. Characterization of a leucine zipper-containing protein identified by retroviral insertion in avian neuroretina cells. J Biol Chem 1996;271:30790–7.

22. Chen S-L, Zhang XK, Halverson DO, et al. Characterization of human N8 protein. Oncogene 1997;15:2577–88.

23. Proux-Gillardeaux V, Galli T, Callebaut I, Mikhailik A, Calothy G, Marx M. D53 is a novel endosomal SNARE-binding protein that enhances interaction of syntaxin 1 with synaptobrevin 2 complex *in vitro*. Biochem J 2003;370:213–21.

24. Todaro GJ, Green H. Quantitative studies of the growth of mouse embryo cells in culture and their development into established cell lines. J Cell Biol 1963;17:299–313.

25. Lewis JD, Shearer MH, Kennedy RC, Bright RK. Surrogate tumor antigen vaccination drives determinant spreading, the induction of systemic tumor immunity, and the rejection of spontaneous lung metastases. Cancer Res 2005;65:2938–46.

26. Bright RK, Kimchi ET, Shearer MH, Kennedy RC, Pass HI. SV40 Tag-specific cytotoxic T lymphocytes generated from the peripheral blood of malignant pleural mesothelioma patients. Cancer Immunol Immunother 2002;50:682–90.

27. Siegel PM, Massague J. Cytostatic and apoptotic actions of TGF-β in homeostasis and cancer. Nat Rev Cancer 2003;3:807–20.

28. Derynck R, Akhurst RJ, Balmain A. TGF-β signaling in tumor suppression and cancer progression. Nat Genet 2001;29:117–29.

29. Zeng L, Sachdev P, Yan L, et al. Vav3 mediates receptor protein tyrosine kinase signaling, regulates GTPase activity, modulates cell morphology and induces cell transformation. Mol Cell Biol 2000;20:9212–24.

30. Alghisi GC, Ruegg C. Vascular integrins in tumor angiogenesis: mediators and therapeutic targets. Endothelium 2006;13:113–35.

31. Wilhelmsen K, Litjens SH, Sonnenberg A. Multiple functions of the integrin α6β4 in epidermal homeostasis and tumorigenesis. Mol Cell Biol 2006;26:2877–86.

32. Janes SM, Watt FM. New roles for integrins in squamous-cell carcinoma. Nat Rev Cancer 2006;6:175–83.

33. Miyazaki K. Laminin-5 (laminin-332): unique biological activity and role in tumor growth and invasion. Cancer Sci 2006;97:91–8.

34. Carver LA, Schnitzer JE. Caveolae: mining little caves for new cancer targets. Nat Rev Cancer 2003;3:571–81.

35. Lawler J, Detmar M. Tumor progression: the effects of thrombospondin-1 and 2. Int J Biochem Cell Biol 2004;36:1038–45.

36. Chang X, Liang R, Zhou J, et al. Malignant transformation of NIH3T3 cells induced by ectopic expression of PC-1 gene. Chin J Path 2005;34:42–6.

37. Hanahan D, Weinberg RA. The hallmarks of cancer. Cell 2000;100:57–70.

38. Fidler IJ. The pathogenesis of cancer metastasis: the "seed and soil" hypothesis revisited. Nat Rev Cancer 2003;3:1–6.

39. Wang L, Guo Y, Huang W-J, et al. CARD10 is a novel caspase recruitment domain/membrane associated guanylate kinase family member that interacts with BCL10 and activates NF-κB. J Biol Chem 2001;276:21405–9.

40. Behrens J. Cadherins and catenins: role in signal transduction and tumor progression. Cancer Metastasis Rev 1999;18:15–30.

41. Enlund F, Persson F, Stenman G. Molecular analysis of the candidate tumor suppressor gene, *PLAGL1*, in benign and malignant salivary gland tumors. Eur J Oral Sci 2004;112:545–7.

42. Basyuk E, Coulon V, LeDigarcher A, et al. The candidate tumor suppressor gene *ZAC* is involved in keratinocyte differentiation and its expression is lost in basal cell carcinomas. Mol Cancer Res 2005;3:483–92.

43. Massague J, Blain SW, Lo RS. TGFβ signaling in growth control, cancer and heritable disorders. Cell 2000;103:295–309.

44. Akhurst RJ, Derynck R. TGF-β signaling in cancer—a double-edged sword. Trends Cell Biol 2001;11:S44–51.

45. Bachman KE, Park BH. Duel nature of TGF-β signaling: tumor suppressor vs. tumor promoter. Curr Opin Oncol 2004;17:49–54.

46. Elliot RL, Blobe GC. Role of transforming growth factor β in human cancer. J Clin Oncol 2005;23:2078–93.

47. Chen T, Jackson C, Costello B, et al. An intronic variant of the *TGFBR1* gene is associated with carcinomas of the kidney and bladder. Int J Cancer 2004; 112:420–5.

48. Bian Y, Caldes T, Franken P, et al. TGFBR1*6A may contribute to hereditary colorectal cancer. J Clin Oncol 2005;23:3074–8.

49. Jonson T, Albrechtsson E, Axelson J, et al. Altered expression of TGFB receptors and mitogenic effects of TGFB in pancreatic carcinomas. Int J Oncol 2001;19:71–81.

50. Kim IY, Ahn H-J, Zelner DJ, et al. Loss of expression of transforming growth factor β type I, type II receptors correlates with tumor grade in human prostate cancer tissues. Clin Cancer Res 1996;2:1255–61.

51. Bright RK, Vocke CD, Emmert-Buck MR, et al. Generation and genetic characterization of immortal human prostate epithelial cell lines derived from primary cancer specimens. Cancer Res 1997;57:995–1002.

52. Zalvide J, DeCaprio JA. Role of pRb-related proteins in simian virus 40 large-T–antigen mediated transformation. Mol Cell Biol 1995;15:5800–10.

Cancer Immunol Immunother (2008) 57:799–811
DOI 10.1007/s00262-007-0416-y

ORIGINAL ARTICLE

Vaccination with metastasis-related tumor associated antigen TPD52 and CpG/ODN induces protective tumor immunity

Laura A. Payton · Jennifer D. Lewis · Jennifer A. Byrne · Robert K. Bright

Received: 29 August 2007 / Accepted: 9 October 2007 / Published online: 26 October 2007

Abstract Tumor protein D52 (TPD52) is involved in transformation and metastasis and has been shown to be over-expressed in tumor cells compared to normal cells and tissues. Murine TPD52 (mD52) shares 86% protein identity with the human TPD52 orthologue (hD52). To study TPD52 protein as a target for active vaccination recombinant, mD52 was administered as a protein-based vaccine. Naïve mice were immunized with either mD52 protein and CpG/ODN as a molecular adjuvant or CpG/ODN alone. Two weeks following the final immunization, mice were challenged s.c. with syngeneic tumor cells that over-express mD52. Two distinct murine tumor cell lines were used for challenge in this model, mKSA and 3T3.mD52. Half of the mice immunized with mD52 and CpG/ODN rejected or delayed onset of mKSA s.c. tumor cell growth, and 40% of mice challenged with 3T3.mD52 rejected s.c. tumor growth, as well as the formation of spontaneous lethal lung metastases. Mice immunized with mD52 and CpG/ODN generated detectable mD52-specific IgG antibody responses indicating that mD52 protein vaccination induced an adaptive immune response. In addition, mice that rejected tumor challenge generated tumor-specific cytotoxic T lymphocytes' responses. Importantly, microscopic and gross evaluation of organs from mD52 immunized mice revealed no evidence of autoimmunity as assessed by absence of T cell infiltration and absence of microscopic pathology. Together, these data demonstrate that mD52 vaccination induces an immune response that is capable of rejecting tumors that over-express mD52 without the induction of harmful autoimmunity.

Keywords Vaccine · Metastasis · mD52 · TPD52 · Murine · CpG

Abbreviations

TPD52	Tumor protein D52
mD52	Murine TPD52
hD52	Human TPD52
3T3.mD52	mD52 Transformed 3T3 cells
ODN	Oligodeoxynucleotide
TAA	Tumor associated antigen

Introduction

The tumor protein D52 (*TPD52*) gene family [1] comprises three genes, *D52* [2], *D53* [1, 3], and *D54* [4, 5]. The first human *D52*-like gene to be identified, human *TPD52 (hD52)*, was found to be over-expressed in approximately 40% of breast carcinomas [2]. Subsequent reports have shown that *hD52* is over-expressed in cancers of the lung [6], prostate [7], colon [8], and ovary [9]. Byrne and colleagues localized the *hD52* gene to human chromosome 8q21 [2], a region frequently gained in breast and prostate carcinomas [10–14], and have since reported that *hD52*

L.A. Payton and J.D. Lewis contributed equally to this study.

L. A. Payton · J. D. Lewis · R. K. Bright (✉)
Department of Microbiology and Immunology,
Texas Tech University Health Sciences Center,
3601 4th Street, MS 6591, Lubbock, TX 79430, USA
e-mail: robert.bright@ttuhsc.edu

J. A. Byrne
Discipline of Paediatrics and Child Health,
Childrens Hospital at Westmead,
The University of Sydney, Sydney, NSW, Australia

Present Address:
L. A. Payton
Department of Surgery, UT Southwestern Medical Center,
Dallas, TX 75390, USA

represents a target for gene amplification in human breast cancer [15]. To our knowledge *hTPD52* is the first and only chromosome 8q21 target gene to have been identified in any cancer type. Additional studies suggest that *hTPD52* and *hTPD53* genes encode regulators of cell proliferation [1]. Murine *TPD52* naturally mirrors human *TPD52* with respect to known function and over-expression in tumor cells, and shares 86% protein identity with the human orthologue. Our recent studies demonstrated that transfection and stable expression of murine *TPD52* (*mD52*) cDNA in mouse 3T3 fibroblasts induced increased proliferation, anchorage independent cell growth, and the ability to form subcutaneous tumors and spontaneous lethal lung metastases in vivo when 3T3.mD52 cells were inoculated subcutaneously into naïve, syngeneic, immuno-competent mice [16]. Together these data strongly suggest that TPD52 is important for initiating and perhaps maintaining a tumorigenic and metastatic phenotype, and thus may be important for tumor cell survival making the TPD52 protein an excellent target for cancer vaccine development.

It has been convincingly demonstrated that unmethylated CpG dinucleotides largely found in bacterial DNA have the capacity to stimulate innate and adaptive immunity [17]. The mechanism of action lies within the ability of oligodeoxynucleotides (ODN), made up of unmethylated CpG dinucleotides, to bind Toll Like Receptor 9 (TLR9) on antigen presenting cells to include dendritic cells (DC) resulting in the enhancement of anti-cancer vaccination [17–19]. It has also been demonstrated that CpG/ODN are stronger than complete Freund's adjuvant in eliciting T_H1-type immune responses, which are believed to be important for the immunologic rejection of solid tumors, following protein antigen immunization [20, 21].

In the present study we sought to determine whether it was possible to induce an immune response to mD52 via active vaccination and to determine whether tumor immunity could be generated in the absence of autoimmunity. Recombinant mD52 protein and ODN 1826 (TCCAT GACGTTCCTGACGTT) [20] were administered to naïve mice in the form of an active vaccination regimen. Immunized mice were challenged subcutaneously with a tumorigenic dose of syngeneic tumor cells naturally over-expressing mD52 protein. Immunization of mice resulted in tumor rejection, the generation mD52 antigen-specific, MHC-restricted cytotoxic T lymphocytes (CTLs) and the production of IgG antibodies against mD52 protein. Pathologic analysis of vital organs shown to express detectable levels of mD25 naturally, revealed no evidence of autoimmunity induction. Together these data indicate that active immunization with mD52 protein and CpG/ODN as an adjuvant is effective at generating an immune response capable of rejecting tumor cells that naturally over-express mD52 protein without the induction of potentially harmful autoimmunity.

Materials and methods

Mice and tumor cell lines

Female 6- to 8-week-old Balb/c mice were purchased from the NIH (Frederick, MD, USA). All animals were cared for and treated according to Institutional Animal Care and Use Committee guidelines at Texas Tech University Health Sciences Center (Lubbock, TX, USA). The tumorigenic Balb/c 3T3.mD52 cell line [16] and the tumorigenic SV40-transformed Balb/c murine kidney cell line designated mKSA were used for tumor challenge following immunization. The C57BL/6 autochthonous TRAMP-C1 and TRAMP-C2 tumor cells lines were used as MHC class-I mis-matched, mD52 positive controls. mKSA and 3T3.mD52 Tumor cell lines were cultured in RPMI 1640 (Fisher Scientific, Pittsburgh, PA, USA) supplemented with 10% heat-inactivated fetal bovine serum, 2 mmol/l L-glutamine, 250 ng/ml fungizone, 50 IU/ml penicillin, 50 μg/ml streptomycin, 50 μg/ml gentamicin sulfate, and 10 mmol/l HEPES. Autochthonous TRAMP cell lines were cultured as previously reported [22].

RT-PCR and real-time RT-PCR analysis

Total RNA was isolated from cell lines using TRIZOL reagent (Bio Whittaker, Walkersville, MD, USA), and 1 μg was reverse transcribed to obtain cDNA as previously described [16]. Murine normal tissue cDNA panels (multiple tissue cDNA panels I and III) were purchased from Clontech (Mountain View, CA, USA). Both *mD52* and *GAPDH* (an internal reference control) amplification reactions were carried out as described previously [16] using 30 cycles for all PCR reactions and annealing temperatures of 62 and 60°C, respectively. All PCR reactions were performed in 50 μl volumes. The results were visualized by electrophoresis using 2% agarose gels containing ethidium bromide.

Real time RT-PCR was performed using cDNA samples generated as described above or using equivalent concentrations of murine normal tissue cDNA panels (Clontech) and the ABI Prism 7000 Sequence Detection System and ABI SYBR green PCR core reagents kit according to the manufacturer's instructions (Applied Biosystems, Foster City, CA, USA). Real time RT-PCR conditions for 40 cycles were as follows: 50°C for 2 min, 95°C for 10 min, 95°C for 15 s, and an annealing temperature of 62°C for 1 min for *mD52* primers (60°C annealing temperature was used for *GAPDH* control reactions). Additional controls

were no template and no enzyme and were included in all real-time RT-PCR reactions as previously described [16].

Recombinant mD52 purification

The MicroSpin GST Purification Module (Amersham Biosciences, Piscataway, NJ, USA) was used to purify recombinant mD52–Glutathione S-transferase (GST) fusion protein using the manufacturer's instructions and previously published methods [4]. Briefly, a 5 ml culture of recombinant *Escherichia coli* expressing mD52–GST fusion protein was grown to log phase and protein expression induced with IPTG. Cultured cells were harvested and lysed by repeated freeze thaw cycles, and the mD52–GST fusion protein was purified using a Glutathione Sepharose 4B MicroSpin column. Protein purity was assessed by SDS-PAGE and silver staining, as well as by western blot analysis using an anti-TPD52 polyclonal antibody (generated by immunizing rabbits with N-terminal, carrier conjugated peptide **GC***AYKKTSETLSQAGQKAS;* italics represents a region of TPD52 protein that is conserved between human and mouse) (Bio Synthesis, Inc, Lewisville, TX, USA). Protein concentration was determined by measuring the absorbance at 280 nm according to the manufacturers' guidelines (Amersham Biosciences). The GST affinity tag was approximated by 1 $A_{280} \sim 0.5$ mg/ml, based on the extinction coefficient of the GST monomer using a Bradford protein assay. mD52 protein concentration was determined based on a 1:1 molar ratio of mD52 to GST in the fusion construct.

Western blot analysis

To determine if vaccination induced anti-mD52 antibodies specific for native denatured mD52 from tumor cells, Western blot analyses were performed using mKSA whole cell lysates, as previously reported by our laboratory [23]. mKSA cells were grown to confluency. Cells were harvested, counted, and whole cell protein lysates were prepared used Pierce Whole Cell Lysis Buffer (Pierce Biotechnology, Inc., Rockford, IL, USA) to obtain lysates of 1×10^8 cell equivalents/ml. Lysates were loaded on a standard reducing SDS-PAGE (4% stacking, 12% resolving) and electrophoresed at 200 V for 1 h, followed by electrolytic transfer to nitrocellulose for immunoblotting. The nitrocellulose membranes were blocked in PBS containing 1% normal goat serum, 1% milk, and 0.02% Tween for 2 h at room temperature. After blocking, membranes were cut into 5 mm strips and incubated overnight at 4°C with a 1:100 dilution of serum collected prior to, and following each immunization. Following incubation with serum, the strips were washed three times with PBS-0.02% Tween. Antibody binding was detected by the addition of goat-anti-mouse IgG horseradish peroxidase conjugated antibody (GAM-HRP) (SIGMA) at a 1:1,000 dilution for 2 h at room temperature. Strips were then washed three times with PBS-0.02% Tween and developed with 3.3 V diaminobenzidine reagent as substrate (Sigma, St. Louis, MO, USA) to visualize mD52-specific antibody reactivity. Strips probed with polyconal rabbit anti-TPD52 polyclonal antibody (generated by immunizing rabbits with N-terminal, carrier conjugated peptide **GC***AYKKTSETLSQAGQKAS;* italics represents a region of TPD52 protein that is conserved between human and mouse) (Bio Synthesis, Inc) served as a positive control.

Immunization and tumor challenge

Individual mice were immunized via intramuscular (i.m.) injection every 14 days with 5–10 μg of recombinant mD52 protein admixed with 5–10 μg of CpG oligonucleotide (ODN 1826 TCCATGACGTTCCTGACGTT) [20] as an alum precipitate for a total of three injections. CpG/ODN in alum alone served as a control immunization. Mice in all groups were bled from the dorsal tail vein prior to immunization and 2 weeks following each immunization. Two weeks following the final immunization, mice in all groups were challenged with the following tumorigenic dose of tumor cells: 3T3.mD52 (1×10^6), or mKSA (5×10^5). Tumor cells were harvested, counted, and re-suspended in versene (PBS/EDTA, Fisher Scientific) to prevent aggregation and 100 μl of viable cell suspension was injected subcutaneously (s.c.) in the right flank of each mouse for tumor challenge. Tumor size was determined by taking perpendicular measurements with calipers every 2 to 3 days, and tumor volume (mm^3) was calculated using the following formula: $(a \times b^2)/2$, where b is the smaller of the two measurements.

Analysis of cytotoxic T lymphocyte (CTL)-mediated tumor cell lysis

T cells from spleens of immunized mice that survived tumor challenge were isolated and subjected to standard CTL-mediated tumor cell lysis analysis. CTLs were generated by culturing spleen cells in the presence of irradiated mKSA or 3T3.mD52 tumor cells (using the same tumor cell line as was used for the in vivo challenge) in the presence of IL-2 (10 ng/ml), IL-7 (5 ng/ml), and IL-12 (5 ng/ml) at 37°C for 5–7 days. Specificity was evaluated by mixing various numbers of CTLs with a constant number of target cells (5×10^3 cells per well) in 96 well round bottom plates. Specific lysis was determined using a Europium time-resolved fluorescence based 2 h method and measured using a Victor3™ plate reader (Perkin Elmer, Boston, MA, USA). Percent lysis was calculated as: % specific lysis = $1 - (E - S)/(M - S) \times 100$, where E represents Eu release in the presence of effector cells, S is spontaneous Eu release in

medium alone and *M* represents maximum Eu released in the lysis buffer [24, 25]. To confirm MHC class-I restricted tumor recognition, CTL blocking assays were performed by incubating tumor cells with anti-H-2K^d (anti-Kd) or anti-H-2K^b (control Ig) mAb prior to incubation with CTLs. Briefly, 10 μl of mAb in PBS (a final concentration of 30 μg/ml) was added to individual wells of 96 well round bottom plates in triplicate. Next, 100 μl tumor cell targets were added to each well and incubated for 30 min at room temperature. Finally, 100 μl of effectors were added to the appropriate wells, and the plates were incubated for 24 h at 37°C. Assays were analyzed using the Victor3™ plate reader (Perkin/Elmer, Wallac).

Flow cytometry

Lymphocytes from spleens cultured as described earlier for CTL assay were stained with monoclonal antibodies specific for CD3, CD4, CD19, NK marker CD49b (detected with the DX5 antibody) and CD8, and MHC class-I expression was assessed on tumors cell lines, using antibodies purchased from BD-Bioscience (San Jose, CA, USA). Cells were fixed in 1% paraformaldehyde at 4°C for 1 h, and then analyzed by flow cytometry using a BD-FacsVantage™.

Assessment of vaccine induced autoimmunity

Kidneys from immune and control mice were blindly evaluated for T cell subset infiltrates using fluorescent immunohistochemistry (IHC) methods (Pathology, Texas Tech University Health Sciences Center). Kidneys from MRL/lpr mice (a murine Lupus model), a generous gift from Dr. Mark Mamula (Yale University), served as positive controls for T cell infiltration analysis by IHC.

Enumeration of 3T3.mD52 spontaneous lung metastases

Analysis of tumor metastasis to the lungs was performed by removing the lungs of animals following euthanization and injection of the lungs with India ink to visualize individual tumor nodules [24]. Briefly, an India ink solution was injected through the trachea and allowed to fill the lungs. The lungs were removed and placed in Fekete's solution for de-staining. Tumor nodules do not absorb India ink, which results in the normal lung tissue staining black and the tumor nodules remaining white. Tumor nodules were counted blindly, and the size was noted by three individuals.

Statistical analysis

When necessary, tumor challenge data were analyzed with a Student's *t* test to determine whether significant differences existed between mean tumor volume for mD52 immunized and that of control immunized groups of mice.

Results

Expression of *mD52* in tumor cell lines and normal tissues

Prior to immunization with murine TPD52 (mD52) and evaluation of protection from tumor cell challenge, expression of *mD52* was determined for tumor cell lines used in this study. The tumorigenic and metastatic cell line 3T3.mD52 was generated in our laboratory and shown to be positive for *mD52* expression previously [16]. Expression of *mD52* by the Balb/c kidney-derived tumor cell line, mKSA and the C57BL/6 tumor cell lines TRAMP-C1 and TRAMP-C2 was confirmed using a Syber green relative quantitation method for real-time RT-PCR (Fig. 1a). All three of the murine tumor cell lines expressed *mD52* at detectable levels at 30 cycles of amplification. The delta Rn for *mD52* expression at 30 cycles of amplification was similar for all three cell lines (Fig. 1, panel i). When comparing the relative expression of *mD52* to the respective expression of *GAPDH* for the same cell line at 30 cycles of amplification, mKSA and TRAMP-C2 cells were similar, whereas TRAMP-C1 demonstrated greater expression of mD52 (Fig. 1a, panel iii). Expression of mD52 protein was confirmed for all tumor cell lines by Western blot analysis using an anti-mD52 antibody. A band of approximately 27 kDa was observed for the 3T3.mD52, mKSA, TRAMP-C1, and TRAMP-C2 cell lines (Fig. 1b). Examination of the 3T3.V empty vector transfected, negative control cell line revealed no detectable levels of mD52 protein expression by Western blot analysis (Fig. 1b). In addition, expression of MHC class-I molecules by the tumor cell lines was evaluated using specific monoclonal antibodies and flow cytometry. All four of the tumor cell lines expressed high levels of surface MHC class-I molecules (not shown). Taken together these data demonstrate that the tumor cell lines, mKSA, 3T3.mD52, TRAMP-C1, and TRAMP-C2 express mD52 protein and MHC class-I molecules.

Others have reported the detection of human *TPD52* expression in some normal tissues. *TPD52* expression was shown to be pronounced in normal human kidney, prostate and breast with very little expression detected in the testes, thymus, and spleen [6]. *TPD52* expression was also demonstrated in human B cells but not in T cells [26]. Since human and mouse TPD52 proteins are 86% identical and we demonstrated natural expression of *mD52* in tumor cell lines (Fig. 1), it was of interest to assess the relative expression of *mD52* in normal murine tissues. We were only interested in relative expression of *mD52* in normal tissues compared to tumor cells to corroborate previous studies and

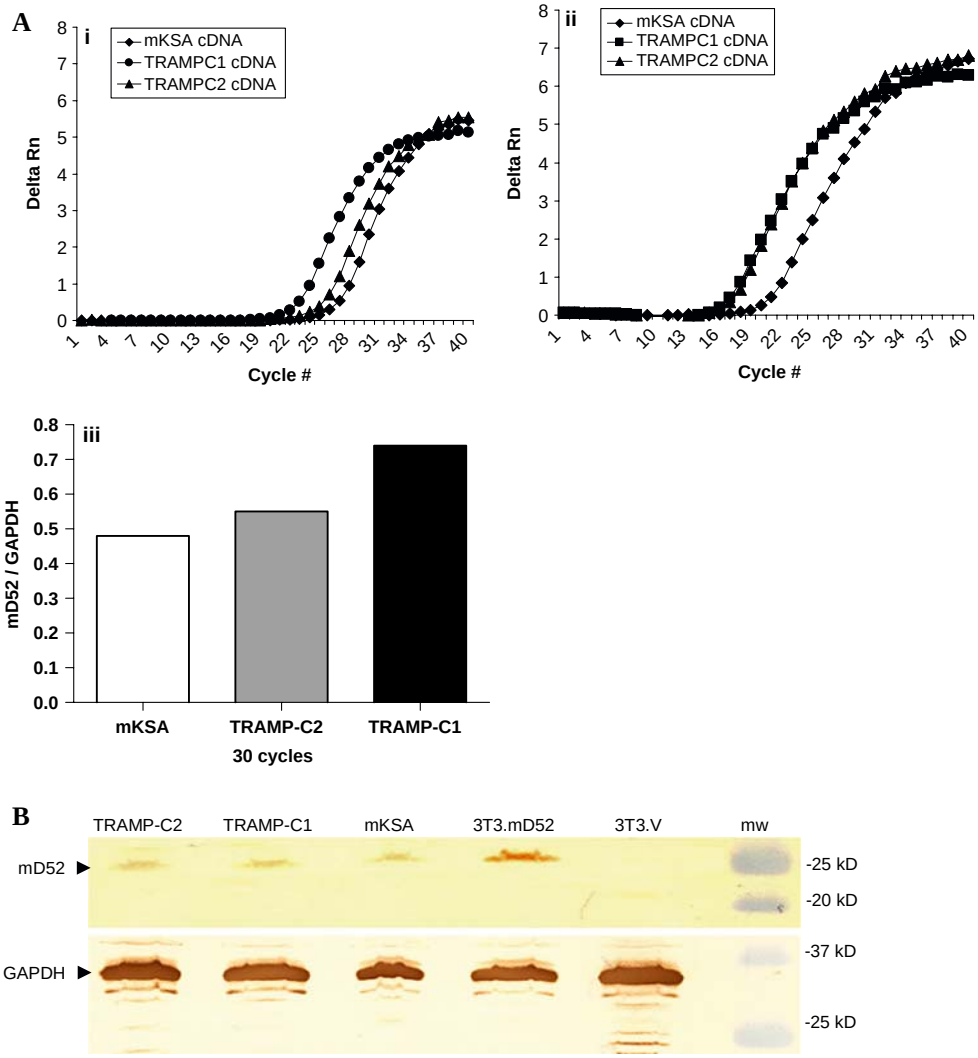

Fig. 1 Expression of Murine TPD52 (mD52) in tumor cell lines. **a** *mRNA expression of mD52 in murine tumor cell lines.* (i) Real-time RT-PCR showing *mD52* expression in mKSA, TRAMP-C1 and TRAMP-C2 murine tumor cell lines. (ii) Real-time RT-PCR showing expression of *GAPDH* in mKSA, TRAMP-C1 and TRAMP-C2 murine tumor cell lines, as an internal reference control. (iii) Relative expression of *mD52* over *GAPDH* in tumor cell lines at 30 cycles of amplication. **b** *mD52 protein expression in murine tumor cell lines.* Western blot analysis of murine tumor cell lysates generated from 1×10^8 cell equivalents demonstrating protein expression of mD52 using an antibody with specificity for mD52. GAPDH served as a control for protein loading. Shown are the representatives of three independent experiments

to justify our evaluation of autoimmunity, given that expression of *mD52* in normal tissues could result in tolerance or autoimmunity following active vaccination, and that absolute quantitation of *mD52* was not necessary at this juncture for evaluation of autoimmunity and tolerance. Sixteen normal murine tissues were examined for relative *mD52* expression using RT-PCR and real-time RT-PCR (Fig. 2). Pronounced expression of *mD52* was observed for kidney, muscle, lung, brain prostate, lymph node, and eye. A much less expression of *mD52* was observed for normal testes, liver, spleen, heart, uterus, stomach, thymus, and placenta (Fig. 2a, panels i and ii). Real-time RT-PCR analysis supported the mD52 expression findings observed for end point RT-PCR (Fig. 2b). Interestingly, expression of *mD52* appeared to be the highest in normal kidney. Real-time RT-PCR produced a delta Rn of approximately 4.5 at 30 cycles of amplification for kidney with lung, spleen, and muscle, for example, producing delta Rn values less than 4.0 (Fig. 2b, panel i). These data indicate that the relative expression pattern of *mD52* in normal murine tissues is similar to what has been reported for human *TPD25* expression in normal tissues. Since *mD52* expression in normal kidneys was the highest among the normal tissues tested, and the kidney is a vital organ, kidney pathology following vaccination with mD52 protein was monitored as an indication of vaccine induced autoimmunity.

Tumor protection following immunization with mD52 protein

To determine whether it was possible to induce tumor protective immunity following vaccination with mD52 protein, groups of mice were immunized with purified recombinant mD52 protein (Fig. 3a) admixed with CpG/ODN, and rejection of subsequent tumor challenge was evaluated. Individual mice were immunized i.m. every 14 days, according to the schedule in Fig. 3b. Immunization groups included mD52 protein admixed with CpG/ODN as an

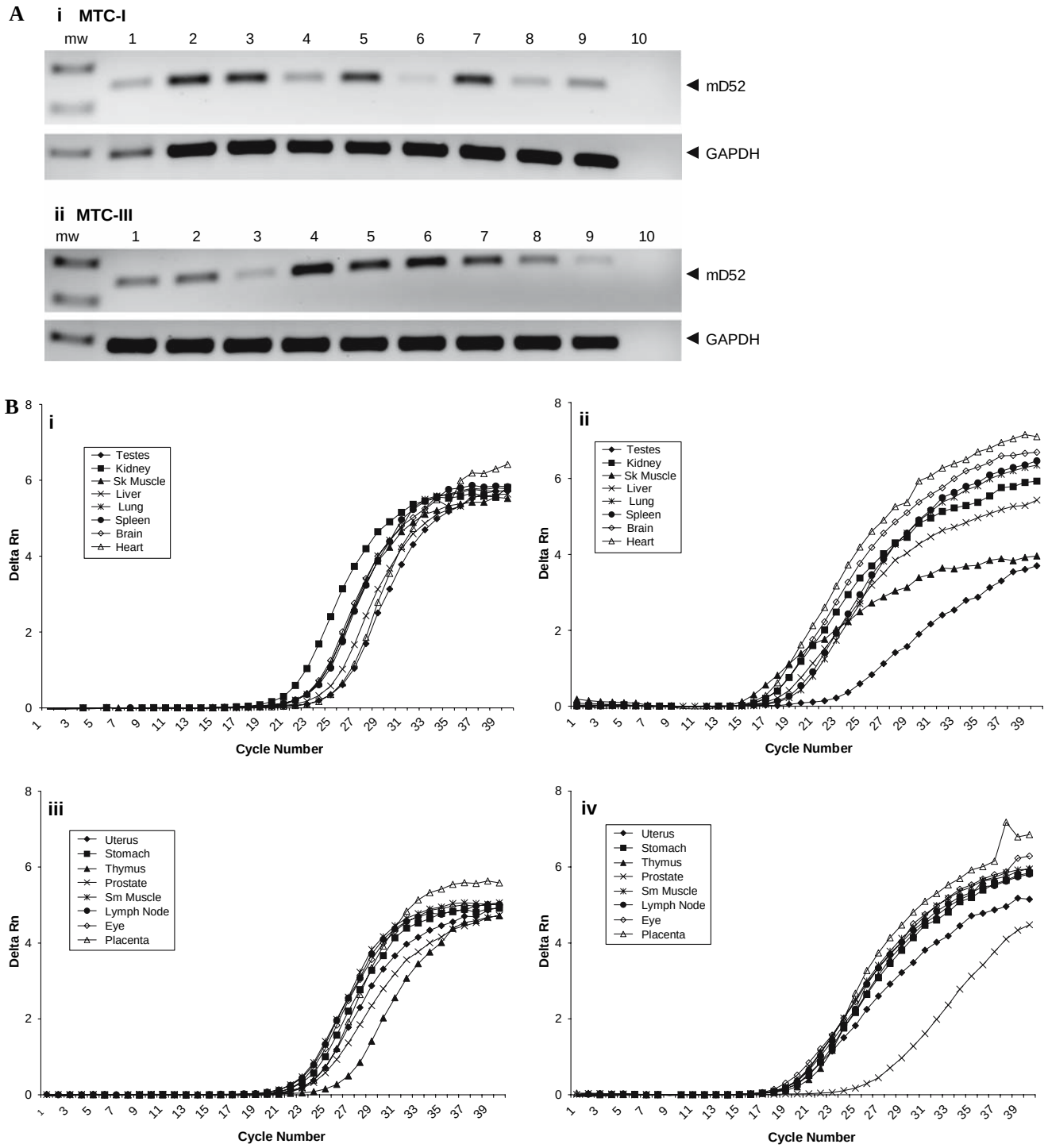

Fig. 2 Expression of Murine TPD52 (*mD52*) in normal tissues. **a** *RT-PCR showing mRNA expression of mD52 in normal tissues.* (i) Multiple tissue cDNA panel-I (*MTC-I*) lane *1*, testes; lane *2*, kidney; lane *3*, skeletal muscle; lane *4*, liver; lane *5*, lung; lane *6*, spleen; lane *7*, brain; lane *8*, heart; lane *9*, manufacturer's control (pooled mouse liver cDNA); lane *10*, H_2O (no template control). (ii) Multiple tissue cDNA panel-III (*MTC-III*) lane *1*, uterus; lane *2*, stomach; lane *3*, thymus; lane *4*, prostate; lane *5*, smooth muscle; lane *6*, lymph node; lane *7*, eye; lane *8*, placenta; lane *9*, manufacturer's control (pooled mouse liver cDNA); lane *10*, H_2O (no template control). GAPDH expression served as a control. *mw* molecular weight standard. **b** *Real-time RPT-PCR showing expression of mD52 in normal murine tissues.* (i) Real-time RT-PCR showing expression of *mD52* in normal tissue panel MTC-I. (ii) Real-time RT-PCR showing expression of *GAPDH* in normal tissue panel MTC-I. (iii) Real-time RT-PCR showing expression of *mD52* in normal tissue panel MTC-III. (iv) Real-time RT-PCR showing expression of *GAPDH* in normal tissue panel MTC-III. Shown are the representatives of three independent experiments

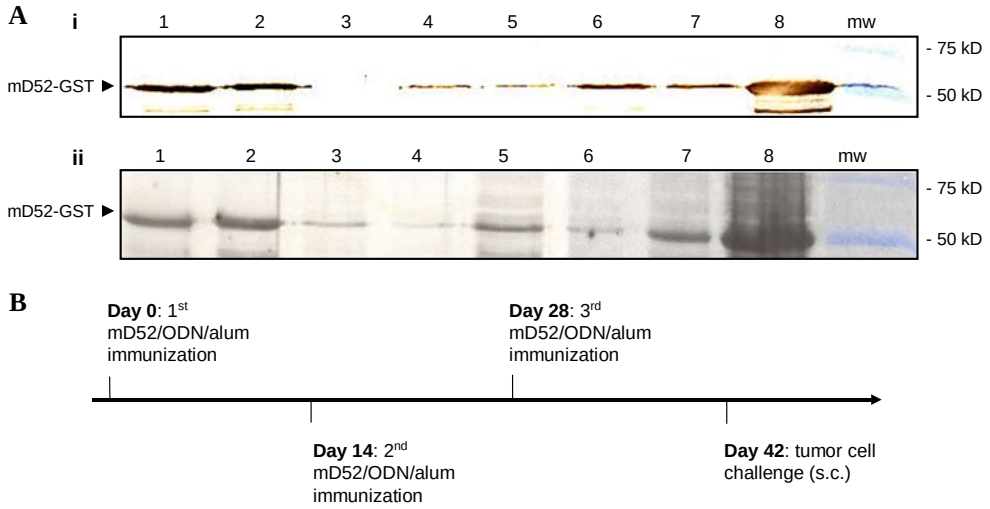

Fig. 3 Purification of mD52 protein and mD52 immunization schedule. **a** *Purification of recombinant mD52 protein.* (i) Western blot analysis of purified mD52-GST fusion protein, lane *1*, second elution of purified protein; lane *2*, first elution of purified protein; lanes *3* and *4*, subsequent washes; lanes *5* and *6*, subsequent flow through samples prior to washing; lane *7*, insoluble material from freeze thaw lysate; lane *8*, freeze thaw lysate prior to loading on affinity column. *mw* molecular weight standard. (ii) Silver stained SDS-PAGE gel exact representation of the western blot shown in (i). *mw* molecular weight standard. **b** *Schematic diagram of the schedule for immunization with purified recombinant mD52 protein* (see Materials and methods for concentration of protein and CpG/ODN)

alum precipitate or CpG/ODN in alum alone as control immunization. Since the vaccine was administered as protein in alum, the induction of immunity prior to tumor challenge was assessed by the detection of anti-mD52 IgG antibodies. Following each immunization, serum samples were collected and monitored for the presence of anti-mD52 antibodies using Western blot analysis. Mice immunized with mD52 protein and CpG/ODN generated detectable IgG antibodies to mD52 following three immunizations (Fig. 4a, post1 and post2), whereas mice immunized with CpG/ODN alone in alum generated no detectable IgG antibodies (not shown). Serum samples collected prior to immunization were also negative for IgG antibodies with specificity for mD52 protein as determined by Western blot analysis (Fig. 4a, pre1 and pre2). These data demonstrate that immunity to mD52 can be induced following immunization with recombinant protein admixed with CpG/ODN in alum. In addition, IgG antibodies with specificity for mD52 do not appear to exist in mice prior to immunization with mD52 and CpG/ODN. Interestingly, immunization with recombinant mD52 protein in alum in the absence of CpG/ODN failed to induce detectable IgG antibodies (not shown).

To determine whether tumor immunity was induced following immunization with mD52 protein and CpG/ODN in alum, mice were challenged s.c. with a tumorigenic dose of syngeneic mKSA tumor. Tumor inoculation and growth was determined as described in the Materials and methods section. Fifty percent of mice immunized with mD52 protein admixed with CpG/ODN in alum rejected a tumorigenic challenge with mKSA tumor cells (Fig. 4b, panel ii), whereas none of the animals immunized with CpG/ODN in alum were capable of rejecting a tumorigenic challenge with mKSA (Fig. 4b, panel i). Similarly, mice immunized with recombinant mD52 in alum without CpG/ODN failed to reject mKSA tumor challenge (not shown). These data demonstrate that immunization with mD52 protein and CpG/ODN in alum prior to challenge with tumor cells that naturally express mD52 protein resulted in rejection of the tumor challenge compared to control immunized animals.

Induction of cytotoxic T lymphocytes following immunization with mD52 protein

Immunization with mD52 and CpG/ODN induced mD52-specific IgG antibodies (Fig. 4a) suggesting that specific T cells were induced to facilitate the switch to the IgG isotype. Since mD52 expressed by tumor cells is an intracellular protein it was of interest to determine if MHC class-I-restricted CTLs were also induced in mice following immunization with mD52 protein and CpG/ODN, and involved in the rejection of subsequent tumor challenge. Splenocytes were harvested and analyzed for tumor-specific killing as described in the Materials and methods section. The effector cells generated by 5–7 days mKSA mixed lymphocyte tumor culture (MLTC) were determined by flow cytometry to contain approximately 33% CD4+ T cells and 32% CD8+ T cells (not shown). Targets consisted of syngeneic MHC class-I matched 3T3 fibroblasts, 3T3.mD52 tumor

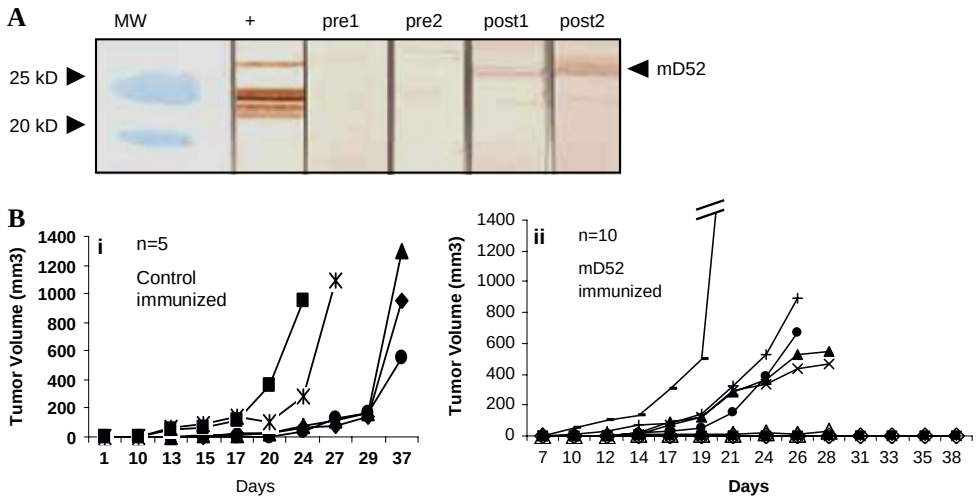

Fig. 4 Immune response following immunization with mD52 protein and challenge with mKSA tumor cells. **a** *Western Analysis of Serum from mD52 Immunized Mice.* Preimmune serum from mouse 1 (*pre1*); and mouse 2 (*pre2*); serum following three immunizations with mD52 and rejection of mKSA tumor challenge mouse 1 (*post1*); and mouse 2 (*post2*). A TPD52 specific antibody that recognizes both human and murine TPD52 was used to detect mD52 protein in mKSA tumor cell lysates (+). *MW* molecular weight standards. Shown are sera from representative animals, and representative results from repeated experiments. **b** *Effect of mD52 immunization on mKSA subcutaneous tumor growth in vivo*. (i) Tumor growth for control immunized mice (CpG/ODN in alum). (ii) Tumor growth for mD52 immunized mice (mD52 protein + CpG/ODN in alum). Animals were immunized i.m. every 14 days with 5–10 μg of mD52 + 5–10 μg of CpG/ODN or 5–10 μg of CpG/ODN alone for a total of three injections followed on day 42 with a s.c. challenge with 5×10^5 live, syngeneic mKSA tumor cells. Shown are representative results for two independent experiments

cells, mKSA tumor cells, and allogeneic MHC class-I mismatched TRAMP-C2 tumor cells. 3T3.mD52, mKSA, and TRAMP-C2 all over-express *mD52*, whereas 3T3 non-transformed fibroblasts do not (Fig. 1a, b) [16].

The CTLs generated from mice immunized with mD52 protein and CpG/ODN in alum and challenged with mKSA tumor cells demonstrated tumor-specific killing in Eu-release assays (Fig. 5a). Both mKSA (H-2K^d) the challenging tumor, and the MHC class-I matched (H-2K^d), mD52 positive cell line 3T3.mD52 were lysed by CTLs (>70 and >35% lysis, respectively, for an effector to target cell ratio of 32:1) (Fig. 5b), whereas the percent-specific lysis was <10% for both control targets 3T3 and TRAMP-C2 (Fig. 5a, b). The control targets either lack the correct MHC class-I molecule (TRAMP-C2; H-2K^b) or the targeted antigen mD52 (3T3; H-2K^d). Taken together, these data suggest that CTLs generated following immunizations with mD52 protein and CpG/ODN in alum are antigen-specific and MHC class-I-restricted. To confirm MHC class-I restricted tumor recognition, CTL blocking assays were performed by incubating tumor cell targets with anti-H-2K^d (anti-Kd) or anti-H-2K^b (control Ig) mAb prior to incubation with CTLs at an effector to target cell ration of 32:1. CTL mediated lysis of both mKSA and 3T3.mD52 was inhibited 90 to 100%, respectively, in the presence of anti-H-2K^d mAb. The control anti-H-2K^b (control Ig) mAb failed to inhibit CTL-specific lysis of either mKSA or 3T3.mD52 (Fig. 5c). These data further support the conclusions that the CTL generated following mD52 and CpG/ODN immunization were mD52 specific and MHC class-I restricted.

Immunization with mD52 does not induce autoimmunity

Since mD52 is a "self antigen", i.e. it is expressed in some normal tissues as well as in tumors, it is possible that tolerance could prevent the induction of an immune response. Conversely, if tolerance is broken and an immune response is generated against mD52, there is the potential for the induction of harmful autoimmunity. As shown by the generation of IgG antibodies and MHC class-I-restricted antigen-specific CTLs to mD52, an immune response was indeed induced against mD52 following immunization, and the response was capable of rejecting mD52-expressing tumor challenge in vivo. Therefore, it was of interest to assess whether autoimmunity was also induced. To assess autoimmunity induction, kidneys of mice that were immunized with mD52 protein and CpG/ODN in alum and survived tumor challenge were harvested and evaluated for T cell infiltration and evidence of microscopic pathology. Individually immunized mice that survived tumor challenge showed no gross morbidity and appeared healthy throughout the study. Immunohistochemical analysis of kidneys showed no T cell infiltrates and no evidence of microscopic pathology compared to kidneys from naïve mice serving as normal controls (Fig. 6). No evidence of gross pathology was

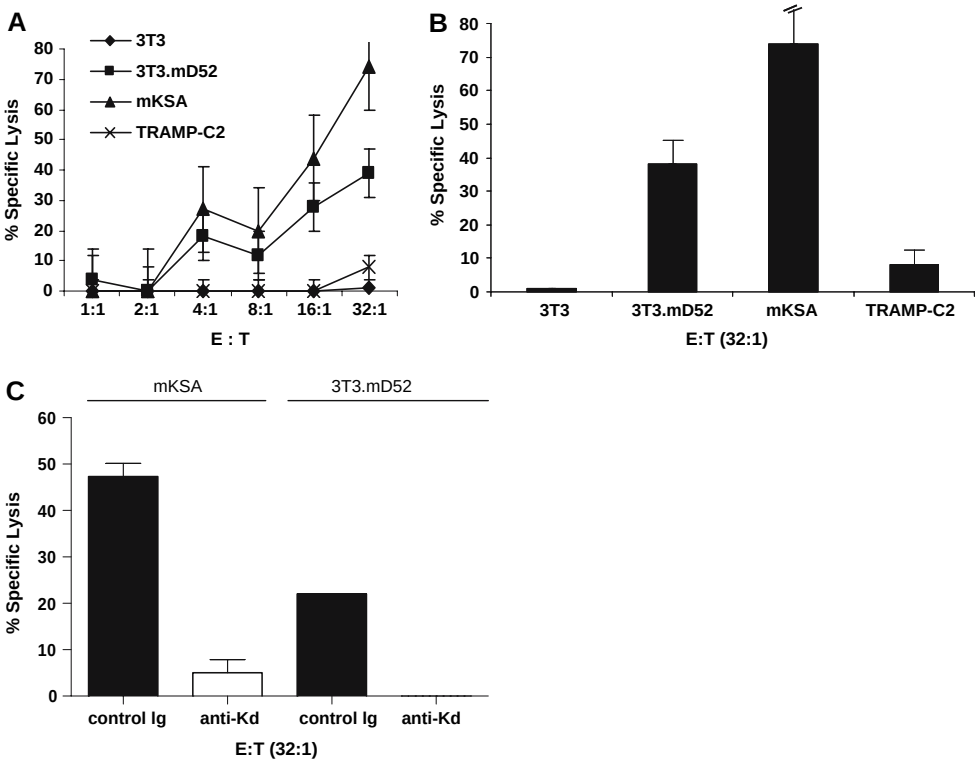

Fig. 5 MHC-restriction and mD52-specificity of CTL from mD52 immunized tumor challenged mice. **a** Specific lysis of mD52 expressing tumor cells; **b** bar graph showing lysis at a single E:T ratio of 32:1. **c** Antibody blocking of CTL lysis of tumor cells. Control Ig, monoclonal antibody specific for mouse H-2K^b MHC class-I; anti-Kd, monoclonal antibody specific for mouse H-2K^d MHC class-I. For **a** and **b** TRAMP-C2 served as an MHC mismatched mD52 expressing negative control. 3T3 served as an MHC matched mD52 minus negative control. 3T3.mD52 and mKSA served as an MHC matched mD52 expressing positive control. Values shown are the mean ± SEM for triplicate determinations and are representative of two independent experiments

observed for livers, lungs or spleens. These data demonstrate that immunization with mD52 protein and CpG/ODN in alum does not result in the induction of autoimmunity.

Prevention of spontaneous lung metastases following immunization with mD52

We reported previously that 3T3.mD52 tumor cells spontaneously metastasize to the lungs, forming lethal tumor burdens [16]. To determine if immunization with mD52 protein and CpG/ODN in alum was capable of preventing lethal lung metastases, animals were challenged s.c. with 3T3.mD52 tumor cells. Enumeration of tumor nodules was performed by harvesting lungs and staining with an India ink solution. Immunization with mD52 protein and CpG/ODN in alum resulted in the rejection of 40% of subcutaneous 3T3.mD52 tumors (Fig. 7a, panel ii), and the prevention of spontaneous lung metastases (Fig. 7b). In contrast, mice immunized with CpG/ODN in alum alone and challenged with 3T3.mD52 developed visible s.c. tumor nodules (Fig. 7a, panel i) and lung metastases (Fig. 7b). Of note, mice that rejected a primary 3T3.mD52 tumor challenge also rejected a second 3T3.mD52 tumor challenge (1×10^6 cells) in the opposite flank, given 90 days after the initial tumor challenge (not shown). Taken together, these data indicate that immunization with mD52 protein and CpG/ODN in alum induces a memory immune response capable of preventing lethal lung metastasis by mD52 positive 3T3.mD52 tumor cells.

Discussion

The use of vaccination against infectious disease in modern medicine has had a major impact on worldwide health. The power of the immune system has also been applied to fight cancer. Anti-cancer vaccines targeting self-proteins have been applied to treat or prevent multiple cancers in preclinical studies and clinical trials [27, 28]. Some examples include targeting MAGE in melanoma [29, 32], PAP [30, 33–36], PSMA [30, 31, 36], and PSA [30, 31, 36–38] in prostate cancer, and MUC1 [28] in breast cancer. Tumor protein D52 (TPD52) is a novel and potentially important tumor associated antigen (TAA) due to its over-expression in a number of fatal and common cancers to include prostate [39, 40], breast [2], ovary [9], and lung [6, 41] carcinomas. Scanlan and colleagues identified human TPD52 (hD52) as a candidate breast cancer TAA by using sera from breast cancer patients to screen a library of expressed genes from breast cancer tissue, demonstrating that hD52 is capable of inducing IgG antibodies [42]. This report suggests that TPD52 may be immunogenic and capable of inducing a cellular immune response, thus warranting study of TPD52 as an anti-cancer vaccine to induce cellular immunity. To address this, we hypothesized that vaccines targeting murine TPD52 (mD52) would induce cellular immune responses capable of rejecting tumor cells that over-express mD52 protein in murine models of cancer. Recombinant mD52 protein was administered along with CpG/oligodeoxynucleotide (ODN) in alum as an intramuscular

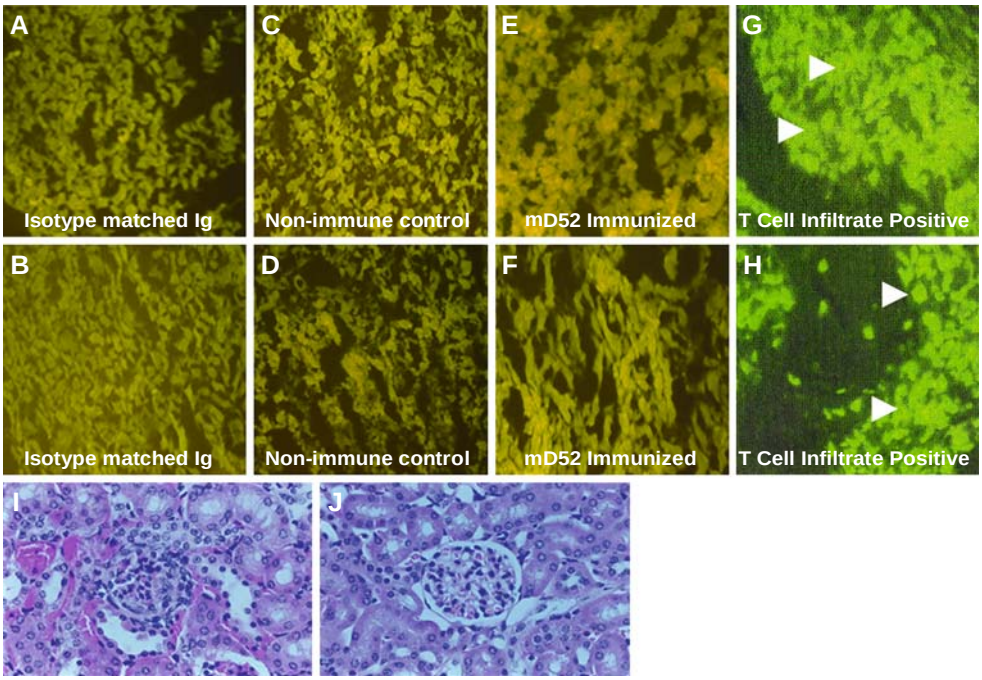

Fig. 6 Evaluation of autoimmune associated kidney pathology following mD52 immunization and tumor rejection. Shown are representative 5 μm, formalin fixed, paraffin embedded sections of kidneys from naïve mice or mice immunized with mD52 and subsequent tumor rejection (×100 magnification). The panels **a** through **h** are representative immuno-fluorescence micrographs staining for T cell infiltration. Panels **a**, **b** IgG-FITC control; panel **c**, **d** CD3-FITC naïve mouse kidneys; panel **e**, **f** CD3-FITC mouse kidneys following mD52 immunization and tumor rejection; panels **g**, **h** CD3-FITC kidneys from MRL/lpr autoimmune lupus mice as a positive control for T cell infiltration as depicted by the brighter fluorescent rings around kidney tubules (*arrows*). Panel **i** H&E stain for naïve mouse kidney; panel **j** H&E stain for kidney from mD52 immunized and tumor challenged animal. All assays were performed by an experienced pathologist and the determinations done blindly. Shown are representative micrographs from individual animals and two independent experiments

vaccine, followed by challenge with a tumorigenic dose of syngeneic tumor cells that naturally over-express mD52 protein.

In the present study we immunized mice with recombinant mD52 protein admixed with CpG/ODN in alum which resulted in the induction of immune responses with specificity for mD52. As a test of tumor immunity we challenged mice with syngeneic tumor cells that over-express mD52, and tumor growth was monitored. All mice that received control immunizations developed lethal tumor burdens and had to be killed (Figs. 4b: panel i, 7a: panel i). In addition, mice immunized with CpG/ODN in alum alone and challenged with the spontaneously metastatic 3T3.mD52 tumor cells developed lung metastases (Fig. 7b). However, mice immunized with recombinant mD52 protein and CpG/ODN in alum resulted in the rejection of tumor challenge in 50% of mice challenged with mKSA tumor cells (Fig. 4b, panel ii) and 40% of mice that received 3T3.mD52 tumor cell challenge (Fig. 7b, panel ii). Mice immunized with mD52 protein and CpG/ODN followed by 3T3.mD52 tumor cell challenge also prevented the formation of spontaneous lethal lung metastases (Fig. 7b). Rejection of mKSA tumor challenge was associated with the induction of mD52-specific, MHC-restricted CTLs (Fig. 5). Importantly, there was no detectable evidence of autoimmunity following immunization with mD52 and CpG/ODN in alum (Fig. 6). Together, these data demonstrate that the "self" TAA mD52 is sufficiently immunogenic when administered as a protein-based vaccine admixed with CpG/ODN as a molecular adjuvant. Moreover, the generation of anti-mD52 CTL resulted in rejection of syngeneic tumor cells that naturally over-express mD52 protein without induction of detectable autoimmunity. The form of recombinant mD52 protein used was a fusion protein of mD52 and GST to facilitate purification (Fig. 3a). It is possible that GST functions as a carrier protein; however, experiments employing mD52-GST protein in the absence of CpG/ODN as a molecular adjuvant followed with mKSA tumor challenge (performed in conjunction with studies represented in Fig. 4) failed to induce protective tumor immunity (not shown). More importantly, the form of mD52 protein recognized by specific CTLs (Fig. 5) and IgG antibodies (Fig. 4) was a natural murine tumor cell derived mD52, not recombinant mD52-GST fusion protein.

It is known that TGF-β1 is involved in tumor-mediated immune suppression. We demonstrated previously that 3T3.mD52 tumor cells secrete significant quantities of TGF-β1 [16] which could account for decreased rejection

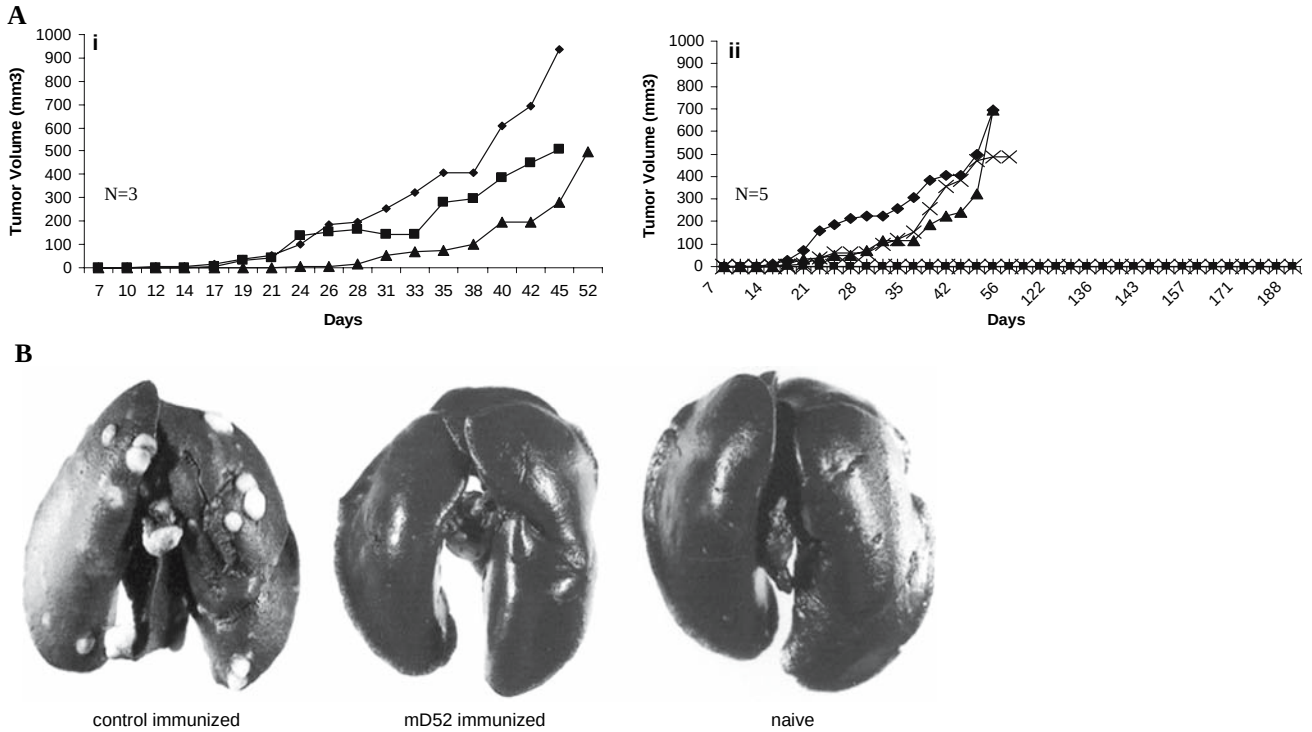

Fig. 7 Immune response following immunization with mD52 protein and challenge with 3T3.mD52 tumor cells. **a** *Effect of mD52 immunization on 3T3.mD52 subcutaneous tumor growth in vivo.* (i) Tumor growth for control immunized mice (CpG/ODN in alum). (ii) Tumor growth for mD52 immunized mice (mD52 protein + CpG/ODN in alum). **b** *Effect of mD52 immunization on 3T3.mD52 spontaneous lung metastasis in vivo.* Control immunized mice, CpG/ODN in alum; mD52 immunized mice, mD52 protein + CpG/ODN in alum. For **a** and **b**, animals were immunized i.m. every 14 days with 5 μg of mD52 + 10 μg of CpG/ODN or 10 μg of CpG/ODN alone for a total of three injections followed on day 42 with a s.c. challenge with 1×10^6 live, syngeneic 3T3mD52 tumor cells. Shown are representative results for two independent experiments

of 3T3.mD52 tumors following immunization compared to mKSA tumors, which secrete nearly 50% less TGF-β1 than 3T3.mD52 tumor cells (not shown). Studies are underway to overcome immune suppression by TGF-β1 and increase protection in mice challenged with 3T3.mD52 or mKSA tumor cells by using TGF-β1 neutralizing mAb in vivo or siRNA to TGF-β1 to knock out or down TGF-β1 expression and secretion in vitro in tumor cells without interfering with in vivo tumorigenic or metastatic characteristics of tumor cells. More traditional adjuvants, such as IFA, different TLR agonists as molecular adjuvants, different routes and schedules of administration of mD52 to increase antitumor efficacy in vivo are also being explored. In addition, studies to assess mD52 vaccination as a treatment of preexisting tumors are underway.

It is now widely accepted that bacterial derived, unmethylated CpG deoxynucleotides are potent molecular adjuvants when administered with active vaccinations regimens [17, 19, 43]. Nearly 10 years have passed since the first report on the potency of CpG DNA as a molecular adjuvant when administered with a protein-based vaccine [20]. In this study Davis and colleagues demonstrated that CpG DNA could overcome the ability of alum and protein vaccines to induce T_H2 immunity in Balb/c mice and instead drive immunity to a T_H1-type response. In addition, they proved that addition of CpG DNA could increase specific T_H1-type IgG2a antibody responses to HBsAg fivefold above HBsAg without CpG DNA. This group subsequently went on to characterize three CpG/ODN classes with distinct immunostimulatory properties [44]. Of importance to our studies was the characterization of what they termed B class CpG/ODN. These CpG/ODN are potent activators of B cells and T_H1-type cytokines capable of driving cellular immunity [44, 45]. The prototype B class CpG/ODN is represented by the ODN 1826 [20, 44, 45]. Since mD52 is an intracellular protein we were interested in the generation of T_H1-type cellular immunity and CTLs which would be necessary for the rejection of mD52 expressing tumors. To this end, we chose the B class CpG/ODN 1826 as our molecular adjuvant. Others have demonstrated that CpG/ODN 1826 is a potent molecular adjuvant for vaccination against various cancers. Vaccine studies utilizing CpG/ODN 1826 admixed with TAA in various murine cancer models include; HPV-16 E7 protein [46], anti-idiotype vaccine that mimics carcinoembryonic antigen (CEA) [47, 48], and synthetic peptide from HER-2/neu oncoprotein in a model of spontaneous

breast cancer [49]. Further support of the immunopotency of CpG/ODN 1826 in mice was the report by Shao and colleagues demonstrating that CpG/ODN 1826 could convert a weak autoantigen like uveitogenic rat interphotoreceptor retinoid-binding protein into a strong auto-antigen that induces uveitis [50]. This study demonstrated that molecular adjuvants based on CpG/ODN 1826 could enable tolerance to be broken to self-antigens delivered as active vaccination strategies.

In the present study we have shown for the first time that the self-TAA mD52 is immunogenic when administered as a recombinant protein-based vaccine admixed with CpG/ODN 1826 in alum. Further, the immune response generated is capable of rejecting tumor cells that naturally over-express mD52 protein without inducing harmful autoimmunity, suggesting the human TPD52 may be a potent vaccine antigen that could be administered to patients to treat or prevent cancers that over-express TPD52.

Acknowledgments This work was supported in part by NIH Grant CA 77351, funds from the Southwest Cancer Treatment and Research Center and by a Howard Hughes Medical Institute grant through the Undergraduate Biological Sciences Education Program to Texas Tech University.

References

1. Byrne JA, Mattei MG, Basset P (1997) Definition of the D52 gene/protein family through cloning of *D52* homologues in human (*hD53*) and mouse (*mD52*). Genomics 35:523–532
2. Byrne JA, Tomasetto C, Garnier JM, Rouyer N, Mattei MG, Bellocq JP, Rio MC, Basset P (1995) A screening method to identify genes commonly overexpressed in carcinomas and the identification of a novel complementary DNA sequence. Cancer Res 55:2896–2903
3. Byrne JA, Mattei MG, Basset P, Gunning P (1998) Identification and *in situ* hybridization mapping of a mouse *Tpd52l1 (D53)* orthologue to chromosome 10A4-B2. Cytogenet Cell Genet 81:199–201
4. Byrne JA, Nourse CR, Basset P, Gunning P (1998) Identification of homo- and heteromeric interactions between members of the breast carcinoma-associated D52 protein family using the yeast two-hybrid system. Oncogene 16:873–882
5. Nourse CR, Mattei MG, Gunning P, Byrne JA (1998) Cloning of a third member of the D52 gene family indicates alternative coding sequence usage in D52-like transcripts. Biochim Biophys Acta 1443:155–168
6. Chen S-L, Maroulakou IG, Green JE, Romano-Spica V, Modi W, Lautenberger J, Bhat NK (1996) Isolation and characterization of a novel gene expressed in multiple cancers. Oncogene 12:741–751
7. Dhanasekaran SM, Barrette TR, Ghosh D, Shah R, Varambally S, Kurachi K, Pienta KJ, Rubin MA, Chinnaiyan AM (2001) Delineation of prognostic biomarkers in prostate cancer. Nature 412:822–826
8. Malek RL, Irby RB, Guo QM, Lee K, Wong S, He M, Tsai J, Frank B, Liu ET, Quackenbush J, Jove R, Yeatman TJ, Lee NH (2002) Identification of Src transformation fingerprint in human colon cancer. Oncogene 21:7256–7265
9. Byrne JA, Balleine RL, Schoenberg Fejzo M, Mercieca J, Chiew YE, Livnat Y, St Heaps L, Peters GB, Byth K, Karlan BY, Slamon DJ, Harnett P, Defazio A (2005) Tumor protein D52 (TPD52) is overexpressed and a gene amplification target in ovarian cancer. Int J Cancer 117:1049–1054
10. Kallioniemi A, Kallioniemi OP, Piper J, Tanner M, Stokke T, Chen L, Smith HS, Pinkel D, Gray JW, Waldman FM (1994) Detection and mapping of amplified DNA sequences in breast cancer by comparative genomic hybridization. Proc Natl Acad Sci USA 91:2156–2160
11. Schoenberg Fejzo M, Ashar HR, Krauter KS, Powell WL, Rein MS, Weremowicz S, Yoon SJ, Kucherlapati RS, Chada K, Morton CC (1996) Translocation breakpoints upstream of the HMGIC gene in uterine leiomyomata suggest dysregulation of this gene by a mechanism different from that of lipomas. Genes Chromosomes Cancer 17:1–6
12. Forozan F, Karhu R, Kononen J, Kallioniemi A, Kallioniemi OP (1997) Genome screening by comparative genomic hybridization. Trends Genet 13:405–409
13. Cher ML, Bova GS, Moore DH, Small EJ, Carroll PR, Pin SS, Epstein JI, Isaacs WB, Jensen RH (1996) Genetic alterations in untreated metastases and androgen-independent prostate cancer detected by comparative genomic hybridization and allelotyping. Cancer Res 56:3091–3102
14. Virgin JB, Hurley PM, Cher MP, Nahhas F, Bebchuk KG, Mohamed AN, Sakr WA, Bright RK, Cher ML (1999) Isochromosome 8q is associated with 8p loss of heterozygosity in a prostate cancer cell line. Prostate 41:49–57
15. Balleine RL, Schoenberg Fejzo M, Sathasivam P, Basset P, Clarke CL, Byrne JA (2000) The *D52 (TPD52)* gene is a candidate target gene for events resulting in increased 8q21 copy number in human breast carcinoma. Genes Chromosomes Cancer 29:48–57
16. Lewis JD, Payton LA, Whitford JG, Byrne JA, Smith DI, Yang L, Bright RK (2007) Induction of tumorigenesis and metastasis by the murine orthologue of tumor protein D52. Mol Cancer Res 5:133–144
17. Krieg AM (2002) CpG Motifs in bacterial DNA and their immune effects. Annu Rev Immunol 20:709–760
18. Krieg AM (2003) CpG motifs: the active ingredient in bacterial extracts? Nat Med 9:831–835
19. Klinman DM (2004) Immunotherapeutic uses of CpG oligodeoxynucleotides. Nat Rev Immunol 4:249–258
20. Davis HL, Weeranta R, Waldschmidt TJ, Tygrett L, Schorr J, Krieg AM (1998) CpG DNA is a potent enhancer of specific immunity in mice immunized with recombinant Hepatitis B surface antigen. J Immunol 160:870–876
21. Lipford GB, Sparwasser T, Zimmermann S, Heeg K, Wagner H (2000) CpG-DNA-mediated transient lymphadenopathy is associated with a state of Th1 predisposition to antigen-driven responses. J Immunol 165:1228–1235
22. Foster BA, Gingrich JR, Kwan ED, Madias C, Greenberg NM (1997) Characterization of prostatic epithelial cell lines derived from transgenic adenocarcinoma of the mouse prostate (TRAMP) model. Cancer Res 57:3325–3330
23. Bright RK, Shearer MH, Kennedy RC (1994) SV40 large tumor antigen associated synthetic peptides define native antigenic determinants and induce protective tumor immunity in mice. Mol Immunol 31:1077–1087
24. Lewis JD, Shearer MH, Kennedy RC, Bright RK (2005) Surrogate Tumor antigen vaccination induces tumor-specific immunity and the rejection of spontaneous metastases. Cancer Res 65:2938–2946
25. Bright RK, Kimchi ET, Shearer MH, Kennedy RC, Pass HI (2002) SV40 Tag-specific cytotoxic T lymphocytes generated from the peripheral blood of malignant pleural mesothelioma patients. Cancer Immunol Immunother 50:682–690

26. Tiacci E, Orvietani PL, Bigerna B (2005) Tumor protein D52 (TPD52): a novel B-cell/plasma-cell molecule with unique expression pattern and Ca^{2+}-dependent association with annexin VI. Blood 105:2812–2820
27. Gilboa E (2004) The promise of cancer vaccines. Nat Rev Cancer 4:401–411
28. Lewis JD, Reilly BD, Bright RK (2003) Tumor associated antigens: from discovery to immunity. Int Rev Immunol 22:81–112
29. Finn OJ (2003) Cancer vaccines: between the idea and the reality. Nature 3:630–641
30. Shen L, Rock KL (2006) Priming of T cells by exogenous antigen cross-presented on MHC class I molecules. Curr Opin Immunol 18:85–91
31. Medzhitov R (2001) CpG DNA: security code for host defense. Nat Immunol 2:15–16
32. Hunt DF, Henderson RA, Shabanowitz J, Sakaguchi K, Michel H, Sevilir N, Cox AL, Appella E, Engelhard VH (1992) Characterization of peptides bound to the class I MHC molecule HLA-A2.1 by mass spectrometry. Science 255:1261–1263
33. Waldman TA (2003) Immunotherapy: past, present and future. Nat Med 9:269–277
34. Liang P, Pardee AB (2003) Analysing differential gene expression in cancer. Nat Rev Cancer 3:869–876
35. Liang P, Pardee AB (1992) Differential display of eukaryotic mRNA by means of the polymerase chain reaction. Science 257:967–971
36. Disis ML, Gooley TA, Rinn K (2002) Generation of T-cell immunity to HER-2/neu protein after active immunization with HER-2/neu peptide-based vaccines. J Clin Oncol 20:2624–2632
37. Chomez P, DeBacker O, Bertrand M (2001) An overview of the *MAGE* gene family with the identification of all human members of the family. Cancer Res 61:5544–5551
38. Burch PA, Breen JK, Buckner JC (2000) Priming tissue-specific cellular immunity in Phase I trial of autologous dendritic cells for prostate cancer. Clin Cancer Res 6:2175–2182
39. Byrne JA, Mattei MG, Basset P (1996) Definition of the tumor protein D52 (TPD52) gene family through cloning of D52 homologues in human (hD52) and mouse (mD52). Genomics 35:523–532
40. Rubin MA, Varambally S, Beroukhim R, Tomlins SA, Rhodes DR, Paris PL, Hofer MD, Storz-Schweizer M, Keufer R, Fletcher JA, His BL, Byrne JA, Pienta KJ, Collins C, Sellers WR, Chinnaiyan AM (2004) Overexpression, amplification, and androgen regulation of TPD52 in prostate cancer. Cancer Res 64:3814–3822
41. Chen SL, Zhang XK, Halverson DO (1997) Characterization of human N8 protein. Oncogene 15:2577–2588
42. Scanlan MJ, Gout I, Gordon CM, Williamson B, Stockert E, Gure AO, Jager D, Chen YT, Mackay A, O'Hare MJ, Old LJ (2001) Humoral immunity to human breast cancer: antigen definition and quantitative analysis of mRNA expression. Cancer Immun 1:4–20
43. Krieg AM, Davis HL (2001) Enhancing vaccines with immune stimulatory CpG DNA. Curr Opin Mol Ther 3:15–24
44. Vollmer J, Weeranta R, Payette P, Jurk M, Schetter C, Laucht M, Wader T, Tluk S, Liu M, Davis HL, Krieg AM (2004) Characterization of three CpG oligodeoxynucleotide classes with distinct immunostimulatory activities. Eur J Immunol 34:251–262
45. van Ojik HH, Bevaart L, Dahle CE, Bakker A, Jansen MJH, van Vugt MJ, van de Winkel JGJ, Weiner GJ (2003) CpG-A and B olidodeoxynucleotides enhance the efficacy of antibody therapy by activating different effector cell populations. Cancer Res 63:5595–5600
46. Kim T-Y, Myoung H-J, Kim J-H, Moon I-S, Kim T-G, Ahn W-S, Sin J-I (2002) Both E7 and CpG-oligodeoxynucleotide are required for protective immunity against challenge with human papillomavirus 16 (E6/E7) immortalized tumor cells: involvement of CD4+ and CD8+ T cells in protection. Cancer Res 62:7234–7240
47. Baral RN, Saha A, Chatterjee SK, Foon KA, Krieg AM, Weiner GJ, Bhattacharya-Chatterjee M (2003) Immunostimulatory CpG oligonucleotides enhance the immune response of anti-idiotype vaccine that mimics carcinoembryonic antigen. Cancer Immunol Immunother 52:317–327
48. Saha A, Baral RN, Chatterjee SK, Mohanty K, Pal S, Foon KA, Primus FJ, Krieg AM, Weiner GJ, Bhattacharya-Chatterjee M (2006) CpG oligonucleotides enhance the tumor antigen-specific immune response of an anti-idiotype antibody-based vaccine strategy in CEA transgenic mice. Cancer Immunol Immunother 55:515–527
49. Nava-Parada P, Forni G, Knutson KL, Pease LR, Celis E (2007) Peptide vaccine given with toll-like receptor agonist is effective for the treatment and prevention of spontaneous breast tumors. Cancer Res 67:1326–1334
50. Shao H, Lei S, Sun SL, Xiang J, Kaplan HJ, Sun D (2003) CpG-containing oligodeoxynucleotide 1826 converts the weak uveitogenic rat interphotoreceptor retinoid-binding protein peptide 1181–1191 into a strong uveitogen. J Immunol 171:4780–4785

Cancer Immunol Immunother
DOI 10.1007/s00262-009-0659-x

ORIGINAL ARTICLE

Memory and cellular immunity induced by a DNA vaccine encoding self antigen TPD52 administered with soluble GM-CSF

Jennifer D. Lewis · Laura A. Sullivan · Jennifer A. Byrne · Werner de Riese · Robert K. Bright

Received: 24 November 2008 / Accepted: 6 January 2009

Abstract Tumor protein D52 (TPD52) is involved in cellular transformation, proliferation and metastasis. TPD52 over expression has been demonstrated in several cancers including prostate, breast, and ovarian carcinomas. Murine TPD52 (mD52) has been shown to induce anchorage independent growth in vitro and metastasis in vivo, and mirrors the function and normal tissue expression patterns of the human orthologue of TPD52. We believe TPD52 represents a self, non-mutated tumor associated antigen (TAA) important for maintaining a transformed and metastatic cellular phenotype. The transgenic adenocarcinoma of the mouse prostate (TRAMP) model was employed to study mD52 as a vaccine antigen. Naïve mice were immunized with either recombinant mD52 protein or plasmid DNA encoding the full-length cDNA of mD52. Following immunization, mice were challenged with a subcutaneous, tumorigenic dose of mD52 positive, autochthonous TRAMP-C1 tumor cells. Sixty percent of mice were tumor free 85 days post challenge with TRAMP-C1 when immunized with mD52 as a DNA-based vaccine admixed with soluble granulocyte-macrophage colony stimulating factor (GM-CSF). Survivors of the initial tumor challenge rejected a second tumor challenge given in the opposite flank approximately 150 days after the first challenge, and remained tumor free for more than an additional 100 days. The T cell cytokine secretion patterns from tumor challenge survivors indicated that a T_H1-type cellular immune response was involved in tumor protection. These data suggest that mD52 vaccination induced a memory, cellular immune response that resulted in protection from murine prostate tumors that naturally over express mD52 protein.

Keywords DNA vaccine · mD52 · TPD52 · TRAMP-C1 · GM-CSF

Abbreviations

TPD52	Tumor protein D52
mD52	Murine TPD52
hD52	Human TPD52
TRAMP	Transgenic adenocarcinoma of the mouse prostate
TAA	Tumor associated antigen

Introduction

Chromosome 8q gain is one of the most frequently identified cytogenetic aberrations in human cancer [1]. Amplification mapping studies have identified several candidate cancer associated genes at chromosome 8q21

J. D. Lewis · R. K. Bright (✉)
Department of Microbiology and Immunology,
Texas Tech University Health Sciences Center,
3601 4th street, MS 6591, Lubbock, TX 79430, USA
e-mail: robert.bright@ttuhsc.edu

J. D. Lewis
e-mail: jennifer.lewis@ttuhsc.edu

L. A. Sullivan
Department of Surgery, University of Texas Southwestern Medical Center, Dallas, TX, USA

J. A. Byrne
Discipline of Paediatrics and Child Health,
Children's Hospital at Westmead, The University of Sydney,
Sydney, NSW, Australia

W. de Riese · R. K. Bright
Department of Urology, Texas Tech University Health Sciences Center, Lubbock, TX, USA

Published online: 24 January 2009

[2, 3] the most definitive of which is *tumor protein D52* (*TPD52* or *D52*) at 8q21.13 [4]. All D52-like sequences either identified or predicted to date include coiled-coil domains, suggesting that protein–protein interactions are integral to their function [5]. Human D52 (hD52) protein is over expressed in breast [4, 6, 7], prostate [8–10] and ovarian cancers [11], and is likely a result of increased gene copy number. Expression microarray analyses predict hD52 over expression in many other cancer types, including multiple myeloma [12, 13], Burkitt's lymphoma [14, 15], pancreatic cancer [16], testicular germ cell tumors [17–19], and melanoma [20, 21].

The murine orthologue of *TPD52* (m*D52*) naturally mirrors h*D52* with respect to known function and over expression in tumor cells, and shares 86% protein identity with the human orthologue [22]. Recently we demonstrated that transfection and stable expression of *mD52* cDNA in mouse 3T3 fibroblasts (3T3.mD52) induced increased proliferation, anchorage independent cell growth, and the ability to form subcutaneous tumors and spontaneous lethal lung metastases in vivo when 3T3.mD52 cells were inoculated subcutaneously into naïve, syngeneic, immunocompetent mice [23]. Together these data strongly suggest that *D52* expression may be important for initiating and perhaps maintaining a tumorigenic and metastatic phenotype and thus may be important for tumor cell survival.

Scanlan and colleagues identified *hD52* as a candidate breast cancer tumor associated antigen (TAA) by using sera from breast cancer patients to screen a library of expressed genes from breast cancer tissue, demonstrating that hD52 protein in tumor cells is capable of inducing IgG antibodies [24]. This report suggests that hD52 protein may be immunogenic and capable of inducing a cellular immune response, thus warranting study of TPD52 protein as an anti-cancer vaccine. In a recent study, we demonstrated for the first time that mD52 is immunogenic when administered as recombinant protein-based vaccine admixed with CpG/ODN 1826 in mice. The immune response generated was capable of rejecting tumor cells that naturally over express mD52 protein without inducing harmful autoimmunity [25]. These data suggest that hD52 protein may also be a potent vaccine antigen that could be administered to patients to treat or prevent cancers that over express *hD52*.

In the present study, we sought to determine whether mD52 DNA vaccination would induce an immune response capable of rejecting tumors in the transgenic adenocarcinoma of the mouse prostate (TRAMP) model of prostate cancer [26]. Approximately 60% of mice were tumor free 85 days post challenge with autochthonous TRAMP-C1 tumor cells when immunized with mD52 as a DNA vaccine admixed with soluble granulocyte-macrophage colony stimulating factor (GM-CSF). Survivors of initial tumor challenge rejected a second tumor challenge given in the opposite flank more that 150 days after the initial challenge was given. These mice remained tumor free for more than an additional 100 days. The T cell cytokine secretion patterns from tumor challenge survivors indicated that a T helper 1-type cellular immune response was involved in tumor protection. Together, these data suggest that mD52 DNA-based vaccination induced a cell-mediated, memory immune response that resulted in protection from prostate tumors that naturally over express mD52 without the induction of discernable harmful side effects.

Materials and methods

Mice and tumor cell lines

Male 6- to 8-week-old C57BL/6 mice were purchased from Jackson Labs (Bar Harbor, ME). All animals were cared for and treated according to Institutional Animal Care and Use Committee guidelines at Texas Tech University Health Sciences Center (Lubbock, TX, USA). The tumorigenic, autochthonous C57BL/6 cell lines TRAMP-C1 and TRAMP-C2 [27] were used for tumor challenge and/or immunoassays, and the tumorigenic SV40-transformed Balb/c murine kidney cell line designated mKSA was used as an mD52 positive MHC mis-matched control target for immunoassays. The mKSA cell line was cultured in RPMI 1640 (Fisher Scientific, Pittsburgh, PA, USA) supplemented with 10% heat-inactivated fetal bovine serum, 2 mmol/l L-glutamine, 250 ng/ml fungizone, 50 IU/ml penicillin, 50 μg/ml streptomycin, 50 μg/ml gentamicin sulfate, and 10 mmol/l HEPES. The autochthonous TRAMP-C1 and TRAMP-C2 cell lines were cultured as previously reported [27].

Immunization and tumor cell challenge

Individual mice were immunized (s.c.) with 100 μg of mD52 DNA admixed with 5 μg of recombinant murine GMCSF for a total of 2 injections given at 14 day intervals followed by a booster immunization given 35 days after the second immunization. Empty vector DNA (pCDNA 3.1 vector minus mD52 cDNA) served as a control immunization. Mice in all groups were bled from the dorsal tail vein prior to immunization and 2 weeks following each immunization. Two weeks following the final immunization, mice in all groups were challenged with a tumorigenic dose of autochthonous TRAMP-C1 (5×10^6) tumor cells. Tumor cells were harvested, counted and re-suspended in PBS (Fisher Scientific, Pittsburg, PA, USA) and 100 μl of viable cell suspension was injected subcutaneously in the right flank of each mouse. Tumor size was determined by

taking perpendicular measurements with calipers every 2–3 days and tumor volume (mm^3) was calculated using the following formula: $(a \times b^2)/2$, where b is the smaller of the two measurements. Mice that survived the primary challenge were re-challenged in the opposite flank with TRAMP-C1 (5×10^6) approximately 150 days after the initial challenge.

To compare mD52 DNA with recombinant mD52 protein as active vaccines, individual mice were immunized either i.m. or s.c. four times at 14 day intervals with 10 μg of recombinant mD52 protein admixed with 10 μg of CpG oligonucleotide (ODN 1826: TCCATGACGTTCCTGACGTT) [25]. The protein vaccines were administered as an alum precipitate and a booster of the same dose was given approximately 2 weeks following the third immunization for a total of four injections. mD52 DNA immunizations were administered as described above. Two weeks after the booster immunizations mice were challenged s.c. with TRAMP-C1 tumor cells (5×10^6) and tumor size was monitored as described above.

Analysis of cytotoxic T lymphocyte (CTL)-mediated tumor cell lysis

T cells from immunized mice were stimulated in vitro by culturing ficol separated spleen cells from immunized mice that survived tumor challenge and subjecting them to standard CTL-mediated tumor cell lysis analysis. CTLs were generated by culturing spleen cells with irradiated TRAMP-C1 tumor cells (using the same tumor cell line as was used for the in vivo challenge) in the presence of IL-2 (10 ng/ml), IL-7 (5 ng/ml), and IL-12 (5 ng/ml) at 37°C for 5–7 days. Specificity was evaluated by mixing various numbers of CTLs with a constant number target cells (5×10^3 cells per well) in 96 well round bottom plates. Specific lysis was determined using a Europium time-resolved fluorescence based 2 h method and measured using a Victor3^{TM} plate reader (Perkin Elmer, Boston, MA, USA). Percent lysis was calculated as: % specific lysis $= 1 - (E - S)/(M - S) \times 100$, where E represents Eu release in the presence of effector cells, S is spontaneous Eu release in medium alone and M represents maximum Eu released in the lysis buffer [25, 28]. To confirm H-2^b-restricted tumor recognition tumor targets included TRAMP-C1 tumor cells (H-2^{b+}, mD52$^+$; cell line used for tumor challenge), TRAMP-C2 tumor cells (H-2^{b+}, mD52$^+$), and mKSA (Balb/c) tumor cells which served as a control MHC mis-matched target (H-2^{d+}, mD52$^+$).

T cell culture and ELISAs for cytokine production

T cells from mD52 DNA immunized mice were stimulated in vitro by culturing ficol separated spleen cells with irradiated TRAMP-C1 tumor cells (the same tumor cell line used for the in vivo challenge) in the presence of IL-2 (10 ng/ml), IL-7 (5 ng/ml), and IL-12 (5 ng/ml) at 37°C for 5–7 days. Assessment of cytokine secretion by tumor-specific T cell cultures was accomplished by applying culture supernatants to commercially available sandwich ELISA kits for IFN-γ, IL-10, IL-4 and IL-17 detection (R&D Systems, Minneapolis, MN, USA). Culture supernatants were harvested from 24 h cultures of T cells (1×10^6 cells/ml in 200 μl of medium in 96 well plates) in medium alone, compared to T cells cultured with various tumor cell targets (1:1 ratio). TRAMP-C1 tumor cells (H-2^{b+}, mD52$^+$; cell line used for tumor challenge), TRAMP-C2 tumor cells (H-2^{b+}, mD52$^+$), mKSA (Balb/c) tumor cells which served as a control MHC mis-matched target (H-2^{d+}, mD52$^+$), and Yac-1 as a control for the presence of non-specific cells. To confirm MHC-I restricted tumor recognition, blocking assays were performed by incubating TRAMP-C1 tumor cells with anti-H-2^b or anti-H-2^d (negative control) mAb prior to incubation with T cells. Briefly, 10 μl of mAb in PBS (final concentration of 30 μg/ml) was added to individual wells of 96 well round bottom plates in duplicate. Next, 100 μl TRAMP-C1 tumor targets was added to each well and incubated for 30 min at room temperature. Finally, 100 μl of T cell effectors was added to the appropriate wells and the plates were incubated for 24 h at 37°C. Assays were analysed using the Victor3^{TM} plate reader (Perkin Elmer, Boston, MA, USA). We preformed all assays with the internal controls provided by the manufacturer and the standards from which standard curves were generated in order to determine concentration of cytokines produced in experimental sets. All the controls provided by the manufacturers worked indicating that the assays were able to detect the cytokines in question.

Elispot assay for IFN-γ production

Following immunization with mD52 DNA and subsequent TRAMP-C1 tumor cell protection, T cell responses specific for TRAMP-C1 tumor cells were assessed using a murine IFN-γ Elispot assay following the manufacturer's instructions (R&D Systems, Minneapolis, MN, USA). Briefly, splenic mononuclear cells from immunized mice that successfully rejected in vivo TRAMP-C1 tumor challenge were isolated and T cells were cultured either alone as a negative control, with 5 μg/ml of the T cell mitogen CON-A as a positive control, with mKSA control tumor cell target (Balb/c H-2^d, MHC mismatched), or with TRAMP-C1 tumor cells and incubated overnight at 37°C and 5% CO_2. T cells were plated at 100,000 cells (100 μl)/well with irradiated tumor cells at 1,000 cells (20 μl)/well. Following T cell/tumor cell incubation, wells were washed a total of four times. Next, 100 μl of detection antibody was added per

well and incubated overnight at 4°C. Following incubation, plates were washed four times as above and 100 µl of streptaviden-AP was added per well and incubated for 2 h at room temperature. After four plate washes, 100 µl of developing solution was added per well and incubated 1 h at room temperature in the dark. Finally, plates were rinsed with water and dried completely at room temperature. The AID Viruspot automated ELISpot reader (CTI Technologies Inc., Columbia, MD, USA) was used to analyze spot counts. Data are represented as the number of IFN-γ spots per 100,000 cells.

Flow cytometry

Lymphocytes from spleens cultured in vitro with TRAMP-C1 as described above were stained with monoclonal antibodies specific for CD3, CD4, CD19, NK marker and CD8. MHC class I expression was assessed on tumors cell lines. Antibodies were purchased from BD-Bioscience (San Jose, CA, USA). Cells were fixed in 1% paraformaldehyde at 4°C for 1 h and then analyzed by flow cytometry using a BD-FacsVantage^{TM}.

Statistical analysis

When necessary, tumor challenge data were analyzed with a *t* test to determine whether significant differences existed between mean tumor volume for mD52 immunized and control immunized mice. Elispot and ELISA data were analyzed using an unpaired *t* test for independent samples with equal variances. A *P* value of less than 0.05 was taken as being of statistical significance (GraphPad Prism 5.0).

Results

Superior CTL induction following immunization with mD52 DNA

Since mD52 is an intracellular protein we were interested in determining if MHC class I restricted CTLs were induced in mice following immunization with mD52 DNA and GM-CSF or mD52 protein and CpG/ODN. Previously, we reported that TRAMP-C1, TRAMP-C2 (C57BL/6, H-2^b) and mKSA (Balb/c H-2^d) all over express *mD52* making these cell lines suitable targets and controls with which to address mD52 vaccine induced tumor immunity [25]. Groups of mice were immunized subcutaneously (s.c.) with either plasmid DNA encoding the full-length cDNA for mD52 admixed with recombinant murine GM-CSF (PeproTech) or with recombinant mD52 protein admixed with CpG/ODN in alum every 14 days as depicted in Fig. 1a and b. In separate experiments mice were immunized intramuscularly (i.m.) with recombinant mD52 protein admixed with CpG/ODN in alum (Fig. 1a) [25]. Following immunizations, splenocytes were harvested and analyzed for tumor-specific killing as described in the methods section. Effector CTLs were generated by 5–7 days TRAMP-C1 mixed lymphocyte tumor culture (MLTC) and were determined by flow cytometry to contain approximately 30% CD4$^+$ T cells and 30% CD8$^+$ T cells (not shown). Targets consisted of syngeneic MHC class I matched, autochthonous TRAMP-C1 and TRAMP-C2 tumor cells, and allogeneic MHC class I mis-matched mKSA tumor cells.

Cytotoxic T lymphocytes generated from mice immunized with mD52 DNA + GM-CSF demonstrated MHC class I restricted lysis of mD52 positive tumor cells (Fig. 2). Specific lysis of the syngeneic TRAMP-C1 and TRAMP-C2 tumor cells, for an E:T ratio of 1:100, averaged nearly 90 and 60% for TRAMP-C1 and TRAMP-C2 tumor cells, respectively (Fig. 2a, b). CTLs generated from mice immunized with mD52 protein and CpG/ODN in alum demonstrated MHC class I restricted lysis of mD52 positive tumor cells whether the vaccine was administered s.c. or i.m. (Fig. 2c–f). Specific lysis of the syngeneic TRAMP-C1 and TRAMP-C2 tumor cells, for an E:T ratio of 1:100, averaged from ~50 to ~80% for TRAMP-C1 tumor cells (Fig. 2c–f) and slightly less for TRAMP-C2 tumor cells (Fig. 2c–f). Whereas, the percent specific lysis was <10% for the H-2^d, mD52+ control target mKSA (Fig. 2a–f). Of note, mice immunized with mD52 DNA s.c. without GM-CSF failed to generate a significant cellular immune response (not shown). Taken together, these data suggest that immunization with mD52 DNA generates superior MHC class I restricted CTL responses against mD52+ tumor cells, and the TRAMP-C1 autochthonous tumor cell line is somewhat more readily lysed than the TRAMP-C2 autochthonous tumor cell line. Based on these data TRAMP-C1 tumor cells were used for all subsequent in vivo tumor challenge experiments.

Superior tumor protection following immunization with mD52 DNA

To determine whether it was possible to induce tumor protective immunity following vaccination with mD52, groups of C57BL/6 mice were immunized with either purified recombinant mD52 protein admixed with CpG/ODN or mD52 DNA admixed with soluble GM-CSF as depicted in Fig. 1, and protection from subsequent TRAMP-C1 tumor challenge was evaluated (Fig. 3). Immunization groups included mD52 protein admixed with CpG/ODN as an alum precipitate administered s.c. or i.m., and mD52 DNA admixed with GM-CSF administered s.c. Control immunizations included CpG/ODN in alum

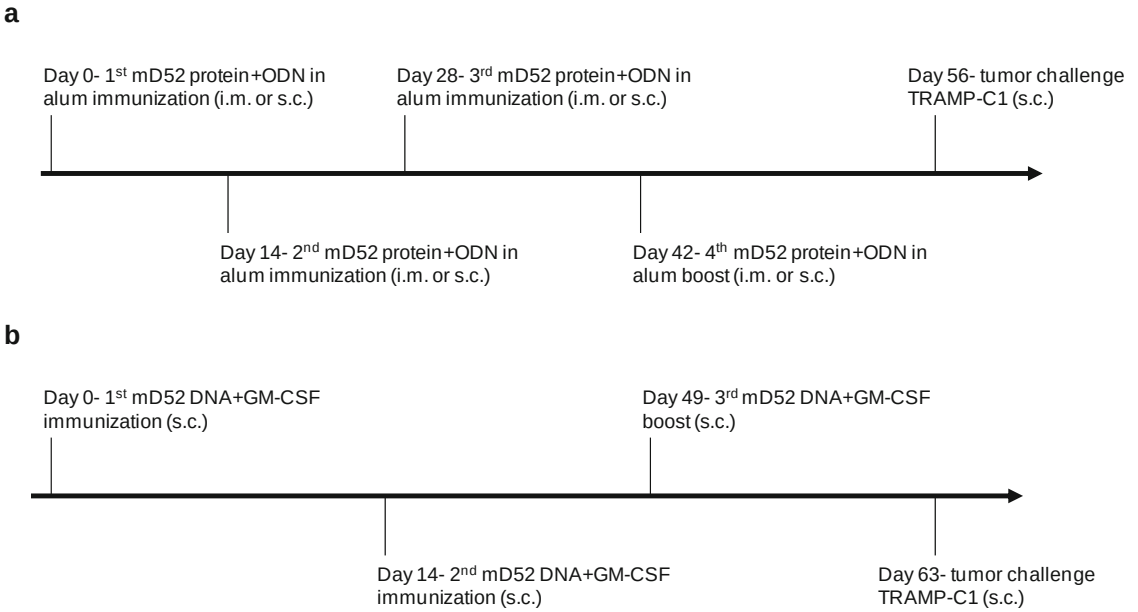

Fig. 1 mD52 DNA and mD52 protein immunization schedules. **a** Immunization schedule for recombinant mD52 protein with ODN in alum. Groups of mice were immunized with mD52 protein admixed with ODN as an alum precipitate either i.m. or s.c. every 14 days for a total of 4 immunizations. Controls included alum alone and ODN in alum administered either i.m. or s.c. Approximately 14 days after the final immunization mice were challenged s.c. with 5×10^6 autochthonous TRAMP-C1 tumors cells. Tumor formation was monitored as described in the methods section. **b** Immunization schedule for mD52 plasmid DNA with soluble GM-CSF in PBS. Groups of mice were immunized with mD52 plasmid DNA admixed with GM-CSF in PBS s.c. on day 0, day 14 and day 49 for a total of 3 immunizations. Controls included empty vector DNA in PBS or PBS alone administered s.c. Approximately 14 days after the final immunization mice were challenged s.c. with 5×10^6 autochthonous TRAMP-C1 tumors cells. Tumor formation was monitored as described in the methods section. See methods for concentrations of protein, CpG/ODN, DNA and GM-CSF. $N = 10$ for each group

administered both s.c. and i.m, alum alone administered both s.c. and i.m, vector only DNA in PBS or PBS alone both administered subcutaneously. The expense of GM-CSF precluded the inclusion of it alone as a vaccine strategy, however numerous published studies have supported the wide spread belief that GM-CSF without antigen is insufficient for inducing protective tumor immunity.

Tumor inoculation and growth was determined as described in the methods section. All mice (100%) immunized with mD52 remained tumor free 50 days following s.c. challenge with a tumorigenic dose of TRAMP-C1 tumor cells, compared to 20% of control immunized mice (Fig. 3). By day 65 post tumor challenge none of the control immunized mice were tumor free. Interestingly, only mice immunized either with mD52 DNA + GM-CSF s.c. or mD52 protein + ODN i.m. remained 60% tumor free by day 65 post tumor challenge. By day 110 post tumor challenge 40% of mice immunized with mD52 DNA + GM-CSF s.c. remained tumor free compared to all other immunizations groups for which all mice had developed s.c. tumors >1 cm × 1 cm (Fig. 3). Of note, 4/10 mice immunized with mD52 DNA + GM-CSF failed to develop palpable tumors at all. These data demonstrate that immunization with mD52 DNA + GM-CSF prior to challenge with TRAMP-C1 tumor cells results in protection from tumor challenge in 40% of mice, compared to mD52 protein + ODN and control immunized animals.

mD52 DNA immunization and tumor protection induces a tumor-specific memory response

Next, we evaluated whether immunization with mD52 DNA admixed with murine GM-CSF was capable of eliciting memory immune responses against secondary challenge with TRAMP-C1 tumor cells. Groups of mice were given three injections with mD52 DNA + GMCSF every two weeks as described in Fig. 4a. A total of 14 days following the final booster immunization animals were challenged with a tumorigenic dose of TRAMP-C1 tumor cells s.c. in the right flank. Primary tumor formation was monitored for 268 days and approximately 80% of the immunized animals remained tumor free (Fig. 4b). Approximately, 150 days following the initial tumor challenge (day 192 following the first immunization), all mice that were tumor free were given a second inoculation of TRAMP-C1 tumor cells in the opposite (left) flank. All mice (100%) that received the secondary tumor challenge in the opposite flank remained tumor free for approximately 6 months following the final immunization which equals 110 days following secondary challenge

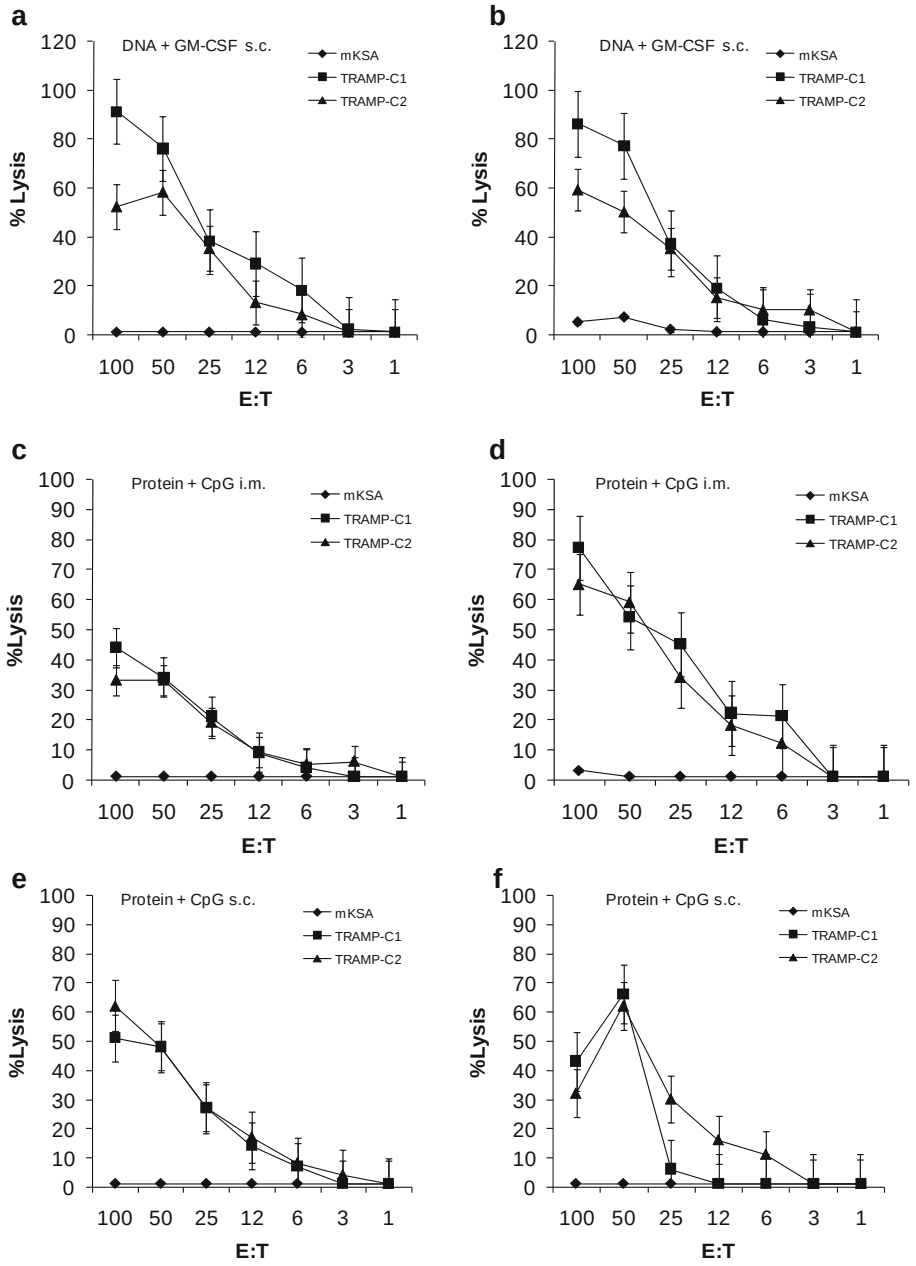

Fig. 2 Cytotoxic T lymphocyte response following immunization with mD52 DNA or mD52 protein. **a**, **b** CTL responses from mice immunized with mD52 DNA + GM-CSF in PBS administered s.c. **c**, **d** CTL responses from mice immunized with mD52 protein + CpG (ODN) in alum administered i.m. **e**, **f** CTL responses from mice immunized with mD52 protein + CpG (ODN) in alum administered s.c. The autochthonous C57BL/6 TRAMP-C1 and TRAMP-C2 cell lines were derived from spontaneous tumors from the TRAMP model of prostate cancer. The Balb/c derived tumor cell line mKSA served as a control for MHC class I restriction. Shown are CTL responses from 2 representative mice from each vaccine group. Values shown are the mean ± SEM for triplicate determinations

(Fig. 4c). It is likely the animals would have remained tumor free for much longer however, the experiment was terminated after 10 months for the evaluation of cellular immunity. Of note, the secondary tumor challenge was given 150 days after the primary challenge, and both the primary and secondary challenge were rejected. The fact that the animals rejected two tumor challenges separated by nearly 5 months without receiving an immunization beyond day 28, along with the significant delay from primary tumor challenge before the secondary tumor challenge was given suggests induction of tumor-specific memory immunity as a result of immunization with mD52 DNA + GM-CSF.

Immunization with mD52 DNA does not induce autoimmunity

Since mD52 is a "self antigen", that is it is expressed in some normal tissues as well as in tumors to include TRAMP-C1 tumor cells [25], it is possible that tolerance could prevent the induction of an immune response. Conversely, if tolerance is broken and an immune response is generated against mD52, there is the potential for the induction of harmful autoimmunity. As shown by the generation of antigen-specific CTLs to mD52 expressing tumors (Fig. 2), and by the induction of an immune response against mD52 following immunization that was

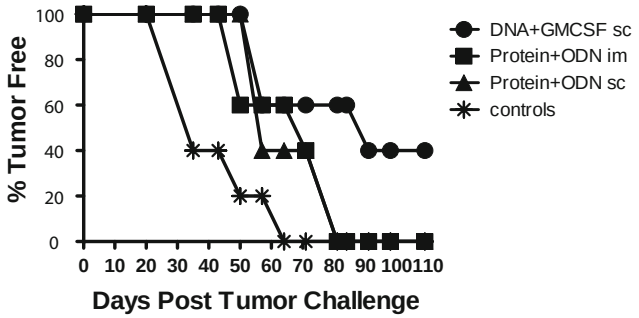

Fig. 3 Protection from TRAMP-C1 tumor cell challenge following mD52 immunization. Mice were immunized according to the schedule in Fig. 1 and as described in the methods section. Subcutaneous tumor growth was measured over time and compared for each immunization group as % tumor free mice over time (days post tumor challenge). Shown are representative results for repeated experiments comparing mice immunized with mD52 DNA + GM-CSF administered s.c. (*DNA + GMCSF sc*) to mice immunized with mD52 protein +CpG (ODN) administered i.m. (*Protein + ODN im*) or administered s.c. (*Protein + ODN sc*). All control immunizations are shown as a single representative line graph (*controls*) and include ODN in alum, alum alone, empty vector DNA in PBS and PBS alone. $N = 10$ for each group

capable of rejecting mD52-expressing tumor challenge in vivo (Fig. 4), it is clear that indeed tolerance to the self antigen mD52 was broken by active vaccination. Therefore, it was of interest to assess whether autoimmunity was also induced. Following methods previously reported by our lab, autoimmunity induction was assessed in the kidneys of mice that were immunized with mD52 and survived tumor challenge [25]. Individual mice that were immunized with mD52 and survived tumor challenge showed no gross morbidity and appeared healthy throughout the study. Immunohistochemical analysis of the kidneys [25] showed no T cell infiltrates and no evidence of microscopic pathology compared to kidneys from naïve mice serving as normal controls (not shown). No evidence of gross pathology was observed for livers, lungs or spleens. These data support the conclusions that immunization with mD52 DNA + GM-CSF does not result in the induction of autoimmunity.

Induction of T_H1-type cellular immunity following immunization with mD52 DNA

Since mD52 is expressed as an intracellular protein by tumor cells it was important to determine if cellular immune responses were induced in animals that were immunized with mD52 and rejected primary and secondary tumor challenges. As shown in Fig. 2, we established that vaccination with mD52 induced CTL responses that were tumor-specific. It was of interest to determine if vaccine induced cellular immunity reflected a T_H1-type response, thus supporting the generation of CTLs. Splenocytes were harvested from mice that were immunized with mD52 DNA + GM-CSF and survived both a primary and a secondary tumor challenge with TRAMP-C1 tumor cells and cultured with irradiated TRAMP-C1 cells for 5–7 days in the presence of IL-2. Following the MLTC, splenocytes were harvested ficol separated, and incubated in vitro with irradiated tumor cells for 24 h as described in the methods section. Next, supernatants were collected and assayed by ELISA for the presence of IL-4, IL-17, IFN-γ and IL-10 (Fig. 5). Neither IL-4 nor IL-17 was detected in supernatants from cultured T cells derived from vaccinated mice that survived tumor challenge (not shown). These data indicate that neither a T_H2 nor a T_H17 cellular immune response was induced by mD52 DNA vaccination nor did they play a role in tumor protection. This finding was not surprising given that we detected specific-CTL responses as a result of mD52 vaccination (Fig. 2). As expected we were able to detect IFN-γ in supernatants from cultured T cells derived from vaccinated mice that survived tumor challenge (Fig. 5a). The amount of IFN-γ present in 24 h supernatants was at least twice as much when TRAMP-C1 or TRAMP-C2 were the targets compared to control targets. For example, T cells from mouse 3 secreted 500–600 pg of IFN-γ/ml/24 h when TRAMP-C1 or TRAMP-C2 tumor cells were the targets compared to approximately 250 pg/ml/24 h or less when Yac-1 or mKSA were the targets (Fig. 5a). These data suggest that there are mD52-induced, TRAMP tumor cell-specific T cell responses in immunized mice that survived TRAMP-C1 tumor cell challenge. This was confirmed by the ability of H-2^b, class I MHC specific mAb to significantly inhibit production of IFN-γ when included in 24 h cultures of T cells and TRAMP-C1 target cells (Fig. 5a, $P < 0.05$). Class I MHC-specific antibody inhibition was consistently about 50% of that of T cells and TRAMP-C1 target cells without antibody. Anti-H-2^d mAb failed to inhibit IFN-γ production by T cells cultured with TRAMP-C1 tumor cells (not shown). The background observed when T cells were cultured with control targets could be attributed to non-specific NK-like or LAK-like cells, given that the MLTC was not selected for $CD8^+$ T cells and contained relatively large amounts of IL-2. However, taken together these data indicate that mD52 DNA immunization induces an antigen-specific, class I MHC-restricted cellular immune response that is likely responsible for the observed tumor protection in vivo.

Previously, we reported that mD52 expression in tumor cells was associated with increased tumor secretion of TGF-β1 [23]. It has been suggested that TGF-β1 and IL-10 may induce regulatory T cells that could dampen immunity to self antigens [29]. Interestingly, we did not observe 100% tumor protection in any of our vaccine experiments, and knowing that mD52 is a self TAA along with the fact

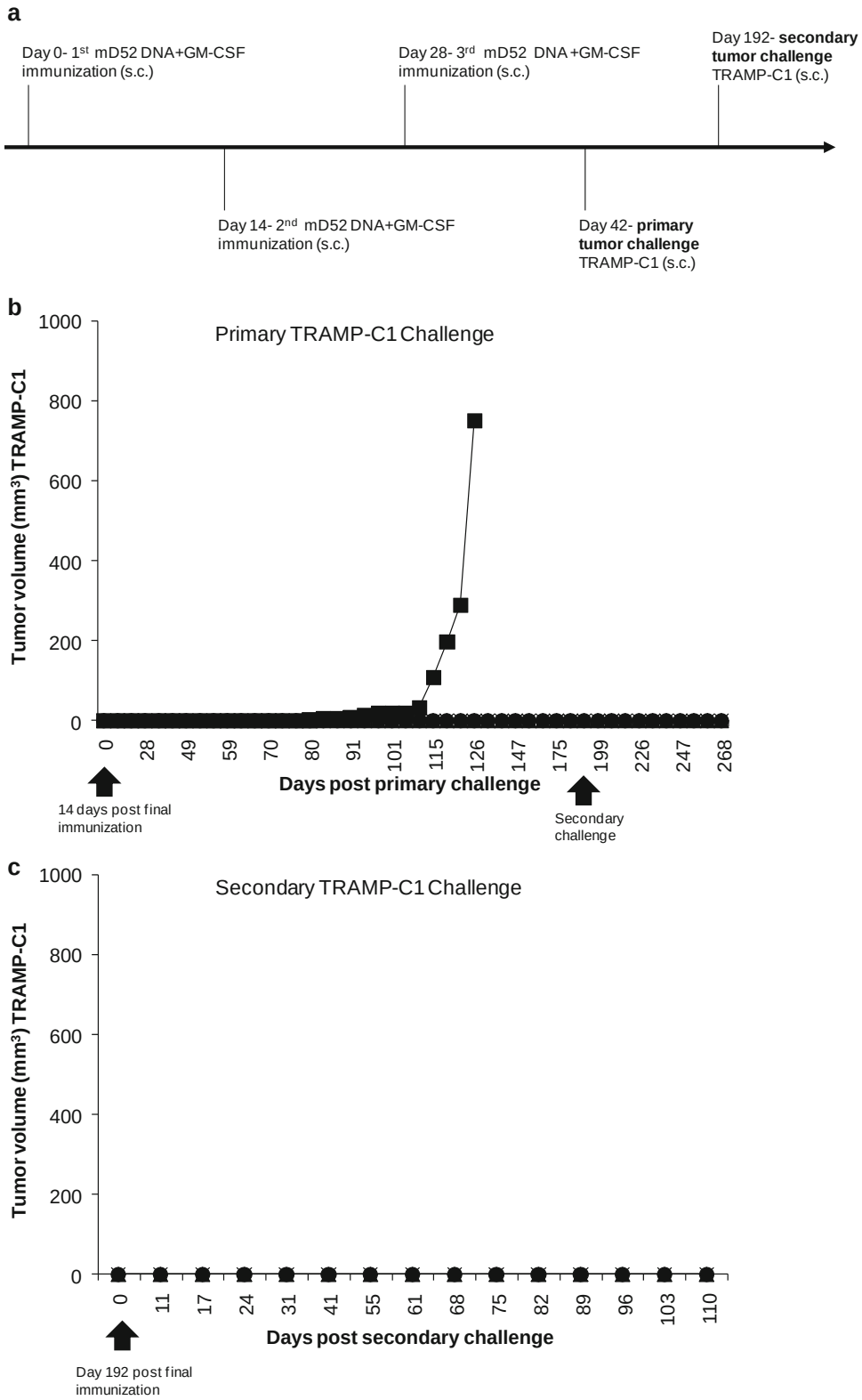

Fig. 4 Immunization with mD52 DNA + GM-CSF induces memory against tumor challenge. Groups of mice were immunized with mD52 DNA admixed with murine GM-CSF administered s.c. as described in the methods sections. **a** Mice were immunized three times s.c. every 14 days and challenged with 5×10^6 autochthonous TRAMP-C1 tumor cells s.c. (*right flank*) 14 days after the last immunization (*primary tumor challenge*). On day 192, approximately 150 days after the primary tumor challenge, mice that rejected the primary tumor challenge in the right flank were given a secondary s.c. tumor challenge with 5×10^6 TRAMP-C1 tumor cells in the left flank. **b** Primary TRAMP-C1 tumor challenge, right flank. Shown is s.c. TRAMP-C1 tumor volume over time (*days post primary challenge*) for mice immunized with mD52 DNA + GM-CSF s.c. Day 0 is the 14 days after the final immunization. An *arrow* marks day 192 when the secondary TRAMP-C1 tumor challenge was administered in the opposite flank. **c** Secondary TRAMP-C1 tumor challenge, left flank. Shown is s.c. TRAMP-C1 tumor volume over time (*days post secondary challenge*) for mice immunized with mD52 DNA + GM-CSF s.c. that rejected a s.c. primary TRAMP-C1 tumor challenge in the right flank. Day 0 is the 192 days after the final immunization, and 150 days after protection from the primary TRAMP-C1 tumor challenge. $N = 5$ for the primary tumor challenge. Shown are representative results for repeated experiments

that mD52 expressing tumors secrete TGF-β1, we were interested in determining if IL-10 was involved in the vaccine induced immune response. IL-10 secretion by T cells generated as described above was measured by specific ELISA. Unlike IL-4 and IL-17 we were able to detect IL-10 in supernatants from all immunized and tumor challenge survivor mice (Fig. 5b). However, the amount of INF-γ was as much as ten-fold more than IL-10, suggesting

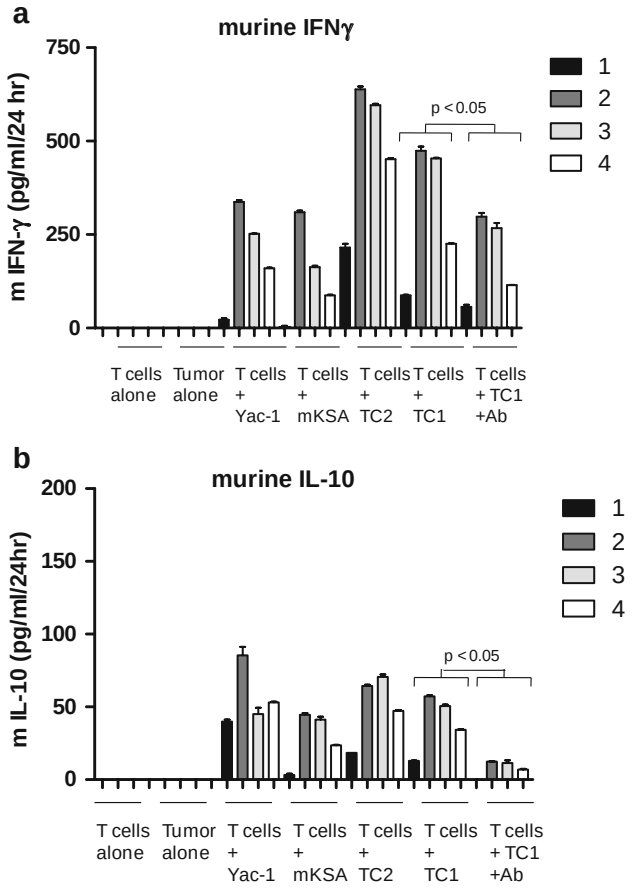

Fig. 5 T lymphocyte cytokine production following mD52 DNA + GM-CSF immunization and tumor protection. Shown are results from standard antigen capture ELISAs measuring the production of cytokines in the supernatants of splenocytes harvested from mice that were immunized with mD52 DNA + GM-CSF and survived both a primary and a secondary tumor challenge with TRAMP-C1 tumor cells and cultured with irradiated TRAMP-C1 cells for 5–7 days in the presence of IL-2. Data are presented as bar graphs depicting pg/ml/24 h of cytokine for T cells cultured alone or with various targets. Targets include: TRAMP-C1 (TC1), TRAMP-C2 (TC2), Yac-1 (control for NK cells) and mKSA tumor cells (MHC class I mis-matched control). To confirm MHC class I restriction T cells were cultured with TRAMP-C1 in the presence of mAb specific for H-2^b class I MHC (T cells + TC1 + Ab). Tumor alone represents each of the tumor cell targets cultured alone. Bars numbered in the legend 1–4 represent each of 4 individual mice. **a** ELISA for the detection of murine IFN-γ, **b** ELISA for the detection of murine IL-10. Shown are representative results for repeated experiments. Values shown are the mean ± SEM for duplicate determinations. Data were analyzed using an unpaired *t* test for independent samples with equal variances and $P < 0.05$ was determined to be significant (GraphPad Prism 5.0)

that IFN-γ played a more dominant role in tumor protection and that in survivor mice the vaccine overcame any possible involvement of regulatory T cells. We did not evaluate cytokine production in vaccinated mice that failed to reject primary tumor challenge. However, it is interesting to speculate that the amount of IL-10 may have been as much as ten-fold greater than INF-γ in vaccinated mice that developed tumors suggesting that in some cases regulatory T cells may have dampened the response to the self antigen mD52 following vaccination. The background observed when T cells were cultured with control targets could be attributed to non-specific NK-like or LAK-like cells generated in bulk MLTC in the presence of IL-2. For all ELISA experiments, Yac-1 served as a control for NK-like or LAK-like non-specific cell activity in the bulk MLTC and mKSA served as an mD52 positive, class I MHC mismatched target. T cells cultured alone without tumor cells and tumor cells cultured alone without T cells failed to secrete detectable levels of any of the cytokines evaluated (Fig. 5a–d).

To examine further the induction of T_H1-type immunity we performed overnight IFN-γ Elispot assays using uncultured T cells from immunized mice that survived tumor challenge. As observed for the ELISA assays, we did not detect IFN-γ production unless T cells were cultured with tumor cell targets (Fig. 6). The number of detectable IFN-γ spots was 2–3 times greater when T cells were cultured with TRAMP-C1 cells than when T cells were cultured with control mKSA tumor cell targets and the difference in spot count was determined to be statistically significant (Fig. 6, $P < 0.0001$). In order to illustrate the difference in the number and intensity of spots, representative Elispot wells were included in Fig. 6. The majority of the spots in wells with T cells + mKSA target cells are uniform, pinpoint and very low in intensity, compared to spots in wells with T cells + TRAMP-C1 tumor cells. If we chose to use a more stringent spot size and intensity setting most, if not all the spots in the T cells + mKSA wells would not have been counted. In contrast most of the spots would have been counted in the T cells + TRAMP-C1 wells, indicating that vaccination induced a specific anti-TRAMP-C1 T_H1 immune response. However, the overall number of large and intense spots in the T cells + TRAMP-C1 wells is relatively few. This could reflect a low precursor frequency of mD52-specific T cells, which would be expected given that mD52 is a self TAA. Overall the Elispot data support the conclusions of the CTL assays in Fig. 2 and the ELISA assays in Fig. 5, that mD52 DNA vaccination induces a tumor protective, T_H1-type cellular immune response.

Discussion

This study was undertaken to determine whether vaccines targeting murine TPD52 (mD52) would induce cellular immune responses capable of rejecting TRAMP-C1 tumor cells that over express mD52 protein in a murine model of prostate cancer. For vaccine strategy comparisons, groups

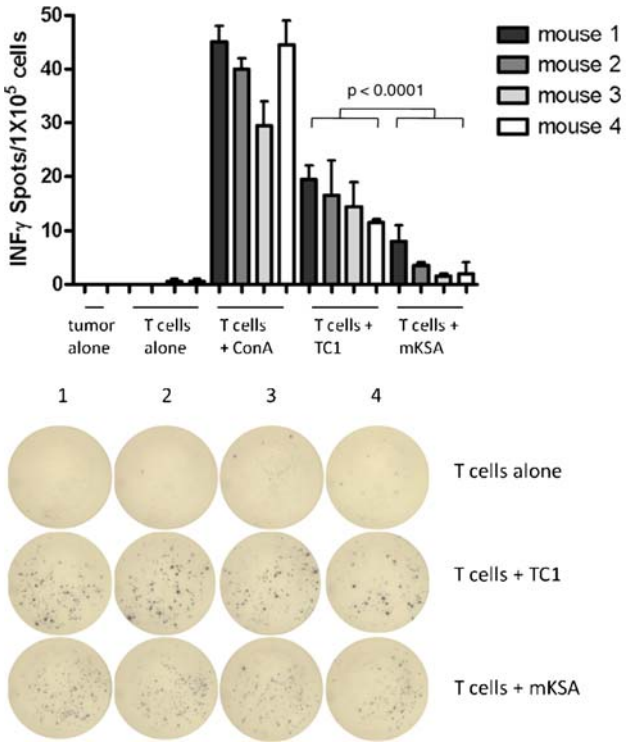

Fig. 6 mD52 DNA + GM-CSF induces tumor reactive T_H1-type cellular immunity. Shown are results from an IFN-γ EliSpot for splenocytes harvested from mice that were immunized with mD52 DNA + GM-CSF and survived both a primary and a secondary tumor challenge with TRAMP-C1 tumor cells and cultured overnight with irradiated target cells. Data are presented as bar graphs depicting IFN-γ spots/1 $\times$ 10^5 T cells cultured alone or with various targets. Targets include: TRAMP-C1 (TC1), and mKSA tumor cells (MHC class I mis-matched control). The mitogen conconavolin A (ConA) served as a positive control for the stimulation of cytokine secretion. Tumor alone represents each of the tumor cell targets cultured alone. *Bars* numbered in the legend 1–4 represent each of 4 individual mice. Shown are representative results for repeated experiments. Values shown are the mean ± SEM for duplicate determinations. Data were analyzed using an unpaired *t* test for independent samples with equal variances and $P < 0.05$ was determined to be significant (GraphPad Prism 5.0)

of male C57BL/6 mice were immunized subcutaneously (s.c.) either with plasmid DNA encoding the full-length cDNA for mD52 admixed with recombinant murine GM-CSF or with recombinant mD52 protein admixed with CpG/ODN in alum every 14 days as depicted in Fig. 1a and b. In separate experiments mice were immunized intramuscularly (i.m.) with recombinant mD52 protein admixed with CpG/ODN in alum (Fig. 1a), as previously reported by our group [25]. All three vaccinations approaches outlined in Fig. 1 were capable of inducing CTLs with specificity for $mD52^+$ TRAMP-derived tumor cells, however, DNA + GM-CSF administered s.c. induced superior CTLs (Fig. 2). Subsequent experiments demonstrated that DNA + GM-CSF as a vaccine approach induced cellular immunity that resulted in tumor protection in vivo (Fig. 4b), and elicited immunologic memory (Fig. 4c) against a subsequent TRAMP-C1 tumor cell challenge (summarized in Table 1). As shown in Fig. 2, we established that vaccination with mD52 DNA + GMCSF induced CTL responses that were tumor-specific. Neither IL-4 nor IL-17 was detected in supernatants from cultured T cells derived from vaccinated mice that survived tumor challenge (Fig. 5a, b). These data suggest that neither a T_H2 nor a T_H17 cellular immune response was induced by mD52 DNA + GM-CSF vaccination and did not likely contribute to or interfere with tumor protection. We were able to detect IFN-γ in supernatants from cultured T cells derived from vaccinated mice that survived tumor challenge (Fig. 5c), suggesting that mD52-induced specific T_H1-type T cell responses in immunized mice that survived TRAMP-C1 tumor cell challenge. This was confirmed by the ability of $H\text{-}2^b$, class I MHC specific mAb to inhibit production of IFN-γ (Fig. 5c). Previously, we reported that mD52 expression in tumor cells was associated with increased tumor secretion of TGF-β1 [23]. It has been suggested that TGF-β1 and IL-10 may induce regulatory T cells that could dampen immunity to self antigens [29]. Interestingly, we did not observe complete tumor protection in our vaccine experiments. Knowing that mD52 is a self TAA and that mD52 expressing tumors secrete TGF-β,1 we were interested in determining if IL-10 was involved in the vaccine induced immune response. We were able to detect IL-10 in supernatants from immunized and tumor challenge survivor mice (Fig. 5d). However, the amount of INF-γ was as much as 10-fold more than IL-10, suggesting that IFN-γ played a more dominant role in tumor protection and that in survivor mice the vaccine may have overcome any possible involvement of regulatory T cells. We did not evaluate cytokine production in

Table 1 Summary of mD52 vaccine induced protection from TRAMP-C1 tumor cell challenge

Vaccine	T cell response[a]	Tumor protection[b]	Memory response
DNA + GM-CSF s.c.	CTL, IFN-γ	40–80%	100%
Protein + CpG i.m.	CTL	0	ND
Protein + CpG s.c.	CTL	0	ND
Controls[c]	none	0	ND

[a] In vitro T cell response following mD52 vaccination. CTL, tumor cell lysis; IFN-γ, cytokine secretion determined by ELISA and EliSpot

[b] Protection from subcutaneous TRAMP-C1 tumor challenge greater than 110 days post challenge

[c] Controls include: PBS alone, alum alone, alum + CpG, vector plasmid DNA

vaccinated mice that failed to reject primary tumor challenge. However, it is interesting to speculate that the amount of IL-10 may have been as much as 10-fold greater than INF-γ in vaccinated mice that developed tumors suggesting that in some cases regulatory T cells may have dampened the response to mD52 following vaccination. This possibility is currently under investigation. To examine further the induction of T_H1-type immunity we performed IFN-γ Elispot assays using uncultured T cells from immunized mice that survived tumor challenge. The number of detectable IFN-γ spots was 2–3 times greater when T cells were cultured with TRAMP-C1 tumor cells than when T cells were cultured with controls (Fig. 6). Overall, the Elispot data support the conclusions of the CTL assays in Fig. 2 and the ELISA assays in Fig. 5, that mD52 DNA vaccination induces a tumor protective, T_H1-type cellular immune response.

Previously, we immunized mice i.m. with recombinant mD52 protein admixed with CpG/ODN in alum which resulted in the induction of immune responses with specificity for mD52. As a test of tumor immunity, we challenged mice with syngeneic tumor cells that over expressed mD52. Approximately, one half (40–50%) of the mice immunized with recombinant mD52 protein and CpG/ODN in alum rejected s.c. tumor challenge or spontaneous lung metastasis. The observed mD52 vaccine induced tumor protection was associated with the induction of mD52-specific, MHC-restricted CTLs and no detectable evidence of autoimmunity was observed [25]. This previous report demonstrated for the first time that the "self" TAA mD52 is sufficiently immunogenic when administered i.m. as a protein-based vaccine. Moreover, the generation of anti-mD52 CTL resulted in protection from syngeneic tumor cells that naturally over expressed mD52 protein without induction of detectable autoimmunity.

Anti-cancer vaccines targeting self proteins have been applied to treat or prevent multiple cancers in preclinical studies and clinical trials [30, 31]. Tumor protein D52 (TPD52) is a novel and potentially important TAA due to its' over expression in a number of fatal and common cancers to include prostate [8–10], breast [4, 6, 7] and ovarian [11] carcinomas. The human orthologue of TPD52 has been identified as a candidate breast cancer TAA by using sera from breast cancer patients to screen a library of expressed genes from breast cancers, demonstrating that TPD52 is capable of inducing IgG antibodies which would have required induction of T cell help [24]. This report suggests that TPD52 may be immunogenic in humans and also capable of inducing a cellular immune response, thus warranting study of TPD52 as an anti-cancer vaccine to induce cellular immunity.

It is widely accepted that inflammatory cytokines are potent mediators of adaptive immunity against solid tumors. Many cytokines have been and are being evaluated as reagents to augment vaccines as well as other modes of immunotherapy against cancer. Arguably the most studied and perhaps the most potent cytokine for enhancing immune responses against cancer is GM-CSF. GM-CSF has proven to be the most potent immunostimulatory product when applied as a transgene in whole tumor cell-based vaccine studies in murine tumor models [32, 33] and in human clinical trials for multiple cancers to include melanoma and non-small cell lung cancer [32]. Recently, Disis and colleagues [34] demonstrated that recombinant GM-CSF protein administered as a soluble cytokine in conjunction with a self antigen rat neu-DNA-based vaccine, skewed the response towards cell-mediated immunity. The idea of DNA-based tumor vaccines administered with soluble GM-CSF as an adjuvant was further explored by McNeel and colleagues in a rat model where prostatic acid phosphatase (PAP) served as the self—TAA targeted by vaccination [35]. In this study, DNA vaccination + soluble GM-CSF proved to be more effective at generating specific T_H1-type immunity than recombinant virus expressing PAP as a viral vector vaccine. In a clinical trial of DNA vaccination of prostate cancer patients it was demonstrated that DNA encoding prostate specific antigen (PSA) administered with soluble GM-CSF was safe and induced both cellular and humoral immunity against PSA protein [36].

In the present study, we have shown for the first time that the self TAA mD52 is immunogenic when administered as DNA-based vaccine admixed with the soluble cytokine GM-CSF. Further, the cellular immune response generated is capable of rejecting tumor cells that naturally over express mD52 protein without inducing harmful autoimmunity in a model of murine prostate cancer. These findings suggest that the human orthologue of TPD52 may be a vaccine antigen that could be administered to patients to treat or prevent cancers that over express TPD52. For future studies we will assess roles of immune effector cell subsets in tumor protection in vivo by depletion of $CD4^+$ T cells, $CD8^+$ T cells, NK cells or $CD25^+$ regulatory T cells (Treg) using specific monoclonal antibodies. In addition, heterologous prime boost vaccination approaches will be evaluated by immunizing with DNA followed by protein or protein followed by DNA. Since we have in our possession the cDNA for the human orthologue of TPD52 we will also explore the efficacy of a xenogeneic antigen, DNA-based prime boost strategy.

Acknowledgments This work was supported in part by; funds from the Southwest Cancer Treatment and Research Center, the Department of Urology at TTUHSC and by a Howard Hughes Medical Institute grant through the Undergraduate Biological Sciences Education Program to Texas Tech University.

References

1. Myllykangas S, Himberg J, Bohling T, Nagy B, Hollment J, Knuutila S (2006) DNA copy number amplification profiling of human neoplasms. Oncogene 25:7324–7332
2. Rodriguez V, Chen Y, Elkahloun A, Dutra A, Pak E, Chandrasekharappa S (2007) Chromosome 8 BAC array comparative genomic hybridization and expression analysis identify amplification and overexpression of TRMT12 in breast cancer. Genes Chromosomes Cancer 46:694–707
3. Hicks J, Krasnitz A, Lakshmi B, Navin NE, Riggs M, Leibu E, Esposito D, Alexander J, Troge J, Grubor V, Yoon S, Wigler m, Ye K, Borresen-Dale AL, Naume B, Schlicting E, Norton L, Hagerstrom T, Skoog L, Auer G, Maner S, Lundin P, Zetterberg A (2006) Novel patterns of genome rearrangement and their association with survival in breast cancer. Genome Res 16:1465–1479
4. Balleine RL, Fejzo MS, Sathasivam P, Basset P, Clarke CL, Byrne JA (2000) The hD52 (TPD52) gene is a candidate target gene for events resulting in increased 8q21 copy number in human breast carcinoma. Genes Chromosomes Cancer 29:48–57
5. Boutros R, Fanayan S, Shehata M, Byrne JA (2004) The tumor protein D52 family: many pieces, many puzzles. Biochem Biophys Res Commun 325:1115–1121
6. Byrne JA, Tomasetto C, Granier JM, Rouyer N, Mattei MG, Bellocq JP, Rio MC, Basset P (1995) A screening method to identify genes commonly overexpressed in carcinomas and the identification of a novel complementary DNA sequence. Cancer Res 55:2896–2903
7. Pollack JR, Sorlie T, Perou CM, Rees CA, Jeffrey SS, Lonning PE, Tibshirani R, Botstein D, Borresen-Dale AL, Brown PO (2002) Microarray analysis reveals a major direct role of DNA copy number alteration in the transcriptional program of human breast tumors. Proc Natl Acad Sci USA 99:12963–12968
8. Wang R, Xu J, Saramaki O, Visakorpi T, Sutherland WM, Zhou J, Sen B, Lim SD, Mabjeesh N, Amin M, Dong JT, Petros JA, Nelson PS, Marshall FF, He Zhau, Chung LW (2004) *PrLZ*, a novel prostate-specific and androgen-responsive gene of the TPD52 family, amplified in chromosome 8q21.1 and overexpressed in human prostate cancer. Cancer Res 64:1589–1594
9. Wang R, Xu J, Mabjeesh N, Zhu G, Zhou J, Amin N, He D, Marshall FF, He Zhau, Chung LW (2007) PrLZ is expressed in normal prostate development and in human prostate cancer progression. Clin Cancer Res 13:6040–6048
10. Rubin MA, Varambally S, Beroukhim R, Tomlins SA, Rhodes DR, Paris PL, Hofer MD, Storz-Schweizer M, Kuefer R, Fletcher JA, Hsi BL, Byrne JA, Pienta KJ, Collins C, Sellers WR, Chinnaiyan AM (2004) Overexpression, amplification and androgen-regulation of TPD52 in prostate cancer. Cancer Res 64:3814–3822
11. Byrne JA, Balleine RL, Schoenberg Fejzo M, Mercieca J, Chiew Y-E, Livnat Y, St. Heaps L, Peters G, Byth K, Karlan BY, Slamon DJ, Harnett P, deFazio A (2005) Tumor protein D52 (TPD52) is overexpressed and a gene amplification target in ovarian cancer. Int J Cancer 117:1049–1054
12. Largo C, Alvarez S, Saez B, Blesa D, Martin-Subero JI, Gonzalez-Garcia I, Brieva JA, Dopazo J, Siebert R, Calasanz MJ, Ciqudosa JC (2006) Identification of overexpressed genes in frequently gained/amplified chromosome regions in multiple myeloma. Haematologica 91:184–191
13. Tiacci E, Orvietani P-L, Bigerna B, Pucciarini A, Liso A, Pacini R, Verducci B, Pulford K, Pileri S, Gambacorta M, Carbone A, Benedetti R, Sciurpi MT, Binaglia L, Byrne JA, Falini B (2005) A new monoclonal antibody (b-28p) identifies the human tumor protein D52 (TPD52) as a novel B-cell/plasma cell associated molecule with a unique expression pattern. Blood 105:2812–2820
14. Dave SS, Fu K, Wright GW, Lam LT, Kluin P, Boerma EJ, Greiner TC, Weisenburger DD, Rosenwald A, Ott G, Müller-Hermelink HK, Gascoyne RD, Delabie J, Rimsza LM, Braziel RM, Grogan TM, Campo E, Jaffe ES, Dave BJ, Sanger W, Bast M, Vose JM, Armitage JO, Connors JM, Smeland EB, Kvaloy S, Holte H, Fisher RI, Miller TP, Montserrat E, Wilson WH, Bahl M, Zhao H, Yang L, Powell J, Simon R, Chan WC, Staudt LM (2006) Molecular diagnosis of Burkitt's lymphoma. N Engl J Med 354:2431–2442
15. Hummel M, Bentink S, Berger H, Klapper W, Wessendorf S, Barth TF, Bernd HW, Cogliatti SB, Dierlamm J, Feller AC, Hansmann ML, Haralambieva E, Harder L, Hasenclever D, Kühn M, Lenze D, Lichter P, Martin-Subero JI, Möller P, Müller-Hermelink HK, Ott G, Parwaresch RM, Pott C, Rosenwald A, Rosolowski M, Schwaenen C, Stürzenhofecker B, Szczepanowski M, Trautmann H, Wacker HH, Spang R, Loeffler M, Trümper L, Stein H, Siebert R (2006) A biologic definition of Burkitt's lymphoma from transcriptional and genomic profiling. N Engl J Med 354:2419–2430
16. Loukopoulos P, Shibata T, Katoh H, Kokubu A, Sakamoto M, Yamazaki K, Kosuge T, Kanai Y, Hosoda F, Imoto I, Ohki M, Inazawa J, Hirohashi S (2007) Genome-wide array-based comparative genomic hybridization analysis of pancreatic adenocarcinoma: identification of genetic indicators that predict patient outcome. Cancer Sci 98:392–400
17. Skotheim RI, Autio R, Lind GE, Kraggerud SM, Andrews PW, Monni O, Kallioniemi O, Lothe RA (2006) Novel genomic aberrations in testicular germ cell tumors by array-CGH, and associated gene expression changes. Cell Oncol 28:315–326
18. Korkola JE, Heck S, Olshen AB, Reuter VE, Bosl GJ, Houldsworth J, Chaganti RS (2008) In vivo differentiation and genomic evolution in adult male germ cell tumors. Genes Chromosomes Cancer 47:43–55
19. McIntyre A, Summersgill B, Lu YJ, Missiaglia E, Kitazawa S, Oosterhuis JW, Looijenga LH, Shipley J (2007) Genomic copy number and expression patterns in testicular germ cell tumours. Br J Cancer 97:1707–1712
20. Hoek KS (2007) DNA microarray analyses of melanoma gene expression: a decade in the mines. Pigment Cell Res 20:466–484
21. Roesch A, Becker B, Bentink S, Spang R, Vogl A, Hagen I, Landthaler M, Vogt T (2007) Ataxia telangiectasia-mutated gene is a possible biomarker for discrimination of infiltrative deep penetrating nevi and metastatic vertical growth phase melanoma. Cancer Epidemiol Biomarkers Prev 16:2486–2490
22. Byrne JA, Mattei MG, Basset P (1996) Definition of the tumor protein D52 (TPD52) gene family through cloning of D52 homologues in human (hD53) and mouse (mD52). Genomics 35:523–532
23. Lewis JD, Payton LA, Whitford JG, Byrne JA, Smith DI, Yang L, Bright RK (2007) Induction of tumorigenesis and metastasis by the murine orthologue of tumor protein D52. Mol Cancer Res 5:133–144
24. Scanlan MJ, Gout I, Gordon CM, Williamson B, Stockert E, Gure AO, Jager D, Chen YT, Mackay A, O'Hare MJ, Old LJ (2001) Humoral immunity to human breast cancer: antigen definition and quantitative analysis of mRNA expression. Cancer Immun 1:4–20
25. Payton LA, Lewis JD, Byrne JA, Bright RK (2008) Vaccination with metastasis-related tumor associated antigen TPD52 and CpG/ODN induces protective tumor immunity. Cancer Immunol Immunother 57:799–811
26. Gingrich JR, Barrios RJ, Morton RA, Boyce BF, DeMayo FJ, Finegold MJ, Angelopoulou R, Rosen JM, Greenberg NM (1996)

Metastatic prostate cancer in a transgenic mouse. Cancer Res 56:4096–4102
27. Foster BA, Gingrich JR, Kwon ED, Madias C, Greenberg NM (1997) Characterization of prostatic epithelial cell lines derived from transgenic adenocarcinoma of the mouse prostate (TRAMP) model. Cancer Res 57:3325–3330
28. Lewis JD, Shearer MH, Kennedy RC, Bright RK (2005) Surrogate tumor antigen vaccination induces tumor-specific immunity and the rejection of spontaneous metastases. Cancer Res 65:2938–2946
29. Li MO, Flavell RA (2008) Contextual regulation of inflammation: a duet by transforming growth factor-β and interleukin-10. Immunity 28:468–476
30. Gilboa E (2004) The promise of cancer vaccines. Nat Rev Cancer 4:401–411
31. Lewis JD, Reilly BD, Bright RK (2003) Tumor associated antigens: from discovery to immunity. Int Rev Immunol 22:81–112
32. Dranoff G (2002) GM-CSF-based cancer vaccines. Immunol Rev 188:147–154
33. Sandler AD, Chihara H, Kobayashi G, Zhu X, Miller MA, Scott DL, Krieg AM (2003) CpG oligonucleotides enhance the tumor antigen-specific immune response of a granulocyte macrophage colony-stimulating factor-based vaccine strategy in neuroblastoma. Cancer Res 63:394–399
34. Disis ML, Shiota FM, McNeel DG, Knutson KL (2003) Soluble cytokines can act as effective adjuvants in plasmid DNA vaccines targeting self tumor antigens. Immunobiology 207:179–186
35. Johnson LE, Frye TP, Chinnasamy N, Chinnasamy D, McNeel DG (2007) Plasmid DNA vaccine encoding prostatic acid phosphatase is effective in eliciting autologous antigen-specific CD8 + T cells. Cancer Immunol Immunother 56:885–895
36. Pavlenko M, Roos AK, Lundqvist A, Palmborg A, Miller AM, Ozenci V, Bergman B, Egevad L, Hellström M, Kiessling R, Masucci G, Wersäll P, Nilsson S, Pisa P (2004) A phase I trial of DNA vaccination with a plasmid expressing prostate-specific antigen in patients with hormone-refractory prostate cancer. Br J Cancer 91:688–694

[CANCER RESEARCH 63, 1040–1045, March 1, 2003]

CD4+ T Lymphocytes Play a Critical Role in Antibody Production and Tumor Immunity against Simian Virus 40 Large Tumor Antigen[1]

Ronald C. Kennedy,[2] Michael H. Shearer, Allison, M. Watts, and Robert K. Bright

Department of Microbiology and Immunology, Texas Tech University Health Science Center, Lubbock, Texas 79430

ABSTRACT

The role of CD4+ T lymphocytes in antitumor immunity has been largely attributed to providing signals required for the priming of MHC class I-restricted CD8+ cytotoxic T lymphocytes, and CD8+ cytotoxic T lymphocytes are thought to serve as the predominant mediators of tumor killing *in vivo*. We decided to evaluate the role of T lymphocyte subsets in tumor immunity induced by recombinant SV40 large tumor antigen (Tag) within an experimental murine pulmonary metastasis model of SV40 Tag-expressing tumors. Studies in BALB/c mice used *in vivo* depletion of either CD4+ or CD8+ T cells in the induction phase of the immune response to SV40 Tag. These studies indicate that CD4+ T cells but not CD8+ T cells were critical in the production of antibodies to SV40 Tag and in tumor immunity as the result of recombinant SV40 Tag immunization. On the basis of the predominance of the IgG1 isotype in the antibody response to SV40 Tag immunization, Th2 type CD4+ T cells appeared to be involved. SV40 Tag immunization was not as effective in the induction of tumor immunity in therapeutic modalities when compared with the prophylactic setting. Our results suggest that CD4+ T cells, along with antibody responses, play a role in the induction of tumor immunity to a viral-encoded tumor antigen.

INTRODUCTION

SV40 Tag[3] is a viral-encoded oncoprotein that represents a tumor-specific antigen and a target for *in vivo* tumor immunity (reviewed in Ref. 1). It has been demonstrated previously that immunization with baculovirus-derived recombinant SV40 Tag induces complete protection from i.p. tumor challenge of BALB/c mice with a syngeneic SV40-transformed cell line designated mKSA (2). In addition, SV40 Tag immunization is able to induce complete protection from the development of lung tumor foci in an experimental pulmonary metastasis model whereby mKSA cells are inoculated i.v. (3, 4). In characterizing the *in vitro* immune response induced by SV40 Tag immunization it was observed that in BALB/c mice, Tag does not induce detectable levels of Tag-specific CTLs; however, it does induce Tag-specific serum antibodies (5). *In vitro* assays using peritoneal exudate cells taken from immunized mice revealed that ADCC was functioning as a mechanism of tumor cell death (5). Neither complement-dependent cytotoxicity nor NK cells appeared to play a role in tumor cell death. This provided indirect *in vitro* evidence that antibodies to SV40 Tag were important in the observed tumor immunity. We were interested in additionally discerning the *in vivo* mechanism of tumor protection induced by SV40 Tag immunization and determining whether humoral immune responses were important. The prevailing belief regarding the immunological rejection of cancer is that T lymphocyte-mediated immunity is essential for the destruction of most solid tumors with CD8+ CTLs representing the major effector cell mediating tumor cell destruction. Because CD8+ CTL responses were not induced by SV40 Tag immunization, we believed that CD4+ T lymphocytes might be a critical mediator of the observed tumor immunity by providing help for the induction of antibodies to SV40 Tag. To evaluate this possibility, we decided to examine the T-cell subsets involved in providing the observed tumor immunity. Therefore, we depleted BALB/c mice of either CD4+ or CD8+ T cell subsets during the course of immunization with SV40 Tag and subsequently challenged the mice i.v. with mKSA tumor cells to evaluate tumor immunity. On the basis of the results of our experiments, it appears that functional CD4+ T cells, but not CD8+ T cells, along with the presence of SV40 Tag-specific antibody are critical for the development of tumor immunity in this model. Additionally, the predominance of the murine IgG1 isotype in the antibody response to SV40 Tag immunization suggests the role of Th2-type CD4+ T cells in the induction of these immune responses. Although SV40 Tag immunization was capable of reducing lung tumor foci and increasing survival time in mice treated therapeutically with existing tumors, it was not as effective as was observed in a prophylactic setting where complete tumor immunity was observed.

MATERIALS AND METHODS

Cells and Mice. The SV40-transformed BALB/c mouse kidney fibroblast cell line designated mKSA (6) was used for tumor challenge. Cells were cultured in DMEM with L-glutamine (Life Technologies, Inc., Rockville, MD) and supplemented with 0.1 mM nonessential amino acids, 100 units/ml penicillin, 500 μg/ml streptomycin (Mediatech, Washington, DC), and 10% heat-inactivated fetal bovine serum (BioWhittaker, Walkersville, MD). Cells were incubated in a humidified, 5% CO_2 atmosphere at 37°C. Before injection, cells were detached from flasks by 5-min exposure to PBS and 1 mM EDTA (pH 7.5). Cells were washed, resuspended in PBS, counted, and adjusted to the appropriate density with additional PBS before inoculation. Six to 8-week-old female BALB/c mice were obtained from Jackson Laboratories (Bar Harbor, ME) and maintained under standard conditions. Treatment and care of the animals were in accordance with institutional guidelines and the Animal Welfare Assurance Act.

***In Vivo* Depletion of CD4+ and CD8+ T Cells.** Mabs GK1.5 (rat IgG2b antimurine CD4) and YTS169.4 (rat IgG2b antimurine CD8) were used for *in vivo* depletion of the CD4+ and CD8+ T-cell subsets, respectively. The rat IgG Mabs were purified by affinity chromatography, and total protein content was quantified by absorbance at 280 nm. Purified rat Mabs and a control rat IgG preparation were administered by i.p. injection of 100 μg of antibody in 0.1 ml PBS, according to the schedule specified in Fig. 1. Groups of Mab-depleted and control immunized mice were sacrificed 12 days after the last immunization with the rat antibodies (corresponding to day 21 or tumor cell challenge, see Fig. 1), and splenocytes and lymph node preparations were analyzed by flow cytometry for CD4+ (stained with clone RM4–4 conjugated to fluorescence isothiocyanate) and CD8+ (stained with clone 2.43 conjugated to phycoerythrin) T-cell subsets. These are commercially available rat Mabs that detect epitopes distinct from those recognized by the depleting Mabs. Flow cytometry indicated a >95% depletion in the specific CD4+ or CD8+ T-lymphocyte populations when compared with control mice (data not shown). Our flow cytometry methods have been described elsewhere (5, 7)

Immunization and Tumor Challenge. SV40 Tag was prepared using a baculovirus expression vector system (8). Groups of 5 BALB/c mice were immunized i.p. with an alum precipitate of recombinant SV40 Tag as described

Received 4/18/02; accepted 12/27/02.

The costs of publication of this article were defrayed in part by the payment of page charges. This article must therefore be hereby marked *advertisement* in accordance with 18 U.S.C. Section 1734 solely to indicate this fact.

[1] Supported in part by Grant CA-77351 from the NIH.

[2] To whom requests for reprints should be addressed, at Department of Microbiology and Immunology, Texas Tech University Health Sciences Center, 3601 4th Street STOP 6591, Lubbock, TX 79430. Phone: (806) 743-2414; Fax: (806) 743-2334; E-mail: ronald.kennedy@ttuhsc.edu.

[3] The abbreviations used are: Tag, large tumor antigen; ADCC, antibody-dependent cell-mediated cytotoxic; CTL, cytotoxic T lymphocyte; Mab, monoclonal antibody; NK, natural killer.

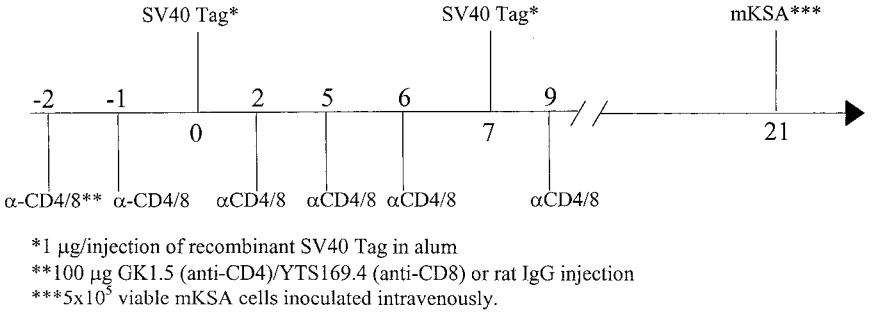

Fig. 1. Schedule for SV40 Tag immunization, CD4 depletion, CD8 depletion, and tumor challenge. Mice were depleted of T-cell subsets by injections of 100 μg of Mab GK1.5 (anti-CD4), Mab YTS169.4 (anti-CD8), or rat IgG at -2, -1, 2, 5, 6, and 9 days. Groups of mice were sacrificed at day 21, and CD4 and CD8 T-cell populations analyzed by flow cytometry. SV40 Tag immunization consisted of 1 μg Tag in alum at day 0 and 7. Groups of mice that were challenged with tumor cells received 5×10^5 viable mKSA cells i.v. at day 21. Tumor cell-challenged mice were sacrificed 14 days after challenge, and lungs were removed and analyzed for tumor foci formation.

previously (2, 5). Control groups of 5 mice each received alum alone. Injections of 1 μg of SV40 Tag were administered at 1-week intervals for a total of two injections (Fig. 1). Serum was obtained from each mouse before immunization (preimmune), and at 7 days after the first and second immunization. Mice were challenged 14 days after the second SV40 Tag injection, with 5×10^5 viable mKSA cells being delivered i.v. in 50 μl of sterile PBS. In the first set of experiments, mice were sacrificed 14 days after challenge, and the number of lung tumor foci was determined using a computer-based image analysis system (9). In the second set of experiments, 1 mouse from each group was sacrificed 21 days after challenge, and lung tumor foci were examined. Tumor immunity was determined in the remaining 4 mice/group based on survival (3–5). To evaluate the effects of SV40 Tag immunization on established tumors, mice were inoculated with 5×10^5 mKSA cells, i.v., and then immunized with recombinant SV40 Tag on days 3, 9, and 15 after tumor challenge. Control groups of mice received alum rather than SV40 Tag in alum. Eighteen days after tumor challenge, 3 mice from each group were euthanized, and lungs were obtained. The remaining 7 mice were used to determine survival time.

ELISA. Detection of SV40 Tag-specific serum antibody was carried out using ELISA as described previously (2, 4, 5). Briefly, 200 ng of recombinant SV40 Tag in borate-buffered saline was coated onto 96-well microtiter plates overnight at 4°C. Nonspecific binding was blocked by the addition of 200 μl of 10% normal goat serum borate-buffered saline and incubated at 37°C for 1 h. Mouse serum was added at various dilutions and incubated for 1 h at 37°C. Anti-SV40 Tag reactivity was detected using horseradish peroxidase-conjugated goat antimouse IgG Fc-specific reagent (Sigma, St. Louis, MO) diluted 1:1000 in blocking solution. Plates were developed with peroxidase substrate 2,2′-azino-di(3-ethyl-benzthiazoline sulfonic acid) containing 0.01% H_2O_2. An absorbance at 410 nm ($A_{410\ nm}$) determined to be approximately three times the absorbance values obtained for 1:10 dilutions of the preimmune sera was established as a cutoff for positive reactivity and antibody end point titer determinations. Immune serum was examined using serial 4-fold dilutions, beginning with a dilution of 1:50, and the dilution that resulted in the last absorbance above the cutoff was the end point titer. Anti-SV40 Tag antibodies failed to bind a control recombinant antigen (hepatitis B surface antigen) in similar assays (data not shown). All of the serum samples were run in triplicate and reported as the reciprocal end point titer. These methods have been described in detail elsewhere (4, 5). To determine the IgG antibody isotype distribution, immune serum at a 1:100 dilution was added to SV40 Tag-coated microtiter wells in triplicate as described above. IgG1 and IgG2a anti-SV40 Tag responses were determined using sheep antimouse IgG1- and IgG2-specific isotyping reagents (Binding Site, San Diego, CA) that were conjugated with horseradish peroxidase, and the assays were performed as described above. Two murine monoclonal anti-SV40 Tag preparations, PAb 405 (IgG1) and PAb 419 (IgG2a), were used as controls. The IgG2a:IgG1 ratios were determined from the mean absorbance values as has been described previously (10, 11).

Determination of Tumor Cell Foci in the Lungs. The left lung of each animal was removed after euthanization and stained by intratracheal injection of the lobes with 10% India ink. Lungs were then suspended in Fekete's destaining solution. To remove subjectivity in the counting of tumor cell foci in the lungs of inoculated mice, we have used a computer-assisted method (9). After destaining 15 min, the number of foci visible on the ventral surface of the lung was quantified using an IS-1000 digital Imaging System (Alpha Innotech Co., San Leandro, CA). Density threshold parameters were defined to ensure that the foci counted consistently fell above a gray scale value of 25 (compared with black lung background). Size threshold parameters were set to count only those foci falling above 4 pixels in diameter on the computer image. SE was determined to demonstrate variability within each group (9).

RESULTS

***In Vivo* Depletion and Recombinant SV40 Tag Immunization.** The schedule used for the *in vivo* depletion of CD4 and CD8 T-cell subsets using rat antimouse CD4 and CD8 Mabs is depicted in Fig. 1. The specific rat Mab for CD4 depletion (GK1.5) and CD8 depletion (YTS169.4) have been used by other investigators previously (12, 13), and we used a similar schedule for *in vivo* depletion. In our initial studies, groups of 5 mice each were depleted with either GK1.5 (CD4), YTS169.4 (CD8), or similarly immunized with purified rat IgG as a control before and after immunization with recombinant SV40 Tag. Serum was obtained before and 7 days after each injection with SV40 Tag, and mice were sacrificed on day 21 (corresponding to tumor cell challenge) and 12 days after the last injection with the rat IgG preparations. Lymph node and splenocytes were obtained and examined by flow cytometry for CD4 and CD8 expression when compared with the control rat IgG immunized group. In each instance, the levels of CD4+ in the GK1.5-treated group and CD8+ in the YTS169.4-treated group were decreased by >95% when compared with the rat IgG immunized group (data not shown). This suggested that the depletion scheme used in Fig. 1 would reduce the levels of CD4 and CD8 subpopulations in the treated mice. To evaluate the effects of this *in vivo* depletion, we also examined the antibody response to SV40 Tag as the result of the recombinant protein immunization. As shown in Table 1, mice treated with either the rat IgG preparation or YTS169.4 (anti-CD8) generated detectable anti-SV40 Tag responses after the second SV40 Tag injection. Mean antibody titers were 3040 (rat IgG-treated) and 1760 (anti-CD8-treated) with similar ranges of antibody responses (800–3200). The group treated with GK1.5 (anti-CD4), along with a control group of mice that received alum alone, failed to produce detectable anti-SV40 Tag responses. These data suggested that the anti-CD4 treatment group of mice were functionally depleted, as no antibody response to SV40 Tag was observed. Alternatively, the anti-CD8 treatment group appeared to possess functioning CD4+ T cells, as SV40 Tag immunization

Table 1 *Antibody titers to SV40 Tag in mice treated with anti-CD4, anti-CD8, or rat IgG*

Immunization	Antibody titers mean (range) day 7 after first immunization	Antibody titers mean (range) day 7 after second immunization
Alum	<50	<50
Tag/rat IgG	<50	3040 (800–3200)
Tag/anti-CD4	<50	<50
Tag/anti-CD8	<50	1760 (800–3200)

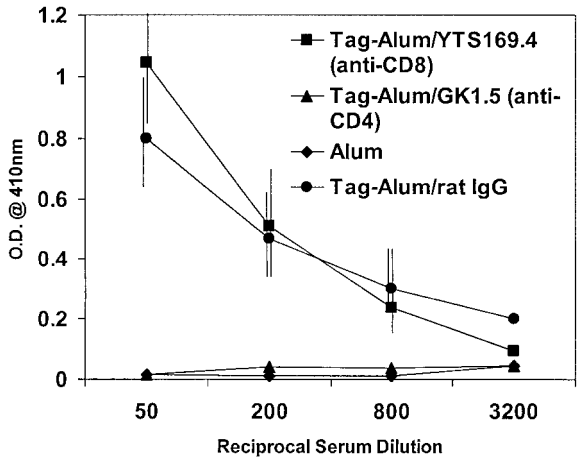

Fig. 2. Representative SV40 Tag-specific antibody binding curves from SV40 Tag-immunized mice treated with anti-CD4 Mab, anti-CD8 Mab, or rat IgG. The mean absorbance ($A_{410\ nm}$) values for the various 4-fold dilutions of groups of 5 mice each are shown; *bars*, ±SD.

generated antibodies to SV40 Tag. No IgG anti-SV40 Tag responses were observed in any of the groups of mice after the first injection, which is similar to what we have observed previously after a single injection of SV40 Tag.

To compare the antibody responses in the rat IgG control-treated and anti-CD8-treated groups of mice, we examined the binding of sera at various dilutions to SV40 Tag by ELISA. A representative set of binding curves is shown in Fig. 2. It is apparent from the binding curves that the anti-SV40 Tag antibody responses in the rat IgG- and anti-CD8-treated groups of mice were similar with respect to the slope of the binding curve and the titer. No anti-SV40 Tag-specific antibodies were observed in the alum immunized or the anti-CD4-treated groups of mice. Together, these data indicate that our Mab treatment regimen is successful for functionally depleting CD4+ T cells, and that the antibody response to SV40 Tag does not appear to differ in the rat IgG- and anti-CD8-treated groups of mice.

Anti-CD4-treated Mice Are Susceptible to Tumor Formation. In the next set of experiments, we evaluated whether anti-CD4 and anti-CD8 treatment before recombinant SV40 Tag immunization had an effect on tumor immunity. Groups of 5 mice each received anti-CD4, anti-CD8, or rat IgG treatment before and after immunization with SV40 Tag as described in Fig. 1 and were challenged i.v. with mKSA tumorigenic cells 14 days after the second SV40 Tag immunization. Tumor immunity was determined 14 days after mKSA challenge by evaluating the presence of lung tumor foci in an experimental model of pulmonary metastasis that has been described previously (3, 4). As shown in Table 2, the rat IgG- and anti-CD8-treated groups of mice developed anti-SV40 Tag responses after the second SV40 Tag injection. The alum immunized and anti-CD4-treated groups of mice failed to develop detectable antibodies to SV40 Tag. These data are similar to the data described in Table 1. However, after tumor cell challenge, both the alum immunized and anti-CD4-treated groups of mice developed lung tumor foci in each of the 5 individual mice. The numbers of lung foci ranged from 6 to 12 (average of 10) for the alum immunized and 1 to 9 (average of 5) for the anti-CD4-treated mice. No lung tumor cell foci were observed in any of the rat IgG- and anti-CD8-treated mice indicating that tumor immunity was complete. To additionally examine the level of tumor immunity, additional groups of mice were treated and immunized as described in Fig. 1, and tumor immunity was evaluated in a single mouse 21 days after mKSA tumor cell experimental challenge. The remaining 4 mice/group were evaluated for tumor immunity based on survival time. Representative tumor cell foci present in the lungs from alum-immunized (Fig. 3*A*) and anti-CD4-treated mice (Fig. 3*C*) differ from the lack of tumor cell foci in the lungs from rat IgG-treated (Fig. 3*B*) and anti-CD8-treated (Fig. 3*D*) mice 21 days after tumor cell challenge. The number of tumor foci quantitated by computer-assisted video image analysis in the alum-immunized mouse was 23 foci *versus* 44 foci in the anti-CD4-treated mouse. This increase in the number of tumor foci in the anti-CD4-treated mice late in the experimental metastasis model may reflect the fact the CD4+ T cells may exhibit direct antitumor effects. However, this is not observed early in tumor foci development in the lungs, because alum-immunized and anti-CD4-treated mice had similar numbers of tumor foci when lungs were evaluated 14 days after tumor cell challenge (Table 2). The survival time for the remaining alum- and anti-CD4-treated mice ranged from 20 to 24 days after challenge. The rat IgG- and anti-CD8-treated mice survived >60 days (data not shown). These data clearly point to a critical role that CD4+ T cells have in the induction of antibody responses and in tumor immunity as the result of recombinant SV40 Tag immunization.

Next, we determined the IgG isotype distribution of the antibody response to SV40 Tag in rat IgG- and anti-CD8-treated mice (Table 3). It is apparent that IgG1 was the predominant antibody response to SV40 Tag immunization in both groups of mice when compared with IgG2a. The IgG2a:IgG1 anti-SV40 Tag ratios ranged from 0.03 to 0.07 in the rat IgG-treated group and 0.02 to 0.08 in the anti-CD8-treated group. These data indicate that the immune response

Table 2 *Antibody titers and development of lung metastases in mice treated with anti-CD4, anti-CD8, or rat IgG*

Immunization	Antibody titers day 7 after first immunization	Antibody titers day 7 after second immunization	Lung foci number
Alum	<50	<50	6
	<50	<50	10
	<50	<50	12
	<50	<50	10
	<50	<50	12
Tag/rat IgG	<50	3200	0
	<50	3200	0
	<50	3200	0
	<50	800	0
	<50	3200	0
Tag/α-CD4	<50	<50	1
	<50	<50	6
	<50	<50	5
	<50	<50	9
	<50	<50	4
Tag/α-CD8	<50	800	0
	<50	800	0
	<50	3200	0
	<50	800	0
	<50	800	0

(A) alum, (B) SV40 Tag/rat IgG, (C) SV40 Tag/Anti-CD4, (D) SV40 Tag/Anti-CD8

Fig. 3. Representative lung tumor cell foci in mice treated with anti-CD4 or anti-CD8 Mabs and immunized with recombinant SV40 Tag. *A*, tumor cell foci in the lung of a control alum immunized mouse. *B*, lack of tumor cell foci in the lung of a rat IgG treated and SV40 Tag-immunized mouse. *C*, tumor cell foci in the lung of an anti-CD4-treated and SV40 Tag-immunized mouse. *D*, lack of tumor cell foci in the lung of an anti-CD8-treated and SV40 Tag-immunized mouse.

Table 3 *IgG antibody isotypes in mice that developed anti-SV40 tag responses*

Immunization	IgG1[a]	IgG2a[a]	IgG2a/IgG1
Tag/rat IgG	1.19	0.087	0.07
	1.084	0.037	0.03
	0.94	0.049	0.05
	0.49	0.035	0.07
	0.98	0.071	0.07
Tag/anti-CD8	0.44	0.010	0.02
	0.70	0.057	0.08
	0.91	0.049	0.05
	0.88	0.051	0.06
	0.56	0.031	0.05

[a] The values represent the mean absorbance value from triplicate determinations at a 1:100 dilution of the individual sera. Positive controls including monoclonal antibodies to SV40 Tag preparations, PAb 405 (IgG1) and aPAb 419 (IgG2a).

to multiple injections of SV40 Tag is Th2 biased, because IgG1 is the predominant subclass of antibody that is synthesized. Little to no IgG2a anti-SV40 Tag was observed in these mice. The synthesis of IgG2a is associated with a Th1-biased immune response (10, 11, 14).

To determine what effects recombinant SV40 Tag immunization had on established tumors, we challenged mice with tumor cells before the initiation of SV40 Tag injections. We selected a tumor cell challenge dose similar to that used in the prophylactic immunization experiments, and the selection of the time point after challenge to obtain lungs from mice was based on the latest time when control group mouse survival became questionable. As shown in Table 4, the control alum-treated mice had a higher number of tumor foci (mean value of 29.33; $n = 3$) when compared with the SV40 Tag immunized mice (mean value of 6.66; $n = 3$). Similarly, the survival time was increased in the group of mice that received SV40 Tag (mean survival time of 35 days) when compared with control mice (mean survival time of 21 days). The SV40 Tag immunization was capable of reducing the number of lung tumor foci and increasing the survival time in a therapeutic modality; however, it was not as effective as was observed in a prophylactic setting where complete tumor immunity was observed.

DISCUSSION

The role of CD4+ T-helper cells in antitumor immunity has been largely attributed to providing signals required for the priming of MHC class I-restricted CD8+ CTLs. The CD8+ CTLs are thought to serve as the predominant mediators of tumor killing *in vivo*. Indeed, many studies that involve the induction of antitumor immune responses *in vivo* target tumor antigen-specific CTL responses (Refs. 15–25, reviewed in Ref. 26). In a number of these instances CD4+ T cells were required for the induction of CD8+ CTLs that exhibited antitumor immunity (17, 20, 22, 23). The involvement of both CD4+ and CD8+ T lymphocytes has been reported in immunity against polyoma virus-induced tumors (27), whereas CD8+ CTL responses specific for the viral-encoded human papillomavirus type 16 tumor antigen E7 correlated with both tumor immunity and the regression of established tumors (28, 29). The antitumor immune responses were dependent on E7-specific CD8+ cells but not CD4+ T cells (28). Although the majority of vaccination strategies for the treatment of solid malignancies focus on the generation of CD8+ CTL responses, antibody-based therapies have been successful against some cancers in the clinical setting (reviewed in Ref. 30). These antibody-based immunotherapies involve passive administration of Mabs specific for CD20 and HER-2/*neu* for the treatment of non-Hodgkin's lymphoma and breast cancer, respectively. Thus, it is reasonable to speculate that antibodies induced by tumor vaccination strategies may exhibit antitumor immunity in some systems.

Previous studies from our laboratories suggested that antibodies to SV40 Tag may play a role in tumor immunity resulting from immunization with recombinant SV40 Tag (2, 4, 5). In comparative studies using other SV40 Tag immunization modalities, such as anti-idiotypes or SV40 Tag synthetic peptides where only partial tumor immunity was observed, the presence of tumor immunity appeared to correlate with the levels of antibodies to SV40 Tag (31, 32). Additional studies demonstrated recombinant SV40 Tag failed to generate any detectable CD8+ CTL responses, whereas antibodies to SV40 Tag were induced and were capable of mediating ADCC against the mKSA tumor cells *in vitro* (5). The role of antibodies that mediated complement-dependent cytotoxicity and direct NK cell activity against mKSA tumor cells as *in vitro* mechanisms in the observed recombinant SV40 Tag-induced tumor immunity was ruled out. In this present study, the predominance of the IgG1 anti-SV40 Tag suggests a biased for a Th2 type CD4+ T-cell response. The lack of an IgG2a anti-SV40 Tag response being induced by multiple injections of recombinant SV40 Tag suggests that Th1 type CD4+ T-cell responses are not involved in the observed tumor immunity in this model. In murine systems, the IgG1 subclass is most effective at mediating ADCC in the context of CD32 (FcγRII) effector cells, whereas the IgG2a subclass is more effective at mediating ADCC using CD64 (FcγRI) effector cells (reviewed in Ref. 33). Because these two Fc receptors are not expressed on NK cells, these data, along with our previous report (5), support the possible role of ADCC and macrophage/monocytes effector cells in the complete tumor immunity resulting from recombinant SV40 Tag immunization. Additional studies to evaluate the direct role of macrophages/monocytes as possible effectors cells involved in ADCC in this system are warranted. The potential exists whereby ADCC may play only a partial role in the observed complete tumor immunity, and CD4+ T cells, particularly Th2 type cells, may also have direct effects that complement the antitumor activities of antibodies that can mediate ADCC. This could include the secretion of cytokines and their potential for direct cytotoxic and/or apoptotic events against tumor cells that also impart a necessary component of the observed tumor immunity. Nonetheless, our study clearly supports a role for both CD4+ T cells and antibodies as components of tumor immunity.

It was of interest to note that in a therapeutic setting, immunization with recombinant SV40 Tag had only partial antitumor effects on pre-existing tumors when compared with immunization in a prophylactic modality. These partial effects included less of a tumor burden as assessed by the number of tumor lung foci and an increase in survival time when compared with control groups. This was not a surprising observation, as a number of murine tumor systems have indicated that immunization is only effective either before or early after tumor cell inoculation (34–37). Indeed, some potential therapeutic effects were observed with recombinant SV40 Tag immunization after tumor cell challenge. However, because tumor immunity in the therapeutic setting was not complete to examine mechanistic aspects related to the induction of tumor immunity in this system, we selected the prophylactic modality where complete tumor immunity was observed.

In this present report, we analyze the role of T-cell subset involvement in mediating tumor rejection in the murine experimental pulmonary metastasis model after immunization with a tumor-specific an-

Table 4 *Effect of SV40 tag immunization on established tumors*

Immunization	Lung foci number mean (range)	Mean survival time mean days (range)
Alum	29.33 (22–40)	21 (18–25)
Tag	6.66 (2–12)	35 (28–44)

tigen. The data described in this present report have implicated an important role for CD4+ T-helper cell function in B-cell priming for antibody production. This is in contrast to reports by another group of investigators who describe the requirement of CD8+ T lymphocytes for recombinant SV40 Tag-induced tumor immunity in their system (37, 38). These investigators determined that whereas CD4+ T-helper cells may play a role in protection, their role is to provide signals to activate CD8+ CTL responses and that these effector cells are responsible for the observed recombinant SV40 Tag-induced tumor immunity (38). It is noteworthy that similar to our studies published previously (4, 5), no CD8+ CTL responses were observed in the spleen or draining lymph nodes that would be indicative of systemic tumor immunity. Rather, CD8+ CTL were observed only at the site of the experimental tumor challenge (38). A number of other important differences between these studies can explain the discrepancies in the results and conclusions of the investigations.

These results are relevant to the treatment of human cancer in both general and specific terms. The use of Mabs as passively administered therapy modalities has been successfully used to treat several types of human cancers, and this directly implicated antibodies in tumor immunity (reviewed in Ref. 30). ADCC and specific effector cells that mediate this form of antitumor immunity appear to play a role. Our studies implicate both the need to activate tumor antigen-specific CD4+ T cells and antibodies as the basis for the observed immunity in this murine tumor model. Thus, active immunization strategies should include the targeting of both antibody induction and CD4+ T-cell activation to impart potentially the most complete form of tumor immunity in cancer scenarios where the mechanism(s) of tumor immunity are unknown. In specific terms, SV40 and SV40 Tag have been reported to be involved in a number of human malignancies (reviewed in Refs. 39–41). Of particular relevance to SV40 Tag vaccination strategies is the association of SV40 with malignant pleural mesothelioma (reviewed in Ref. 42). This is a tumor of the pleura that originates in the serosal lining and is exceptionally lethal. Current therapies, including surgery, radiation, and chemotherapy, are ineffective at slowing the course of the disease. The median survival from the time of diagnosis is rarely >1 year. Thus, the need for new alternative cancer therapies to treat malignant pleural mesothelioma is important. Within mesothelioma cells, it has been shown that SV40 Tag binds essential cellular tumor suppressor gene products, including p53 and pRb, suggesting that SV40 and SV40 Tag may play roles in cellular transformation (43, 44). It was reported recently that SV40 Tag-specific CTLs could be generated from the peripheral blood of malignant pleural mesothelioma patients (45). These CTLs were capable of recognizing mesothelioma tumor cells that expressed SV40 Tag in an MHC class I-restricted manner, suggesting that SV40 Tag represents an immunological target in humans with mesothelioma. The potential exists whereby recombinant SV40 Tag or components thereof may function as a therapeutic cancer vaccination strategy for treating malignant mesotheliomas expressing SV40 Tag (reviewed in Ref. 46). Additionally, asbestos exposure has also been associated with malignant mesothelioma (42). Individuals who are exposed to both SV40 and asbestos have two associated risk factors for developing mesothelioma (47). Such high-risk individuals could be vaccinated using SV40 Tag-based strategies before the onset of symptoms, a scenario that may approximate prophylactic immunization. In these treatment scenarios, the generation of antibodies and CD4+ T cells specific for SV40 Tag would be indicative of immunological responsiveness to the vaccination protocol and based on the studies describe herein using murine systems, a preferred outcome associated with tumor immunity.

REFERENCES

1. Bright, R. K., Shearer, M. H., Pass, H. I., and Kennedy, R. C. Immunotherapy of SV40 induced tumours in mice: a model for vaccine development. Dev. Biol. Stand., *94:* 341–355, 1998.
2. Shearer, M. H., Bright, R. K., Lanford, R. E., and Kennedy, R. C. Immunization of mice with baculovirus derived recombinant SV40 large tumor antigen induces protective tumor immunity to a lethal challenge with SV40 transformed cells. Clin. Exp. Immunol, *91:* 266–271, 1993.
3. Watts, A. M., Shearer, M. H., Pass, H. I., and Kennedy, R. C. Development of an experimental murine pulmonary metastasis model incorporating a viral encoded tumor specific antigen. J. Virol. Methods, *69:* 93–102, 1997.
4. Watts, A. M., Shearer, M. H., Pass, H. I., and Kennedy, R. C. Comparison of SV40 large Tag recombinant protein and DNA immunization in the induction of protective immunity from experimental pulmonary metastasis in a murine model. Cancer Immunol. Immunother., *47:* 343–351, 1999.
5. Bright, R. K., Shearer, M. H., and Kennedy, R. C. Immunization of BALB/c mice with recombinant simian virus 40 large tumor antigen induces antibody dependent cell mediated cytotoxicity against simian virus 40 transformed cells: an antibody based mechanism for tumor immunity. J. Immunol., *153:* 2064–2071, 1994.
6. Kit, S., Kurimura, T., and Dubs, D. R. Transplantable mouse tumor line induced by injection of SV40-transformed mouse kidney cells. Int. J. Cancer, *4:* 384–392, 1969.
7. Shearer, M. H., Chanh, T. C., Dalgleish, A. G., and Kennedy, R. C. Idiotype cascades associated with the CD4-HIV glycoprotein 120 interaction: immunization with anti-idiotypic antibodies induces anti-anti-idiotypic responses with anti-CD4 specificity and *in vitro* neutralizing activity. AIDS Res. Hum. Retrovir., *16:* 77–86, 2000.
8. Lanford, R. E. Expression of simian virus 40 T antigen in insect cells using a baculovirus expression vector. Virology, *167:* 72–81, 1988.
9. Watts, A. M., and Kennedy, R. C. Quantitation of tumor foci in an experimental murine tumor model using computer-assisted video imaging. Anal. Biochem., *256:* 217–219, 1998.
10. Fernando, G. J., Stewart, T. J., Tindle, R. W., and Frazer, I. H. Th2-type CD4+ cells neither enhance nor suppress antitumor CTL activity in a mouse model. J. Immunol., *161:* 2471–2472, 1998.
11. Fernando, G. J., Stewart, T. J., Tindle, R. W., and Frazer, I. H. Vaccine induced Th1-type responses are dominant over Th2 type responses in the short term whereas preexisting Th2 responses are dominant in the long term. Scand. J. Imunol., *47:* 459–465, 1998.
12. Benjamin, R. J., Cobbold, S. P., Clark, M. R., and Waldmann, H. Tolerance to rat monoclonal antibodies: implications for serotherapy. J. Exp. Med., *163:* 1539–1552, 1986.
13. Goronzy, J., Weyand, C. M., and Fathman, C. G. Long-term humoral unresponsiveness *in vivo*, induced by treatment with monoclonal antibody against L3T4. J. Exp. Med., *164:* 911–925, 1986.
14. Horner, A. A., and Raz, E. Immunostimulatory sequence oligodeoxynucleotide: A novel mucosal adjuvant. Clin. Immunol., *95:* S19–S29, 2000.
15. Schreurs, M. W. J., deBoer, A. J., Figdor, C. G., and Adema, G. J. Genetic vaccination against the melanocyte linage-specific antigen gp100 induces cytotoxic T lymphocyte mediated tumor protection. Cancer Res., *58:* 2509–2514, 1998.
16. Correale, P., Cusi, M. G., Sabatino, M., Micheli, L., Pozzessere, D., Nencini, C., Valensin, P. E., Petrioli, R., Giorgi, G., Zurbriggen, R., Gluck, R., and Francini, G. Tumour-associated antigen (TAA)-specific cytotoxic T cell (CTL) response *in vitro* and in a mouse model induced by TAA-plasmids delivered by influenza virosomes. Eur. J. Cancer, *37:* 2097–2103, 2001.
17. Berlyn, K. A., Schultes, B., Leveugle, B., Noujaim, A. A., Alexander, R. B., and Mann, D. L. Generation of CD4+ and CD8+ T lymphocyte responses by dendritic cells armed with PSA/anti-PSA (antigen/antibody) complexes. Clin. Immunol., *101:* 276–283, 2001.
18. Smith, S. G., Patel, P. M., Porte, J., Selby, P. J., and Jackson, A. M. Human dendritic cells genetically engineered to express a melanoma polyepitope DNA vaccine induce multiple cytotoxic T cell responses. Clin. Cancer Res., *7:* 4253–4261, 2001.
19. Hanabuchi, S., Ohashi, T., Koya, Y., Kato, H., Hasegawa, A., Takemura, F., Masuda, T., and Kannagi, M. Regression of human T cell leukemia virus type 1 (HTLV-1) associated lymphomas in a rat model: peptide induced T cell immunity. J. Natl. Cancer Inst., *93:* 1775–1783, 2001.
20. Wu, T. Y., and Fleischmann, W. R., Jr. Murine B16 melanoma vaccination induced tumor immunity: identification of specific immune cells and functions involved. J. Interferon Cytokine Res., *21:* 1117–1127, 2001.
21. Dan, Q., Sanchez, R., Delgado, C., Wepsic, H. T., Morgan, K., Chen, Y., Jeffes, E. W., Lowell, C. A., Morgan, T. R., and Jadus, M. R. Non-immunogenic murine hepatocellular carcinoma Hepa1–6 cells expressing membrane form of macrophage colony stimulating factor are rejected *in vivo* and lead to CD8+ T cell immunity against the parental tumor. Mol. Ther., *4:* 427–437, 2001.
22. Wang, Q., Yu, H., Zhang, L., Ju, D., Pan, J., Xia, D., He, L., Wang, J., and Cao, X. Vaccination with IL-18 gene modified, superantigen coated tumor cells elicits potent antitumor immune responses. J. Cancer Res. Clin. Oncol., *127:* 718–726, 2001.
23. Steitz, J., Bruck, J., Knop, J., and Tuting, T. Adenovirus transduced dendritic cells stimulate cellular immunity to melanoma via a CD4+ T cell dependent mechanism. Gene Ther., *8:* 1255–1263, 2001.
24. Perez-Diez, A., Spiess, P. J., Restifo, N. P., Matzinger, P., and Marincola, F. M. Intensity of vaccine elicited immune responses determines tumor clearance. J. Immunol., *168:* 338–347, 2002.
25. Kumamoto, T., Huang, E. K., Paek, H. J., Morita, A., Matsue, H., Valentini, R. F., and Takashima, A. Induction of tumor specific protective immunity by *in situ* Langerhans cell vaccine. Nat. Biotechnol., *20:* 64–69, 2002.

26. Hobeika, A. C., Clay, T. M., Mosca, P. J., Lyerly, H. K., and Morse, M. A. Quantitating therapeutically relevant T cell responses to cancer vaccines. Crit. Rev. Immunol., *21:* 287–297, 2001.
27. Ljunggren, G., Ljunggren, H-G., and Dalianis, T. T cell subsets involved in immunity against polyoma virus induce tumors. Virology, *198:* 714–716, 1994.
28. Lamikanra, A., Pan, Z. K., Issacs, S. N., Wu, T. C., and Patterson, Y. Regression of established human papillomavirus type 16 (HPV-16) immortalized tumors *in vivo* by vaccinia viruses expressing different forms of HPV-16 E7 correlates with enhanced CD8+ T cell responses that home to the tumor site. J. Virol., *75:* 9654–9664, 2001.
29. Velders, M. P., McElhiney, S., Cassetti, M. C., Eiben, G. L., Higgins, T., Kovacs, G. R., Elmishad, A. G., Kast, W. M., and Smith, L. R. Eradication of established tumors by vaccination with Venezuelan equine encephalitis virus replicon particles delivering human papillomavirus 16 E7 RNA. Cancer Res., *61:* 7861–7867, 2001.
30. Reilly, R. T., Emens, L. A., and Jaffee, E. M. Humoral and cellular immune responses: independent forces or collaborators in the fight against cancer? Curr. Opin. Investig. Drugs, *2:* 133–135, 2001.
31. Shearer, M. H., Bright, R. K., and Kennedy, R. C. Comparison of humoral immune responses and tumor immunity in mice immunized with recombinant SV40 large tumor antigen and a monoclonal anti-idiotype. Cancer Res., *53:* 5734–5739, 1993.
32. Bright, R. K., Shearer, M. H., and Kennedy, R. C. SV40 large tumor antigen associated with synthetic peptides define native antigenic determinants and induce protective tumor immunity in mice. Mol. Immunol., *31:* 1077–1087, 1994.
33. Ravetch, J. V., and Clynes, R. A. Divergent roles for Fc recepts and complement *in vivo*. Ann. Rev. Immunol., *16:* 421–432, 1998.
34. Golumbek, P. T., Lazenby, A. J., Levitsky, H. I., Jaffee, H., Karasuyama, H., Baker, M., and Pardoll, D. M. Treatment of established renal cancer by tumor cells engineered to secrete interleukin-4. Science (Wash. DC), *254:* 713–716, 1991.
35. Hanson, H. L., Donermeyer, D. L., Ikeda, H., White, J. M., Shankaran, V., Old, L. J., Shiku, H., Schreiber, R. D., and Allen, P. M. Eradication of established tumors by CD8+ T cell adaptive immunotherapy. Immunity, *13:* 265–276, 2000.
36. Gorelik, L., and Flavell, R. A. Immune-mediated eradication of tumors through the blockade of transforming growth factor-β signaling in T cells. Nat. Med., *7:* 1118–1122, 2001.
37. Zerrahn, J., Utermohlen, O., Warnecke, G., Deppert, W., and Lehmann-Grube, F. Protective immunity in BALB/c mice against the simian virus 40 induced mKSA tumor resulting from injection of recombinant large T antigen. Requirement of CD8+ T lymphocytes. J. Immunol., *156:* 3919–3924, 1996.
38. Utermohlen, O., Schulze-Garg, C., Warnecke, G., Gugel, R., Lohler, J., and Deppert, W. Simian virus 40 large T antigen specific rejection of mKSA tumor cells in BALB/c mice is critically dependent of both strictly associated tumor specific CD8+ cytotoxic T lymphocytes and CD4+ T helper cells. J. Virol., *75:* 10593–10602, 2001.
39. Butel, J. S. Simian virus 40, poliovirus vaccines, and human cancer: research progress versus media and public interests. Bull. W. H. O., *78:* 195–198, 2000.
40. Jasani, B., Cristaudo, A., Emri, S. A., Gazdar, A. F., Gibbs, A., Krynska, B., Miller, C., Mutti, L., Radu, C., Tognon, M., and Procopio, A. Association of SV40 with human tumors. Semin. Cancer Biol., *11:* 49–61, 2001.
41. Carbone, M., and Pass, H. I. Debate on the link between SV40 and human cancer continues. J. Natl. Cancer. Inst., *94:* 229–230, 2002.
42. Rizzo, P., Bocchetta, M., Poweres, A., Foddis, R., Stekala, E., Pass. H. I., and Carbone, M. SV40 and the pathogenesis of mesothelioma. Semin. Cancer Biol., *11:* 63–071, 2001.
43. Carbone, M., Rizzo, P., Grinley, P. M., Procopio, A., Mew, D. J., Shridhar, V., deBartolomeis, A., Esposito, V., Giuliano, M. T., Steinberg, S. M., Levine, A. S., Giordano, A., and Pass, H. I. Simian virus 40 large T antigen binds p53 in human mesotheliomas. Nat. Med., *8:* 908–912, 1997.
44. De Luca, A., Baldi, A., Esposito, V., Howard, C. M., Bagella, L., Rizzo, P., Caputi, M., Pass, H. I., Giordano, G. G., Baldi, F., Carbone, M., and Giordano, A. The retinoblastoma gene family pRb/p105, p107, pRb2/p130 and simian virus 40 large T antigen in human mesotheliomas. Nat. Med., *8:* 913–916, 1997.
45. Bright, R. K., Kimchi, E. T., Shearer, M. H., Kennedy, R. C., and Pass, H. I. SV40 Tag specific cytotoxic T. lymphocytes generated from the peripheral blood of malignant pleural mestholioma patients. Cancer Immuno. Immunother., *50:* 682–690, 2002.
46. Pass, H. I., Robinson, B. W., Testa, J. R., and Carbone, M. Emerging translational therapies for mesothelioma. Chest, *16:* 455S–460S, 1999.
47. Bocchetta, M., Di Resta, I., Powers, A., Fresco, R., Tosolini, A., Testa, J. R., Pass, H. I., Rizzo, P., and Carbone, M. Human mesothelial cells are unusually susceptible to simian virus 40 mediated transformation and asbestos cocarcinogenicity. Proc. Natl. Acad. Sci. USA, *97:* 10214–10219, 2000.